The development of a SARS-CoV-2 pseudoparticle assay for the detection of neutralizing antibodies in sera from COVID-19 patients

UNIVERSITY of the
WESTERN CAPE

Submitted in fulfilment of the requirements for the degree Master of Science in the Department of Medical Biosciences, Faculty of Natural Sciences at the University of the Western Cape

Ame-Leigh Daniels

Supervisor: Prof. Megan L. Shaw

Department of Medical Biosciences, University of the Western Cape

List of abbreviations

%	percentage
°c	degree Celsius
µg	microgram(s)
µl	microlitre(s)
aa	amino acid(s)
Ab	antibody
ACE-2	Angiotensin-converting enzyme- 2
Ag	antigen
APS	ammonium persulphate
bp	base pair
BSA	bovine serum albumin
CO_2	carbon dioxide
cDNA	complementary deoxyribonucleic acid
CoV	coronavirus
CPE	cytopathic effect
C-terminal	carboxy-terminus
DAPI	4‘‘,6-diamidino-2-phenylindole, dihydrochloride
dH20	distilled water
DMEM	Dulbecco’s modified Eagles Medium
DNA	deoxyribonucleic acid
DTT	dithiothreitol

E. coli	*Escherichia coli*
EDTA	ethylenediaminetetraacetic- acid
ER	endoplasmic reticulum
FBS	foetal bovine serum
g	gram
GFP	green fluorescent protein
HCoV	human coronavirus
HEK	human embryonic kidney
KB	kilobases
mAb	monoclonal antibody
MERS-CoV	Middle East respiratory syndrome coronavirus
mins	minutes
mL	millilitre
MOI	multiplicity of infection
nAb	neutralizing antibody
ng	nanogram
N-terminal	amino-terminus
ORF	open reading frame
PBS	phosphate buffered saline
PCR	polymerase chain reaction
mg	microgram(s)
pp	pseudoparticles
RBD	receptor binding domain

RDM	receptor binding motif
RNA	ribonucleic acid
RT	reverse transcription
RT-PCR	reverse transcription polymerase chain reaction
S	spike
S protein	spike protein
S1	subunit 1
S2	subunit 2
SARS-CoV	severe acute respiratory syndrome coronavirus
SARS-CoV-2	severe acute respiratory syndrome coronavirus-2
SDS-PAGE	sodium dodecyl sulphate polyacrylamide gel electrophoresis
VSV	vesicular stomatitis virus
VSV-G	vesicular stomatitis virus glycoprotein
RPM	rotations per minute

Abstract

The COVID-19 pandemic has caused devastating effects on the global socio-economic landscape. Severe Acute Respiratory Syndrome Coronavirus 2 (SARS-CoV-2) is the causative agent of COVID-19, and infections have led to approximately 7 million fatalities worldwide. Previous findings have confirmed that neutralizing antibodies are a highly predictive measure of immune protection. Thus, measuring SARS-CoV-2 neutralizing responses after infection or vaccination remains a priority, especially in the event of newly emerging SARS-CoV-2 variants.

Due to the limitations of working with live virus in a BSL3 facility, pseudoparticles are an alternative tool used to study viral surface proteins. This research aims to develop a SARS-CoV-2 pseudoparticle system to detect neutralizing antibodies in sera from previously infected or vaccinated individuals. The use of vesicular stomatitis virus (VSV) as a vector for the pseudoparticle system, provides several advantages over the lentivirus system including faster assay time, and lack of interference from antiretroviral drugs present in sera from HIV-positive patients on antiretroviral therapy (ART). The latter is particularly relevant in South Africa where there are more than 7.8 million HIV people living with HIV.

After generating VSV pseudoparticles bearing the SARS-CoV-2 spike from the Wuhan/D614G, Beta, Delta and Omicron variants, a neutralizing assay was optimized using characterized human monoclonal antibodies. The assay was then applied to a sample set of patient sera and the ID_{50} values were compared to those obtained using a lentivirus-based SARS-CoV-2 neutralization assay. The comparison highlighted a strong concordance between the VSV and lentivirus neutralization assays particularly for the Wuhan/D614G and Omicron variants. The findings indicate that the development of a VSV-based neutralization assay is a valuable contribution to our ongoing efforts to characterize protective immune responses arising from SARS-CoV-2 infection or vaccination.

Declaration

I, Ame-Leigh Daniels, declare that this thesis, *The development of a SARS-CoV-2 pseudoparticle assay for the detection of neutralizing antibodies in sera from COVID-19 patients and vaccinees* hereby submitted to the University of the Western Cape for the degree of *Magister Scientiae* (MSc) has not previously been tendered by

me for a degree at any other university or institution, that it is my own work in design and

in execution, and that all materials contained herein have been duly acknowledged.

Ame-Leigh Daniels 10/11/23

Acknowledgments

I would like to express my sincere gratitude to Professor Megan L Shaw, for her guidance as my Masters' supervisor and for the opportunity to do my project in her laboratory.

Thank you to the National Research Foundation (NRF) and Poliomyelitis Research Foundation (PRF) for funding my project.

I would like to offer my special thanks to Dr Kim Lategan her assistance and mentorship through these 3 years.

My sincere appreciation to the Shaw Lab, with special recognition to Dr Bianca Gordan and Jihaan Adonis for all your guidance and patience with me through this journey.

Then to my mother Noleen, I would like to express my deepest gratitude for the unwavering support throughout my studies and for all the prayers. To my immediate family Benjiman, Tamara and my nephews and niece thank you for all the love and support.

To my extended family the Lategan's, thank you for playing such a pivotal role in my life these last few years. My close friends Demi-Che, Michealla and Kathryn thank you for being by my side through it all.

I would like to express my deepest appreciation to the late Kevin John Lategan†, I am grateful for the impact you had on my life, for all the lessons and memories. I wish you could have seen this journey from beginning to end. May your soul forever rest in peace**.**

Lastly I would like to thank God for all He did and continues to do.

List of Figures

List of Table

List of Appendices

Table of Content

Chapter 1. Introduction

SARS-CoV-2 has caused the greatest pandemic of the 21st century so far, infecting approximately 772 million people and causing the deaths of nearly 7 million worldwide. COVID-19 is the disease caused by the coronavirus severe acute respiratory syndrome coronavirus 2(SARS-CoV-2). Coronaviruses cause mild to severe respiratory disease in humans and are the largest of all RNA viruses. They are sub divided into four genera; Alpha, Beta Gamma and Delta with SARS-CoV-2 belonging to the Beta genus, which also includes SARS-CoV-1 (causes severe acute respiratory syndrome or SARS) and MERS-CoV (causes middle east respiratory syndrome or MERS) (Shereen et al. 2020) SARS-CoV-1 and MERS-CoV caused epidemics in 2003 and 2012, respectively.

Coronaviruses were first identified in humans in the 1960's isolating HCoV-229E strain, B814 as the cause of the common cold in humans (Kendall, et al. 1962, Fani, et al. 2020). Since then, more knowledge of human coronaviruses was acquired through the considerable research of isolates HCoV-229E and HCoV-OC43 (Ye, et al. 2020). Studies later identified HCoV-NL63 which demonstrated that coronaviruses have been circulating in the human population for a vast amount of time (Van Der Hoek, et al. 2006). Zoonotic coronavirus infections came under the spotlight in 2003 after the outbreak of SARS-CoV-1 prompted scientists to intensively investigate coronaviruses isolated from domesticated and wild animals (Wertheim et al. 2013).

1.1. Host species of coronaviruses

A broad variety of coronaviruses are harboured in bat populations (Menachery, et al. 2017) and this correlates with evidence presented from Zhang and Holmes who state that both SARS-CoV-1 and MERS-CoV have bats as primary hosts (Zhang and Holmes 2020). Bat-CoV-RaTG13, from the bat species *Rhinolophus affinis*, shares 96% nucleotide homology with SARS-CoV-2, suggesting that SARS-CoV-2 may have originated in bats. Another SARS-like coronavirus isolated from Chinese horseshoe bats (*Rhinolophus sinicus*) shares 79% nucleotide homology with SARS-CoV-2. This is similar to the percent nucleotide homology shared between SARS-

CoV-1 and SARS-CoV-2 (Mackenzie and Smith 2020). However, there is still much speculation and investigation of which animal/animals acted as an intermediate amplification host causing the transmission of SARS-CoV-2 from animal to human.

Studies from Liu, et al and Lam, et al. have both suggested that Malayan Pangolins could be an intermediatory host due to coronaviruses isolated from these animals showing 85.5–92.4% genomic identity with SARS-CoV-2(Liu, et al., Lam, et al. 2020). There is also evidence that six key amino acid residues in the S1 region of the receptor binding site present in the spike protein of coronaviruses isolated from Pangolins are similar to those found in SARS-CoV-2 spike protein (Andersen, et al. 2020). This is an important feature as the spike protein's primary function is to mediate attachment of the virus to target cells.

However, viruses transmitted from an intermediary host to humans should share higher nucleotide similarity than that of the virus transmitted directly from the primary host (Yuan, et al. 2020). This contradicts the theory that Malayan Pangolins could be intermediary host as the nucleotide similarity for RaTG13 coronavirus isolated from the *Rhinolophus affinis* bat is higher than that of coronaviruses isolated from pangolins. However, it is hypothesized that pangolins may have been involved in a recombination event leading to transmission of SARS-CoV-2 to humans (Polatoğlu, et al. 2023).

A variety of animal species are susceptible to SARS-CoV-2 infection, either naturally or experimentally (Figure 1.1). Further studies are needed to positively identify both primary and intermediary hosts and fully understand the transmission chain that led to the initial human infection.

1.2 SARS-CoV-2 pathogenicity

Similar to other coronaviruses, the primary route of transmission of SARS-CoV-2 is via respiratory droplets, with infection occurring by direct or indirect contact with nasal, conjunctival, or oral secretions (Hui, et al. 2020). SARS-CoV-2 targets cells that express the receptor, ACE-2, and due to the variability in distribution of ACE-2 in different organs (Scialo, et al. 2020) this may lead to a broad spectrum of infection sites and patient symptoms. Patients infected with SARS-CoV-2 can have symptoms ranging from mild upper respiratory tract infection to life-threatening sepsis.

In severe cases of COVID-19, it is hypothesized that the course of infection goes through the following stages: Viral invasion and replication, dysregulated immune response, multiple organ damage and recovery. First the virus enters susceptible cells, replicates, and is released before

going on to infect other cells. This causes direct damage and deterioration of parenchymal cells such as alveolar epithelial cells. Simultaneously a large number of pathogen associated molecular pattern (PAMP) and damage associated molecular pattern (DAMP) molecules are produced, which upregulate the innate immune response, leading to inflammatory cell infiltration, excretion of large quantities of cytokines, chemokines, proteases and free radicals (Li, et al. 2021). High levels of these immune responses can lead to the development of

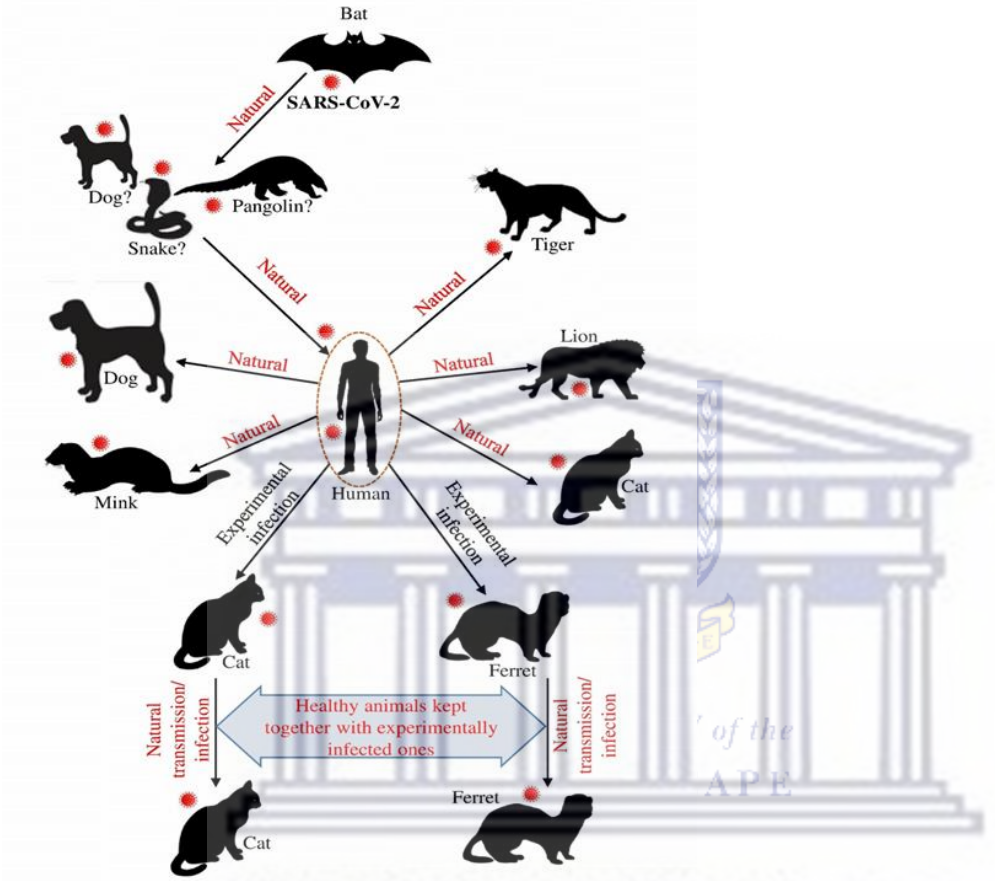

Figure 1. 1. Possible host range of SARS-CoV-2.(Hossain, et al. 2021)

diseases such as acute respiratory distress syndrome (ARDS) (Wang, et al. 2021) and multiple organ dysfunction syndrome (MODS) (Robba, et al. 2020), which cause excess pathological damage to respiratory structures in the lungs (von der Thüsen and van der Eerden 2020). Following the initial critical stage there is a decrease in immune hyperactivity and recovery of some of the damaged organs. However, repercussions of this infection can leave chronic illnesses such as fibrosis, constant inflammation, immunosuppression persistent inflammation, immunosuppression and catabolism syndrome (PICS) and the recently defined sequalae referred to as “long COVID” (Li,et al. 2023).

1.3. Genome organisation of SARS-CoV-2 and its expressed proteins

The SARS-CoV-2 genome is a non-segmented large positive-sense stranded RNA with a length of about 30 kB.The first two thirds of the SARS-CoV-2 genome encodes for two polyproteins, ORF1a and ORF1ab that are proteolytically cleaved into a total of 16 non-structural proteins (nsp) (Figure 1.2). These nsp have various functions in viral replication, viral assembly, and viral pathogenesis (Naqvi, et al. 2020).

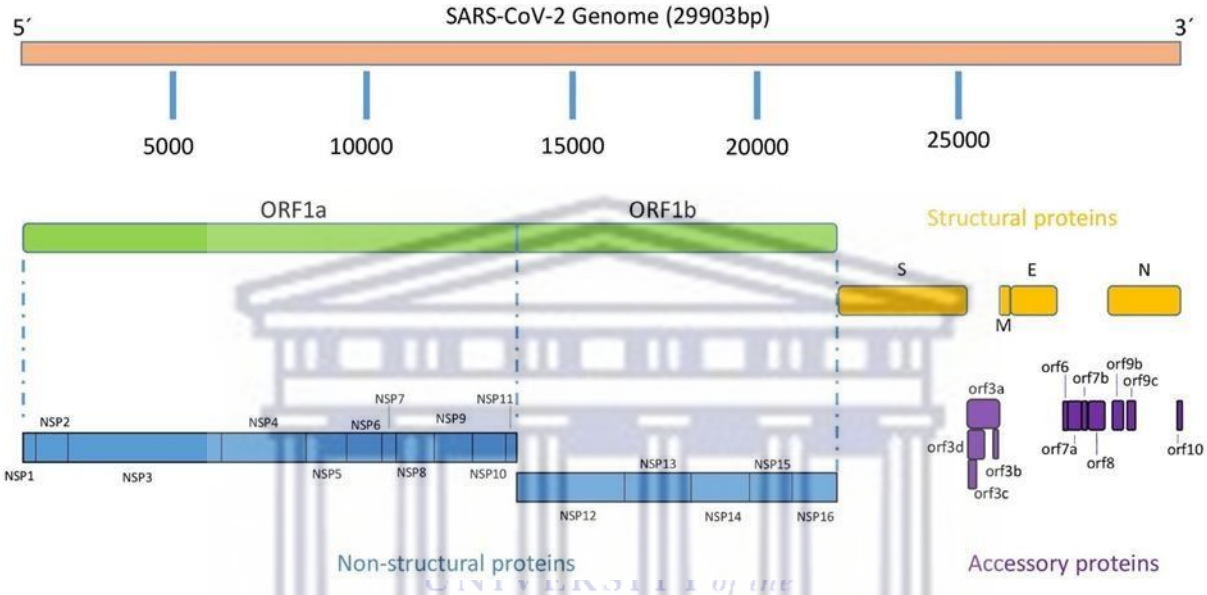

Figure 1. 2 SARS-CoV-2 genome. Starting from the 5' cap to the 3' poly A tail. the genome starts with open reading frame (ORF) 1a and 1ab encode for 16 non-structural proteins. Subsequently followed by ORFs encoding the structural proteins; spike(S), envelope(E), membrane (M) and nucleocapsid (N) along with several accessory proteins. (Redondo, et al. 2021)

SARS-CoV-2 expresses four structural proteins; spike (S), envelope (E), membrane (M), and nucleocapsid (N) proteins. These proteins share high amino acid similarity with the corresponding proteins from SARS-CoV-1 and MERS-CoV. Located on the outside of the virion, the structural glycoprotein spike is responsible for the attachment of the virus to human cells and thereby initiates infection. It is composed of 1273 amino acid residues and is divided into two subunits, namely S1 and S2. The first subunit, S1, mediates attachment of virions to the receptor on the host cell. That subsequently primes the activation of S2 which possesses fusion activity (Wong and Saier Jr 2021) and causes fusion of the viral membrane with the

mammalian cell membrane, effectively allowing release of the viral genome into the cell (Naqvi, et al. 2020).

The M protein, is the most abundant viral protein and recruits other structural proteins to the endoplasmic reticulum (ER)–Golgi intermediate compartment (ERGIC), where virus assembly and budding of takes place (Zhang, et al. 2022). The M protein also aids in morphogenesis via packaging of the genomic RNA into viral particles (Neuman, et al.
2011)

E protein is the smallest of the structural proteins, and it is an integral membrane protein consisting of three subdomains. This protein forms viroporins which are essential for the assembly and release of the virus particles (Cao, et al. 2021). By interacting with M protein it also helps to maintain viral structure (Wong and Saier Jr 2021).

N protein is best known for its ability to bind to genomic RNA to form a ribonucleoprotein complex that is essential for genome replication and translation (Arya, et al. 2021). It also interacts with the structural membrane (M) protein to promote membrane envelope folding and virion assembly (Wong and Saier Jr 2021). The N protein has been described to have various functions that manipulate the cellular machinery e.g. dysregulating the host cell cycle, stimulating the production of proinflammatory markers, suppressing the production of interferon, and inducing apoptosis. (V'kovski, et al. 2021)

Nestled between the structural genes are ORFs encoding the eleven accessory proteins. Four are wedged between the S and E genes (ORFs 3a, b,c,d), four between the M and N genes (6, 7a, 7b, 8) and two found within the N gene (9b,9c). The final accessory protein is encoded is ORF10. Accessory proteins have been shown to participate in viral-host interactions, and regulate apoptosis and immune functions (Zandi, et al. 2022). Furthermore, mutations in accessory proteins such as ORF3a,ORF6, ORF7a, ORF8 and ORF10 have been detected in currently circulating variants of concern (VOC) so they could potentially contribute to the increasing pathogenesis and transmissibility in these SARS-CoV-2 strains (Redondo, et al. 2021).

1.4. The role of SARS -CoV-2 spike protein in virus entry

SARS CoV-2 spike protein(S) is a homotrimer, class I fusion glycoprotein and it contains two functional subunits, S1 and S2 (Figure 1.3). S1 contains the N terminal domain (NTD) and the receptor binding motif (RBM) or receptor binding domain (RBD) and C-terminal domain(CTD).The RBM is the region that mediates binding to the ACE-2 receptor (Lan, et al. 2020).The NTD is not well characterized but it has an important role in maintaining the

structural conformation of spike (Magazine, et al. 2022). Mutations in the NTD are also associated with immune escape, indicating that the NTD is an antibody target (Harvey, et al. 2021). SARS-CoV-2 spike C-Terminal domain (CTD) has a larger binding interface and binding surface area with the ACE-2 receptor than RBD thus making this region a great target site for antibody neutralization (Huang, et al. 2020). Nonetheless, the SARS-RBD still has a higher interaction and affinity for ACE-2 receptor than SARS-CTD

Made up of eight subdomains, S2 has a fusion peptide (FP), fusion peptide proximal domain (FPPR), two heptad repeat subdomains (HR 1 and HR 2), a central helix (CH1), connector domain (CD) a transmembrane subdomain (TM) and the C terminal tail (CT). In the solved 3D structure of SARS-CoV-2 spike protein, the S2 portion forms a trimeric stalk, on top of which is the head-like structure of S1 with the RBD exposed for engagement with the receptor.

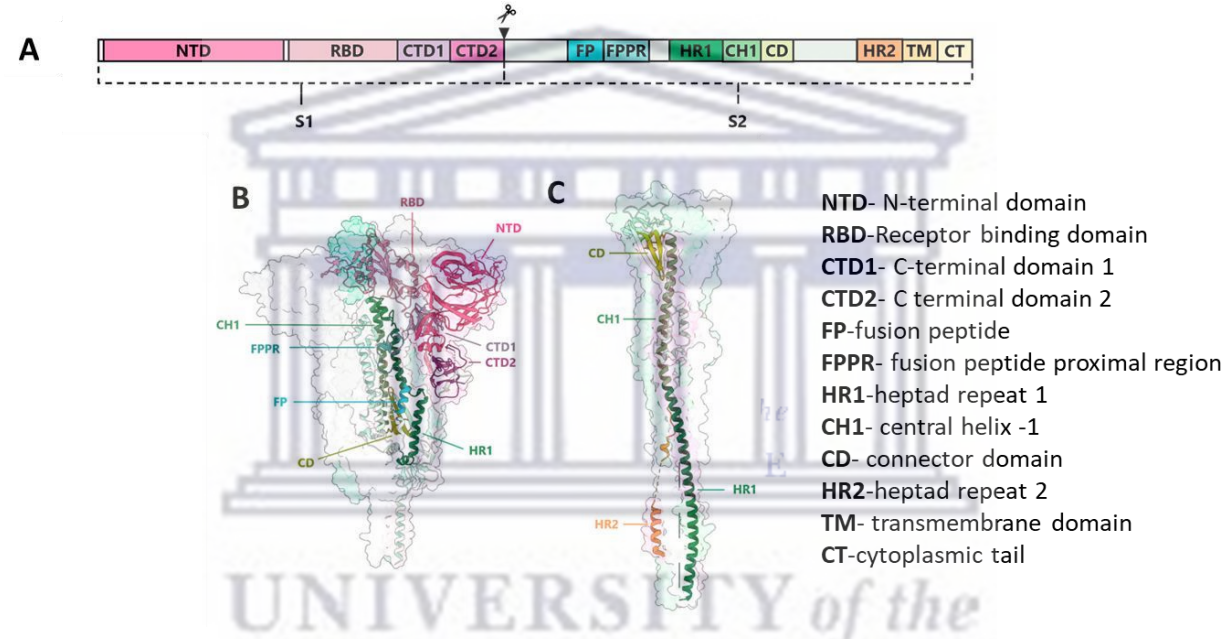

Figure 1. 3 The SARS-CoV-2 spike genome and 3D structure model (A) is the genome for the spike glycoprotein protein(B) is the protein in a pre-fusion state (C) is the protein in postfusion state. Adaptation from (Pedenko, et al. 2023)

Once the spike protein binds to ACE-2 receptors, the interaction causes a conformational change in the spike structure that exposes the S2 fusion peptide which gets inserted into the host cell membrane. While the TM anchors S in the viral membrane, the HR1 and HR2 subdomains are pulled towards each other and form what is known as a six helical bundle (Huang,et al. 2020). The energy involved pulls the viral and host membranes into close proximity, and this then leads to fusion of the two membranes (Weissenhorn, et al. 2007).

1.5. SARS-CoV-2 mutations and variants of concern (VOC)

The SARS-CoV-2 spike gene is very susceptible to mutation with the most vulnerable regions being the RBD and NTD within the S1 subunit of the spike protein. Mutations occurring in the RBD can modify both the biological and immunological characteristics of the virus by interfering with ACE-2 spike binding affinity, increasing virus transmissibility and allowing the virus to escape immune responses) (Scovino, et al. 2022).

There have been approximately 20 000 mutations detected in the SARS-CoV-2 genome between 2020-2022 (Wang, et al. 2023), with the majority being synonymous amino acid changes (Harvey, et al. 2021). This was evident early in the early stages during the emergence of SARS-CoV-2, when the amino acid change D614G was detected in the spike protein. The frequency of this mutation quickly gained 100% prevalence in circulating viruses by June of 2020 (Wang, et al. 2023). The mutation changed the conformation of the spike protein which resulted in increased virus infectivity and transmissibility, thus reducing vaccine efficacy (Yurkovetskiy, et al. 2020). Any mutation able to increases transmissibility, cause an elevation severity of illness and to escape vaccines or other medicinal treatment are known as variants of concern (VOC) (Young, et al. 2022). The classification of these variants is determined by World Health Organization (WHO) and the Centres of Disease Control (CDC) and are done according to the Greek alphabet (Wolfe, et al. 2022)

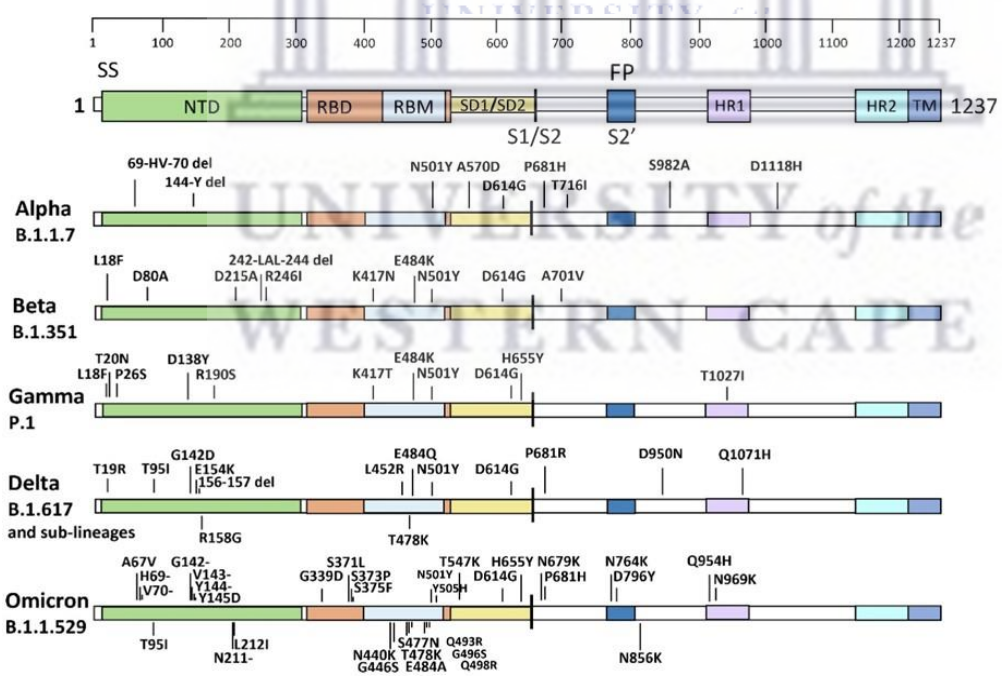

Figure 1. 4 Amino acid mutations and deletions present in the spike protein of SARS-CoV-2 variants of concern (Yoon, et al. 2022)

Other spike amino acid mutations (Figure 1.4), N501Y emerged firstly in the Alpha variant in September 2020 and was also present in the Beta and Gamma variants. This mutation lies in the RBD, and variants carrying N501Y showed increased binding affinity for ACE2 and the ability to evade immune responses (Chakraborty 2022). The Beta and Gamma variants, which emerged in December 2020 and January 2021 respectively, carried an E484K mutation that led to the decrease in neutralization potency of some human sera by 10-fold (Greaney, et al. 2021). The Delta variant, that emerged in May 2021 introduced two additional significant mutations; L452R and T478K. The L452R mutation resulted in enhanced spike stability, increased viral infectivity, and immune evasion. (Motozono, et al. 2021) Whilst T478K caused enhanced viral entry into ACE-2-expressing cells but it had negligible effect on antibody neutralization efficiencies compared to that of the WT (D614G) strain (Wang, et al. 2022). The Omicron VOC was originally detected in South Africa in December 2021 and contained more than 30 mutations in the spike protein, 15 of them in the RBD region and 8 of them causing impairment in antibody neuralization.

1.6. COVID-19 waves in the South African population

There were four waves of COVID-19 experienced in South Africa from March 2020 until January 2022, with each wave defined as a period in which there was a significant increase in the number of COVID-19 cases (Figure 1.5). During these waves the weekly incidence increased above 30 cases per 100 000 individuals (Jassat, et al. 2021). Each wave also saw the emergence and dominance of a new VOC. Wave 1 was dominated by the D614G variant, Wave 2 by the Beta variant, Wave 3 by the Delta variant, and Wave 4 by the Omicron variant (Yang and Shaman 2022).

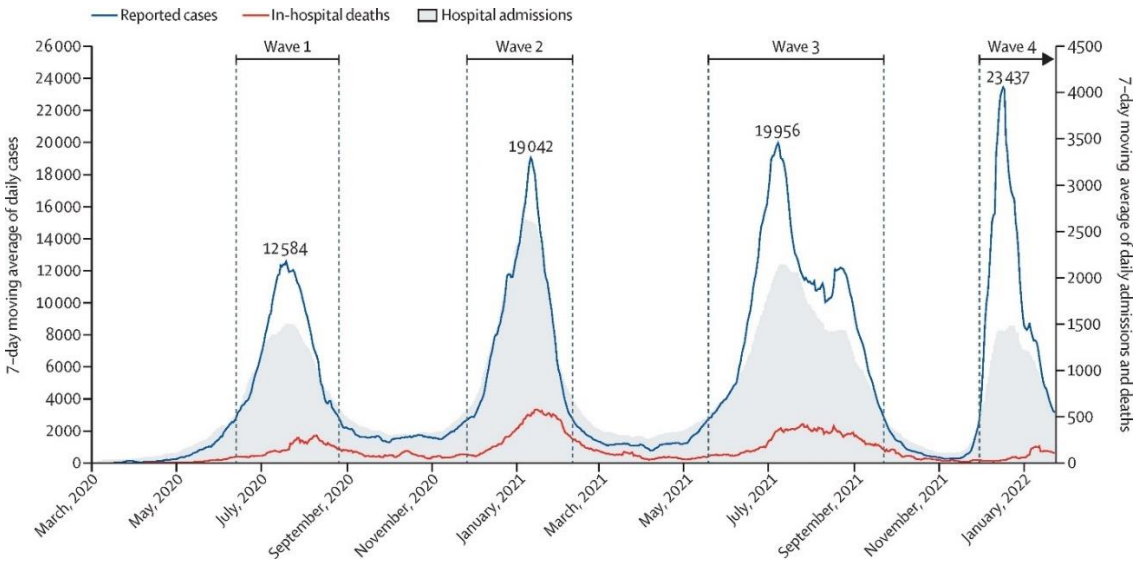

Figure 1.5. Timeline of pandemic waves in the South African population between March 2020 and January 2022 (Jassat, et al. 2022)

1.7. Role of neutralizing antibodies

When the body encounters pathogens such as viruses it triggers various immunological pathways as a mechanism of defence and protection. This involves the activation of B-lymphocytes which produce antibodies specific for the invading pathogen. Some of these antibodies have the ability to bind to the virus and prevent it from infecting a cell. Such antibodies are known as neutralizing antibodies (nAbs), and their presence usually correlates with protection from subsequent infection with the same virus (Abebe and Dejenie 2023). Neutralizing antibodies are produced in both infected individuals, and in those who have been vaccinated against the pathogen (Morales-Núñez, et al. 2021). However, the quality and quantity of the neutralizing antibody response differs from person to person (Gupta and Jaiswal 2022).

SARS-CoV-2 infection elicits virus specific antibodies against several different virus proteins, however only those directed against the S protein have neutralization activity (Figure1.6) (Galipeau et al. 2020, Perkmann, et al. 2021). Although neutralizing antibodies have been described to target both S1 and S2 regions of the spike protein, those that are directed specifically at the RBD appear to have a stronger neutralizing activity (Jackson, et al. 2022,Gattinger, et al. 2022).

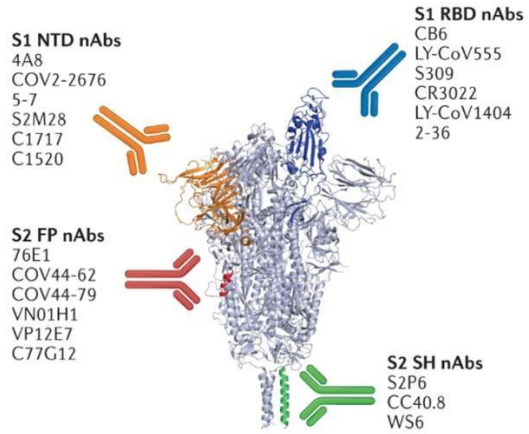

Figure 1.6. Different neutralizing antibodies that bind to various domains in the SARS-CoV-2 spike protein (Chen, et al. 2022)

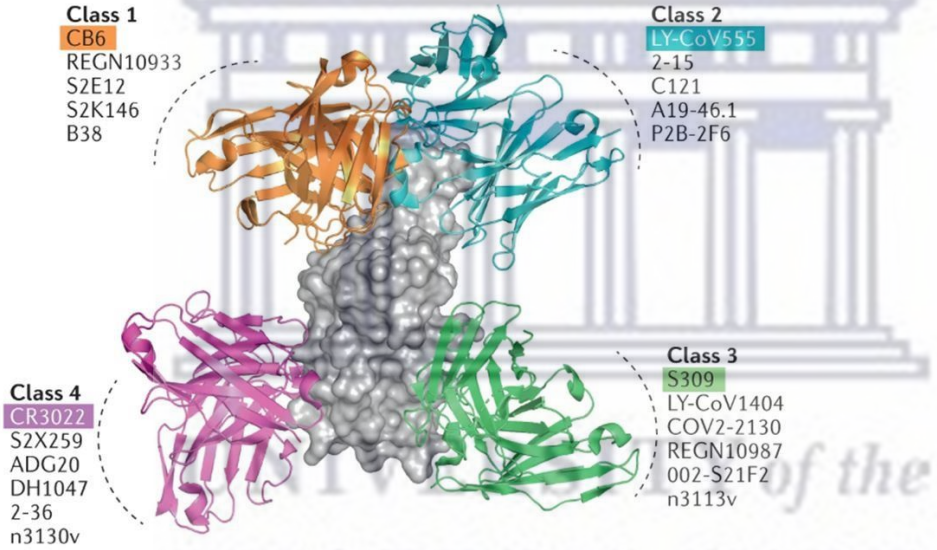

Figure 1. 7 Receptor binding domain specific neutralizing antibodies classified into four classes based on the epitopes they target in the spike protein (Chen, et al. 2022)

These neutralizing antibodies inhibit virus infectivity by blocking binding of the RBD to ACE2 receptors, or by disrupting the viral fusion process (Stephens and McElrath 2020), both of which prevent virus entry.

Analysis of the SARS-CoV-2 neutralizing antibody response can provide critical information on the longevity and stability of the protective immune response, both in response to infection and vaccination (Lau, et al. 2021). Furthermore, such studies can provide accurate predictions

of whether existing antibodies will afford cross-neutralizing activity against a newly emerged virus variant (Khoury, et al. 2021).

Various antibodies have the ability to neutralize more than one variant due to it binding to more conserved areas in the spike protein shared by the different variants. Thus, there is a need to discover neutralizing antibodies that are able to bind to various unmutated regions of the spike domain (Seydoux, et al. 2020).

1.8. Neutralization assay

Neutralization assays are a vital tool to detect and quantify the presence of functional antibodies in sera samples of infected patients and vaccinees. The classical method used for a neutralizing assay is to incubate live virus with serial dilutions of sera, and measure the extent of virus infectivity in permissive cells (e.g. by viral plaque assay or cytopathic effect) (Matusali, et al. 2021). However, an alternative method has been developed that is particularly useful when dealing with highly pathogenic viruses that can only be handled in biosafety level (BSL) 3 or 4 laboratories. Instead of using live virus, an engineered viral pseudoparticle is used that carries the surface glycoprotein of the pathogenic virus, but is otherwise harmless. As well as allowing the assay to be handled in a BSL-2 setting, these pseudoparticles carry a reporter gene so viral entry can be measured using either fluorescence or luminescence. (Figure 1.8)

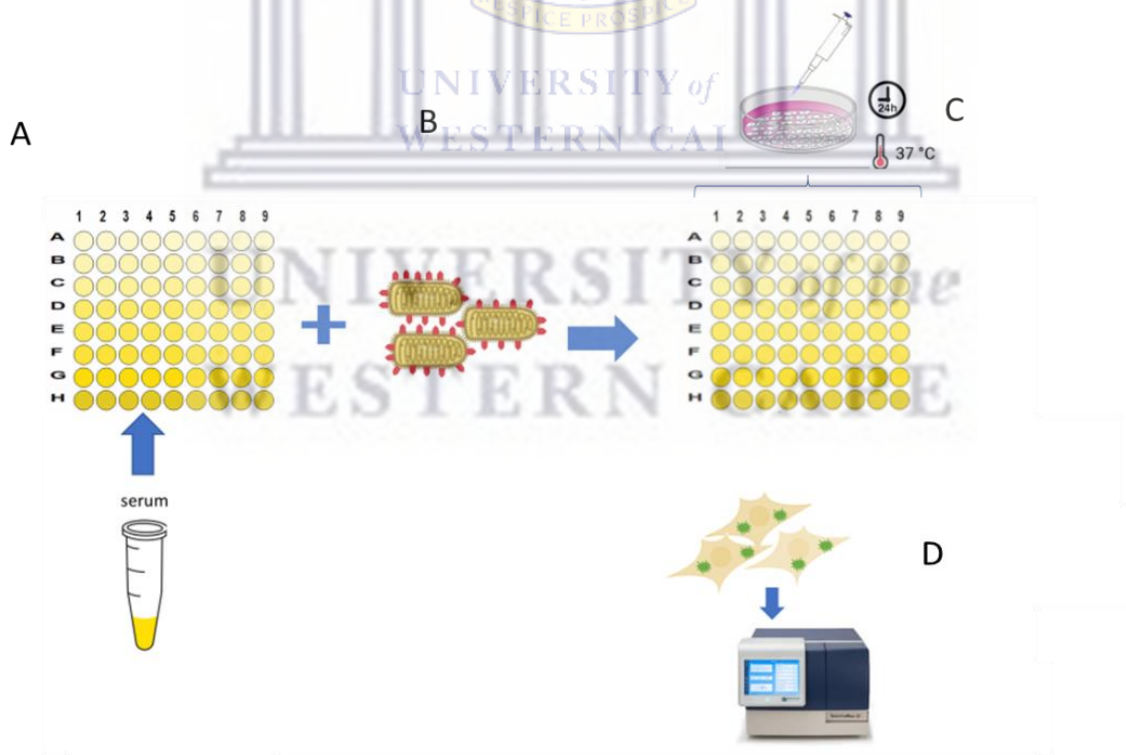

Figure 1. 8 Workflow of neutralization assay using vesicular stomatitis virus pseudoparticles. (A) Sera is serially diluted, (B) a set amount of virus is added to the

sera and incubated for 1hr. Cells are then added (C) to the sera/virus and incubated for 24 hours. After incubation, cells are lysed and luciferase activity quantified using a luminometer (D), providing readings in relative light units (RLU).

Data is usually processed with statistical analysis programmes to determine dose response curves; Figure 1.9 is an ideal shape of a dose response curve to determine inhibitory dilution 50(ID_{50}).

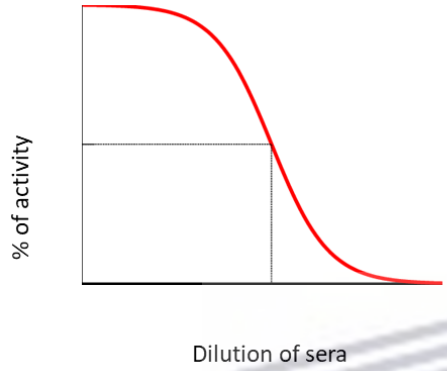

Figure 1. 9 Ideal sigmoidal/curve of best fit/dose response curve. Used to determine inhibitory dilution (ID_{50}) values (Vogt 2008).

The ID_{50} is defined as the reciprocal of the inhibitory dilution that causes 50% inhibition of the sera. The lower the IC_{50} the less neutralizing activity the sera have and the higher the IC_{50} the higher the neutralizing ability (Sarzotti-Kelsoe, et al. 2014).

1.9 Pseudoparticles

Pathogens are classified into four biosafety levels for the purpose of reducing the risk of exposure to a potentially infectious microbe and limiting contamination of the work environment and, ultimately, the community (Burnett, et al. 2009). There are four levels of biosafety with biosafety level (BSL) 1, being for the lowest risk associated organisms and level 4 having the highest risk associated organisms. SARS-CoV-2 is classified as a BSL-3 organism. However, most developing countries across the globe lack the highly trained personnel and infrastructure for BSL-3 facilities, especially in African countries.

One way of overcoming this hurdle and allowing us to study BSL-3 organisms in a BSL-2 setting is by developing pseudotyped viruses. A pseudoparticle is a recombinant virus particle that has the backbone of a less pathogenic virus but expresses the proteins/glycoproteins of more pathogenic viruses on its surface (Li, et al. 2018). The genome of the vector is genetically

modified to not produce its own surface protein, but through transfection or stable cell induction the surface protein of the pathogenic virus can be supplied *in trans* (Travieso, et al. 2022). It is also engineered to carry a reporter gene (fluorescence protein or luciferase) which serves to measure virus entry into cells, and aids in the process of obtaining quantitative data. There are three main pseudovirus packaging systems described that use either lentivirus (LV), vesicular stomatitis virus (VSV) and Murine leukaemia virus (MLV). For the purpose of the project, the focus will be on the VSV system.

1.10. Vesicular stomatitis virus pseudoparticles

Vesicular stomatitis virus (VSV) belongs to the Rhabdovirus family (Figure 1.9), and is found in insect vectors such as flies and midges which predominately targets farm animals (Letchworth, et al. 1999). The is virus considered to be harmless in humans, and any infections are mostly asymptomatic, or cause acute illness with symptoms that may include fever, muscle aches, headache and malaise (Peck,et al. 2020).

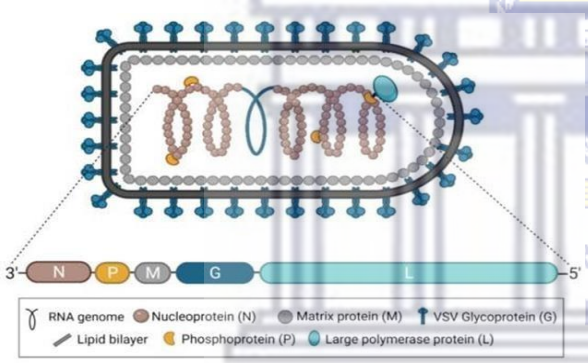

Figure 1. 10 Structure and genome organization of vesicular stomatitis virus. The genome encodes five proteins, N, P, M, G, and L. The glycoprotein (G) is found on the surface of the virus and aids in attachment to target cells (Liu, et al. 2021)

Laboratory strains of VSV have been engineered to replace the endogenous glycoprotein with two reporter genes, firefly luciferase gene (FLUc) and green fluorescence protein (GFP), creating a virus known as VSV*ΔG (FLUc)+VSV-G. To propagate this virus, the G protein must be supplied *in trans*, either by transient transfection or by stable expression. In order to generate a pseudovirus that carries the glycoprotein of another virus, e.g., SARS-CoV-2, cells are transfected with a SARS-CoV-2 spike expression plasmid, and then infected with VSV*ΔG (FLuc)+ VSV-G. The VSV pseudoparticle will acquire the spike glycoprotein during budding (Whitt 2010). (Figure1.10)

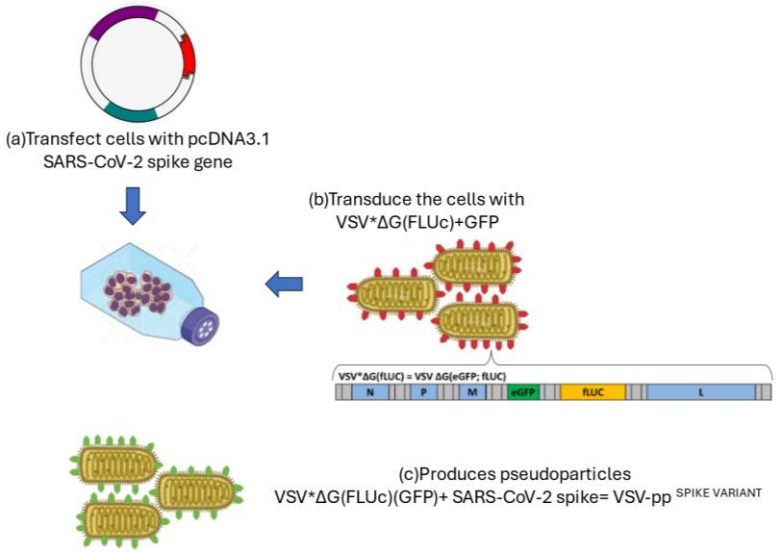

Figure 1. 11 Schematic diagram of the generation of VSV pseudoparticles. (a) Cells are first transfected with the plasmid encoding the desired protein (SARS-CoV-2 spike gene). (b) Cells are infected with the packaging virus VSV*ΔG(FLUc) +VSV-G. (c) Cells release pseudoparticles VSV*ΔG(FLUc)(GFP)+(SARS-CoV-2 spike) = VSVpp$^{spike\ variant}$ into the cell supernatant. *- denotes the open reading frame of enhanced green fluorescent protein

The VSV-based pseudoparticle system has some desirable advantages over the lentivirus-based system. The first one being that the generation of VSV pseudoparticles is less time consuming. It takes a total of 48 hours to generate VSV pseudoparticles whereas it takes up to 72 hours to generate lentivirus pseudoparticles (Fukushi, et al. 2008).

The second advantage relates to the prevalence of HIV infection in the population. A recently published article from De La Torre-Tarazona, González-Robles et al. reported that SARS-CoV-2 neutralizing titres in HIV patients on antiretroviral treatment (ART) are artificially elevated if using lentivirus-based pseudoparticles (De La Torre-Tarazona, et al. 2023). This is because antiretroviral drugs in the serum can inhibit the lentivirus polymerase, leading to decreased expression of the reporter gene, and hence a false positive neutralizing titre. The authors recommended that a VSV backbone be used instead, particularly if quantifying SARS-CoV-2 neutralization activity in HIV patients on ART. This precaution was further supported by Garcia-Beltran, Lam et al. who demonstrated that sera from patients on ART generated a large proportion of false positive results (Garcia-Beltran, et al. 2021).

It is estimated that there are more than 7.7 million HIV positive people in South Africa, of which 4.6 million currently receive ART (Burger, et al. 2022). Thus, the VSV pseudoparticle system is more suitable for conducting studies on SARS-CoV-2 neutralization titres in a dense HIV positive population such as South Africa.

Aim and objectives

Aim: To develop a VSV based pseudoparticle system to detect SARS-CoV-2 neutralizing antibodies in human sera.

Objective 1: Clone the spike gene and express the spike protein from SARS-CoV-2 Wild type and variants (Beta, Alpha, Delta, Omicron)

- Clone SARS-CoV-2 wild type and variant spike genes into the mammalian expression vector pCAGGS.
- Verify expression of the cloned spike proteins by performing both western blots and immunofluorescence assays.

Objective 2: Develop a pseudoparticle entry assay for SARS-CoV-2 wild type and variants

- Generation of VSV pseudoparticles bearing the SARS-CoV-2 spike protein of wild type and Beta, Alpha, Delta, and Omicron variants.
- Establish infection conditions for the pseudoparticles and use reporter gene expression to provide quantitative data on spike-mediated entry.

Objective 3: Establish an assay to detect SARS-CoV-2 neutralizing antibodies in patient serum samples.

- Optimize conditions for assessing neutralization by using a control neutralizing antibodies to inhibit entry of SARS-CoV-2 spike pseudoparticles.
- Use the established neutralization assay to quantify the presence of SARS-CoV-2 neutralizing antibodies present in the sera of COVID-19 patients.

Chapter 2. Methodology

2.1 Amplification and cloning of SARS-CoV-2 spike genes into mammalian expression vectors

2.1.1. Primer design for SARS-CoV-2 spike gene amplification

Oligonucleotide primers were designed to target the SARS-CoV-2 spike open reading frame (ORF) based on the NCBI Reference Sequence: NC_045512.2 (on 18th of July 2020). For the amplification of the spike ORF from subsequent variants, the primer sequences were aligned with the published sequences of the variant spike genes. No mismatches were observed.

Due to the large size of the SARS-CoV-2 spike gene, the ORF was amplified in three overlapping fragments sized between 1210-1355 base pairs. Each fragment was flanked with 15-30 base pair overlapping ends as indicated in Figure 2.1 and Table 2.1. During ligation of the three fragments, endonuclease creates a single stranded 3' overhang that allows for the ligation of these complementary ends (overlapping regions). Thus, the forward primer for Fragment 1 and the reverse primer for Fragment 3 included overlapping sequence corresponding to the cut sites of the pCAGGS vector after *KpnI* digestion.

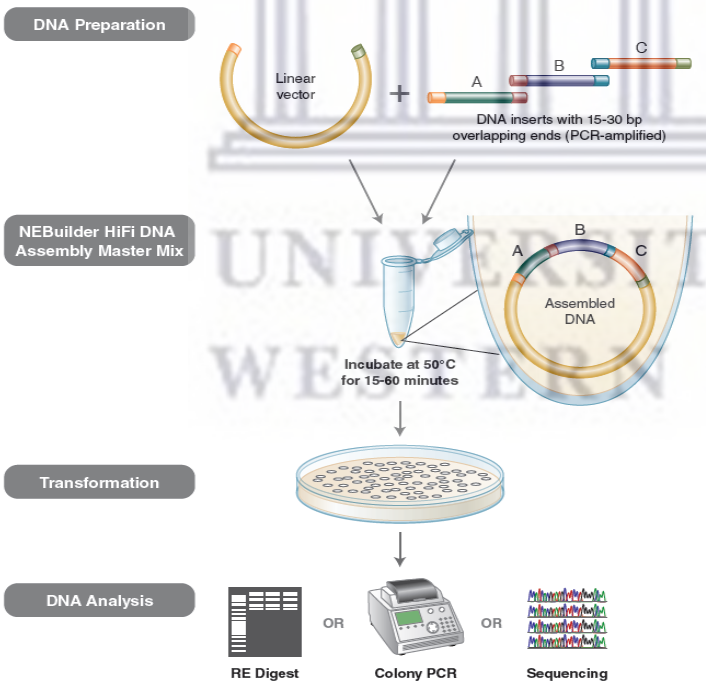

Figure 2.1 Overview of the cloning strategy for the generation of plasmids expressing SARS-CoV-2 spike. Taken from the instructional manual (Biolabs 2022)

Table 2. 1 Primers for the amplification of the SARS-CoV-2 spike gene.

	Forward	Reverse
Fragment 1 ***1210bp***	MLS-1 5'-attcgagctcatcgatgcatggtacACCATG TTTGTTTTTCTTGTTTTATTG-3'	MLS-2 5'-attagtaaagcaGAGATCATTTAATTT AGTAGGAGAC-3'
Fragment 2 ***1355bp***	MLS-3 5'-attaaatgatctcTGCTTTACTAATGT CTATGCAGATTCATTTG-3'	MLS-4 5'-catattgtttgaTGAAGCCAGCATCTGC AAGTG-3'
Fragment 3 ***1327bp***	MLS-5 5'-catattgtttgaTGAAGCCAGCATCTG CAAGTG-3'	MLS-6 5'-catattgtttgaTGAAGCCAGCATCTGC AAGTG-3'

2.1.2. Synthesis of cDNA from RNA

SARS-CoV-2 RNA was isolated from amplified virus stocks of WT, Beta, Alpha and Delta variants (kindly provided by Dr Tasnim Suliman). To generate amplicons for downstream PCR reactions, the RNA was converted to cDNA using New England Biotech LunaScript reverse transcriptase as illustrated below.

Table 2. 2Reaction preparation for the synthesis of cDNA from RNA

	Test sample	No RT control	No template control
LunaScriptRT SuperMix (5X)	4µl	-	4 µl
Viral RNA	4 µl	4 µl	-
No RT control mix	-	4 µl	-
Nuclease free water	12 µl	12 µl	16 µl
Total		20 µl	

Table 2. 3 Thermocycler conditions for the synthesis of cDNA from RNA

Cycle step	Temperature	Time	Cycles
Primer Annealing	25°C	2 minutes	1
cDNA Synthesis	55°C	10 minutes	
Heat Inactivation	95°C	1 minute	

cDNA was stored at -20°C.

2.1.3. PCR amplification of SARS-CoV-2 spike genes

Three separate reactions were performed to generate the three fragments of the SARSCoV-2 spike gene. Reactions were prepared as per manufactures instructions (New England Biolab) using the Q5® High-Fidelity PCR Kit.

Table 2. 4 Q5® High-Fidelity PCR amplification reaction mixtures

Reagent	Volume
Q5 High Fidelity Master Mix(2X)	12.5µl
Forward primer (10 µM)	0.5µl
Reverse primer (10 µM)	0.5µl
Nuclease Free water	9.5µl
Template DNA	2 µl
Total volume	**25µl**

Reactions were placed in the thermocycler under the following conditions:

Table 2. 5 Q5® High-Fidelity PCR amplification reaction thermocycler conditions

Step(s)	Temperature(°C)	Time	Number of cycles
Initial denaturation	98	30s	1
Denaturation	98	10s	35
Annealing	58	30s	
Extension	72	45s	
Final extension	72	2 mins	1

2.1.4 Single restriction enzyme digest

In order to ligate the expression vector and the three PCR fragments, the plasmid vector had to be linearized at the KpnI cut site. Using New England BioLab manufacturer's instructions pCAGGS(1µg) was mixed with 1µl of KpnI-HF (see Appendix 1 Table 5), 3µl of CutSmart buffer and 21µl of nuclease free water. The mixture was then incubated at 37°C for 1hour.

2.1.5 Agarose gel electrophoresis

PCR and digest products were run on a 1% (w/v) agarose gel. This was prepared by combining 1g of agarose powder in 100 ml of TAE buffer and then heated in a microwave until the solutes were dissolved. After allowing the solution to cool down slightly, 1µl(10mg/mL) of ethidium bromide (see Appendix 1, Table 5) was added. The agarose was poured into a casting tray with appropriate combs depending on the specifications of the experiment. The solution was left to solidify for approximately an hour. An equal ratio of DNA: 6X loading dye was loaded into each well. A 1kB ladder (NEB Biolabs) was also loaded, and the gel was then electrophoresed for 60 mins at 100V in TAE buffer. DNA was visualized via UV light and images were captured.

2.1.6 DNA extraction from agarose gels

After samples were run on the agarose gel, DNA was extracted as per manufactures instructions (NucleoSpin Gel and PCR clean up). DNA fragments were visualized on a UV lightbox, excised from the agarose gel, and transferred to an Eppendorf tube. For each 100mg of agarose gel, 200µl of Buffer NTI was added, and the samples were incubated for 10 mins at 50ºC with vertexing in intervals of 2 mins. Once the agar was completely dissolved a NucleoSpin Gel Clean up column was placed in a 2mL Eppendorf tube and up to 700µl of sample was loaded. The collection tube and column were centrifuged for 30s at 11,000 x *g*. Flow through was discarded and the column membrane was washed with Buffer NT3 before centrifuging the column twice at 11,000 x *g* for 1 minute each to allow the membrane to dry completely. The column was then placed in a new 1.5ml tube and 30µl of elution buffer was added at room temperature, before finally centrifuging for 1 minute at 11,000 x *g*.

2.1.7 Ligation of SARS-CoV-2 spike into pCAGGS vector

The 3 PCR fragments of the SARS-CoV-2 spike gene were ligated into the pCAGGS mammalian expression vector using NEBuilder HiFi DNA Assembly Reaction kit from New England BioLabs.

Table 2. 6 Ligation mixture preparation reaction

	Spike gene ligation	Positive control	Negative control
pCAGGS(100ng/µl) (linearised with KpnI)	1µl	-	1µl
Fragment 1(pmol/µl)	3.3µl	-	-
Fragment 2(pmol/µl)	3.7µl	-	-
Fragment 3(pmol/µl)	1.8µl	-	-
NEBuilder HiFi Assembly reaction master mix	10µl	10µl	10µl
Nuclease Free water	0.2µl		9µl
Positive control	-	10µl	-
Total	**20µl**	**20µl**	**20µl**

The samples were incubated for 15 minutes at 50 C, and then stored at -20ºC for subsequent transformation.

2.2. Preparation of plasmid DNA

2.2.1 Transformation of DHα competent *E.coli*

A 50µl vial of high efficiency DHα cells (Appendix 1, Table 1), provided with the NEBuilder HiFi DNA Assembly kit, was briefly thawed on ice, and 2µl of the PCR ligation reaction was added and gently mixed by pipetting and placed on ice for 30 minutes Cells were heat shocked at 42ºC for 30 seconds before immediately placing the tubes back on ice for 2 minutes. S.O.C media was added to the tube and incubated at 37ºC for 1 hour on a shaker with vigorous agitation (225 rpm). 100µl of the mixture was plated onto pre-warmed LB-Ampicillin agar plates which were inverted and incubated at 37°C overnight.

2.2.2. Transformation of JM109 competent *E.coli*

A 50µl vial of Promega JM109 (Appendix 1, Table 1) competent *E.coli* was thawed on ice before adding 1µl of plasmid DNA at a concentration of 10ng/µl. The vial was incubated on ice for 30 minutes and then briefly incubated at 42°C for 30 secs before being transferred back onto ice. 250µl of prewarmed Invitrogen S.O.C media was added to the vial before incubation on a shaking rotator for 1 hour at 225 rpm. 10µl of each transformation reaction was plated onto LB- Ampicillin agar plates, which were inverted and incubated at 37°C overnight.

2.2.3. Small scale generation of plasmid DNA (miniprep)

The extraction of plasmid DNA from transformed *E.coli* was done according to the manufacturer's instructions of the NucleoSpin Plasmid kit from Macherey-Nagel. One isolated colony from an LB-agar plate was inoculated into 3ml of LB broth (Appendix 1, Table 9) containing 50µg/ml of ampicillin antibiotic (Appendix 1,Table 5), and the culture was incubated overnight at 37°C on a shaking rotator. Thereafter, the cultures were transferred into 1.5 mL Eppendorf tubes and centrifuged at 11 000 x g for 30 secs. The supernatant was then discarded and the remaining pellet thoroughly resuspended in resuspension buffer. Cell lysis buffer was then added, and the tube gently inverted. Neutralization buffer was then added to the mixture and the tube inverted until the solution became colourless. Insoluble material was pelleted at 11 000 x g for 10 minutes, and the supernatant was transferred to a NucleoSpin column and centrifuged at 11 000 x g for 1 minute. The silica column was then washed with wash buffer and centrifuged at 11 000 x g for 1 minute. To remove excess wash buffer, the NucleoSpin column was further centrifuged at 11 000 x g for 2 mins. DNA was then eluted from the membrane by addition of elution buffer and centrifuging at 11 000 x g for 1 minute. The plasmid DNA was stored at -20°C for further downstream use.

2.2.4 Double restriction enzyme digest of plasmid DNA

Restriction enzyme digest was done as per manufacturer's instructions (New England BioLabs). Briefly, 1µg of miniprep plasmid DNA was mixed with 1.2µl of CutSmart buffer and 0.3µl of each restriction enzyme. The reaction was incubated overnight at 37°C. The digested plasmid DNA was then analysed on a 1% agarose gel by gel electrophoresis.

2.2.5 Large scale generation of plasmid DNA (maxiprep)

Large quantities of plasmid DNA were prepared using the NucleoBond Xtra Plasmid Purification kit from Macherey-Nagel. Bacterial cultures containing 300ml of LB-broth and 50µg/ml of Ampicillin antibiotic were inoculated with 300µl of starter culture broth, and were incubated overnight at 37°C on a shaking rotator. Cells were pelleted via centrifugation at 4 000 x g for 30 minutes at 4°C, the supernatant was discarded, and the pellets resuspended in resuspension buffer until the mixture became homogenous. Cell lysis buffer was added and the container gently inverted before being incubated for 5 minutes at room temperature. Thereafter, neutralization buffer was added and mixed until a transparent colour with white flocculants appeared. This mixture was then centrifuged at 4 000 x g for 10 minutes to allow for separation of the flocculant and supernatant. The column and filter were equilibrated with equilibration buffer prior to the addition of the supernatant which was allowed to flow through via gravitational flow. The filter was then washed with equilibrium buffer before discarding the column filter and a second wash step was done with wash buffer directly onto the column. The DNA was eluted from the column by the addition of elution buffer heated to 50°C and set aside for elution via gravity flow. The DNA was then mixed with iso-propanol and precipitated via centrifugation at 13 000 x g for 30 minutes at 4°C. DNA pellets were washed with 70% ethanol and centrifuged at 13 000 x g for 5 minutes at room temperature. Pellets were left to dry before resuspending the pellet in TE Buffer. The plasmid DNA was stored at -20°C for further downstream use.

2.2.6 Ethanol precipitation of DNA

Ethanol precipitation was used to purify and concentrate DNA. The DNA was mixed with 1/10th the DNA volume of 3M of sodium acetate and 3 times the DNA volume of 100% ethanol. The solution was then left to precipitate overnight at -20ºC, and the next day the solution was centrifuged at 14 000 RPM at 4ºC for 30 minutes to pellet the DNA. The pellets were then washed twice with 70% ethanol and centrifuged at 14 000 RPM for 10 minutes. Thereafter, the pellets were spun for 30 secs to allow for removal of any excess ethanol. Finally,

the pellets were left to dry at room temperature, and resuspended in nuclease-free water. The DNA were stored at -20ºC.

2.2.7. Quantification of plasmid DNA

Plasmid DNA concentrations were determined using the ThermoFisher Nanodrop 3300. Absorbance readings at 260nm and 280nm (A260/A280) were determined, where a ratio of 1.8 and above indicated that the preparation was relatively free of contaminants.

2.2.8 Sanger Sequencing

In order to verify the correct sequence of the cloned SARS-CoV-2 spike genes. Plasmid DNA clones were sequenced using forward and reverse vector plasmid primers (CAGGS-3 and CGGS-5), in addition to internal forward and reverse primers that bind within the spike ORF (MLS-2, MLS-3, MLS-4, and MLS-5). Samples were sent to Inqaba BioTech labs for Sanger sequencing. Results in the form of chromatograms were analysed using Ape, A plasmid editor and Snapgene. The DNA contigs were aligned against the SARS-CoV-2 spike reference sequence (NC_045512.2) using the BLAST tool in order to check for any mismatches and mutations in the cloned sequences.

2.3. Maintenance of mammalian cell lines

Human embryonic kidney cells (HEK-293T) and African green monkey kidney cells (Vero E6) cells (see Appendix 1, Table 2) were maintained in Dulbecco's Modified Eagles Medium (DMEM) supplemented with 10% foetal bovine serum (FBS) and 1% Amphotericin B/PenStrep (Penicillin-Streptomycin) (Appendix 1, Table 6) and cultured in a T75 tissue culture flask at 5% CO_2 and 37ºC.

HEK-293T cells that stably express human angiotensin converting enzyme 2 (HEK293T/ACE-2) were kindly provided by Prof Penny Moore (NICD). This cell line was maintained in DMEM supplemented with 10% FBS, 1% Amphotericin B/PenStrep, and 3µg/uL Puromycin (see Appendix 1, Table 6).

2.4 Transfection of mammalian cells

HEK-293T cells at a density of 8×10^5 cells per well were transfected in suspension with ThermoFisher Lipofectamine 3000 reagent as per manufacturer's instructions. A 1:3 ratio of DNA to Lipofectamine is used during all transfections and are done according to manufacturer's instructions. As per Figure 2.2, two aliquots of Gibco OptiPRO serum free media were dispensed into individual Eppendorf tubes. Lipofectamine 3000 reagent was added

to tube 1 and plasmid DNA (1µg/µl) and 5 µl of P3000 reagent were mixed together in tube 2. The DNA/P3000 was then mixed with the diluted Lipofectamine 3000, and incubated at room temperature for 15 minutes. The transfection solution was added to cells in a dropwise manner and the cells were incubated at 37ºC for 24 hours.

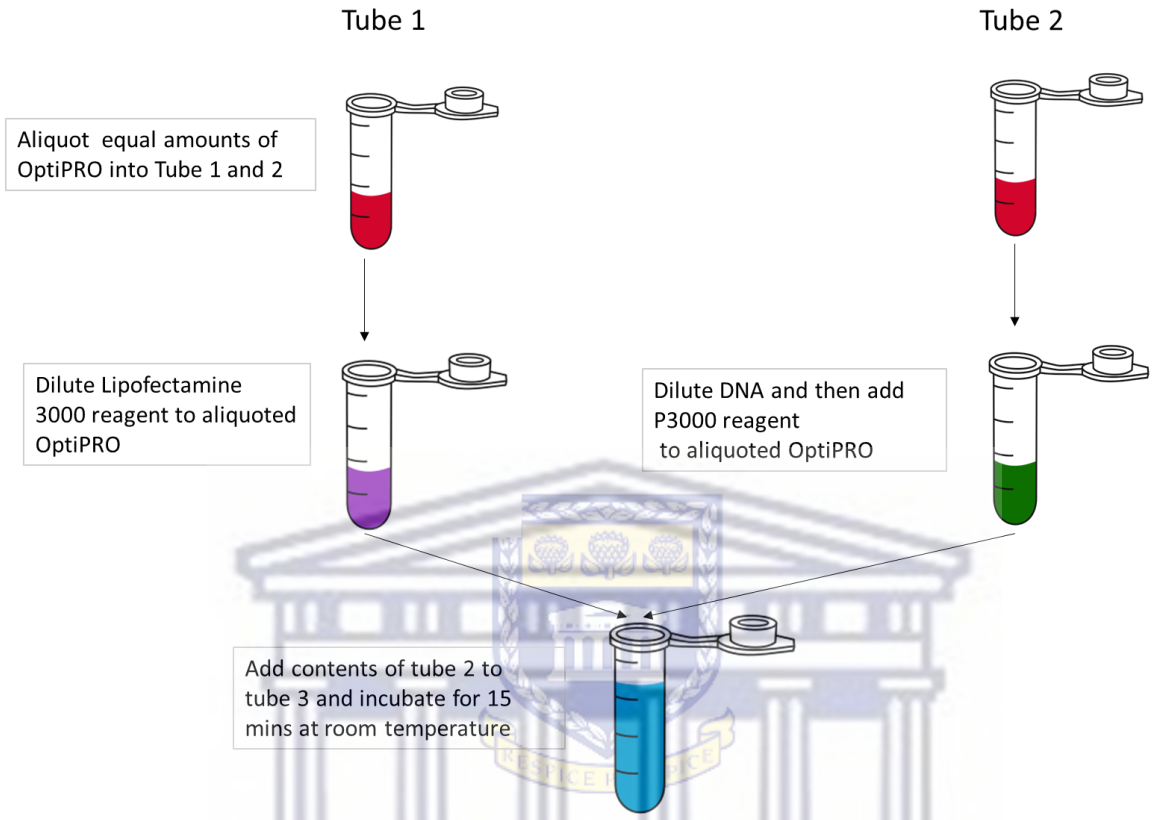

Figure 2. 2 Schematic of preparing reagents for transfection of HEK-293T cells

2.5. Western Blots

Media was removed from cells and was washed twice with 2 X DPBS before the addition of 200µl RIPA buffer to each well. Cells were incubated on ice and gently agitated for 30 minutes. Thereafter cells were manually dislodged from each well and transferred to Eppendorf tubes before centrifuging at 13 000 rpm for 10 mins at 4ºC. Pellets were discarded, and supernatants were stored at -20ºC.

An equal amount of lysate was mixed with an equal amount of 1X SDS-PAGE sample buffer (see Appendix 1, Table 9), the suspension was boiled at 95ºC for 15 minutes, and then loaded into individual wells of the SDS-PAGE gel along with a protein marker. Electrophoresis was performed at 0.02 constant amps for 2 hours. Total proteins were then transferred from the gel to nitrocellulose membrane using Bio-Rad semi- dry transfer system at constant voltage of 25V for 2 hours. The membrane was blocked in 5% non-fat milk (see Appendix 1, Table 9) for 2

hours at room temperature with slight agitation. The primary antibody, mouse monoclonal SARS-CoV-2 spike S1 subunit (R&D systems
MAB105403), was diluted 1/10 000 dilution (0.5mg/mL) in block solution and incubated overnight at 4ºC with slight agitation. The membrane was then washed with PBS-Tween 20 (PBS-T) three times for 10 minutes each.
Subsequently, secondary antibody Goat anti Mouse IgG (H+L) HRP conjugated (Invitrogen, # 31430) was diluted 1/5 000 (0.8mg/mL) in block solution, and added to the membrane which was incubated for 1 hour at room temperature. The membrane was washed in PBS-T three times for 20 minutes each, then 1-2 mL of TMB Membrane Peroxidase Substrate (see Appendix 1, Table 9) (pre-warm to 37ºC) was added to the membrane for 5-10 minutes to allow the substrate to react with the HRP enzyme (resulting in a blue precipitate). To stop the reaction, the membrane was covered with distilled water and then viewed.

2.6. Immunofluorescence

The transfected cells were fixed and permeabilized `with 100% methanol at – 20ºC for 30 minutes, and then washed twice with PBS. Blocking solution (5% bovine serum albumin (BSA) in PBS) was added to each well and incubated for 30 minutes at room temperature. Thereafter primary antibody (SARS-CoV-2 Spike S1 Subunit Antibody (R&D systems MAB105403)) at a 1:1000 dilution(0.5mg/mL) or mouse monoclonal ANTI-FLAG® M2 antibody (Sigma Alrich, F3165) at a 1:1000 dilution (1mg/mL) was added to coverslips and incubated at 1 hour at room temperature. Coverslips were washed 3 times with PBS-T before adding secondary antibody Goat anti-mouse IgG(H+L) highly cross absorbed Alexa Fluor Plus 488 (Invitrogen, # A32723) diluted 1:1000 (2mg/mL) and DAPI for 45 minutes at room temperature in the dark. Coverslips were then washed again 3X with PBS-T and 1X with distilled water before being briefly dabbed on tissue paper to remove excess liquid. Coverslips were then inverted i.e., cell side down, and mounted in Invitrogen ProLong Gold antifade mounting media on a microscope slide. Slides were stored in the dark at 4ºC.

2.6. Generation of pseudoviruses using a VSV-based system

2.6.1 Propagation of VSV*ΔG(FLUc) trans complemented with VSV-G

Vesicular stomatitis virus (VSV) engineered to express firefly luciferase (FLUc) and green fluorescent protein (GFP) in place of the viral glycoprotein (G), was kindly provided by Dr Gert Zimmer at the Institute for Virology, Mittelhäusern, Switzerland. The propagation of VSV*ΔG(FLUc) trans complemented with VSV-G was performed in a 6 well plate that was

pre-treated with poly-L-lysine for 20 minutes and left to dry in a laminar flow hood. HEK-293T cells ($8x10^5$/well) were transfected with an expression plasmid for VSV-G (pCG-1-VSV-G) using Lipofectamine 3000.

After 24 hours the cells were infected with VSV*ΔG(FLUc)+(VSV-G) (see Appendix 1, Table 2) at an MOI of 3 for 1 hour at room temperature with gentle agitation every 15 minutes. The virus was removed from cells before gently washing the cells 6 times with PBS and adding 2% post infection media (1X DMEM supplemented with 2% FBS and %1 Pen/Strep). Cells were incubated for 24 hours at 33ºC before harvesting the supernatant which was then centrifuged at 2000 RPM for 5 minutes and aliquoted into cryovials and frozen at -80ºC.

2.6.2. Titration of VSV*ΔG(FLUc) +(VSV-G) stock

The VSV*ΔG(FLUc) +(VSV-G) stock was titrated using a TCID-50 assay in HEK-293T cells. A 10-fold dilution series of the virus stock was made in a 96-well plate from columns 3-12, to which a suspension of cells at a density of 4×10^5cells/well was added. The infected cells were incubated for 24 hours at 37ºC. The luciferase activity in the infected cells was quantified using Bright-Glo™ Luciferase Assay System (Promega). Briefly, supernatant was removed, and the cells were lysed in 30 µl 1X passive lysis buffer for 10mins, before adding 100µl of BrightGlo substrate. The contents of each well were then transferred to a 96-well white plate and the luminescence was read using the SpectraMax ID3 with an integration time of 1 sec. Relative light units (RLU) were recorded.

The Reed Muench method was used to calculate the TCID 50/mL of the virus stock as follows:

1. A positive (+) sign was assigned to all RLU values >1000, and a negative (-) for all values < than 1000.
2. A percentage for each dilution ranging from 10^{-1}-10^{-10} was calculated by dividing the number of positive signs of each dilution by the number of replicates (8 replicates for a full 96 well plate) x100%
3. LogID50 = Log (dilution with >50% RLU) + [difference of logs or PD x (-Log of dilution factor)] is the equation used to determine TCID 50
4. The proportional distance (PD) or difference in logs value is calculated as follows:
5. The proportional distance (PD) or difference in logs value is calculated as follows:

$$\frac{(\%\ RLU\ at\ the\ viral\ dilution\ that\ shows > 50\%\ ) - 50\%}{(\%\ RLU\ at\ the\ viral\ dilution\ that\ shows > 50\%\ ) - (\%\ RLU\ at\ the\ viral\ dilution\ that\ shows < 50\%\ )}$$

6. LogID50 $\longrightarrow$ ID50 = 10^{LogID50}

7. $\text{TCID50/mL} = \frac{\frac{1}{ID\ 50}}{volume\ of\ virus\ inoculum(mL)}$

2.6.3. Generation of VSV*ΔG(FLUc) +(SARS-CoV-2 spike) pseudoparticles

To generate SARS-CoV-2 spike expressing VSV pseudoparticles, HEK-293T cells were transfected with pcDNA expression plasmids expressing SARS-CoV-2 spike from the wild-type (WT)/D614G, Beta, Delta, and Omicron (BA1) variants of SARS-CoV2, which were kindly provided by Prof Penny Moore (NICD).

After transfection the media was aspirated and the cells washed twice with DPBS. Transfected cells were then infected with VSV*ΔG(FLUc)+VSV-G at an MOI of 3 for 1 hour at room temperature with gentle agitation every 15 minutes. The virus was removed from cells before gently washing cells 6 times and adding 2% Post infection media. Cells were incubated for 24 hours before harvesting supernatant which were then centrifuged at 2000 RPM for 5 minutes and aliquoted in cryovials and frozen at -80ºC.

2.6.4 Titration of VSV*ΔG(FLUc) +(SARS-CoV-2 spike) pseudoparticles

A 2-fold serial dilution of the VSVpp-Spike pseudoparticle preparation was made in a 96 well cell culture plate, before adding 100µl of HEK-293T/ACE-2 cells at a density of 8×10^5cells per well. The infected cells were incubated for 24 hours at 37ºC. Luciferase activity was measured using the Bright-Glo™ Luciferase Assay System (Promega). The media was aspirated off the cells, briefly and 30µl of 1X passive lysis buffer was added to each well and incubated for 10 minutes before adding 100µl of BrightGlo substrate. The contents of each well were then transferred to a 96 well white plate, and luminescence was measured using the SpectraMax ID3 with an integration time of 1 second. Relative light units (RLU) were recorded and plotted on the Y-axis vs. dilution factor on the X-axis. Dilutions that resulted in approximately 100 000 RLUs were used for neutralization assays.

2.7. SARS-CoV-2 neutralization assay

2.7.1. SARS-CoV-2 neutralizing antibodies and human sera

Human monoclonal antibodies (CA1, CB6, 084-7D) targeting the spike protein that have been described to neutralize SARS-CoV-2 were kindly provided by Prof Penny Moore (NICD). The neutralizing antibody, Bebtelovimab (Eli Lilly), was kindly provided by Dr Craig Fenwick (Lausanne University Hospital, Lausanne, Switzerland).

Human sera from COVID-19 patients were obtained from two different cohorts, one from the University of Pretoria, the other the University of Cape Town.

Ethics statement: The use of human antibodies and human sera for research purposes was approved by the Biomedical Science Research Ethics Committee of the University of the Western Cape. Ref No. BM21/9/19.

2.7.2. Optimisation of assay conditions using SARS-CoV-2 spike neutralizing antibodies

A 3-fold serial dilution of the neutralizing antibodies CA-1 (10 µg/mL starting concentration), CB-6 (5µg/mL), 087-4D (50µg/mL), and Bebtelovimab (1µg/mL) was performed in a 96 well culture plate. VSVpp-spike pseudoparticles (variants WT, Beta, Delta and Omicron) were diluted to obtain approximately 100 000 RLU of virus (based on the titration described in 2.6.4) and 50µl was added per well. The antibody and pseudoparticle were mixed and the suspension were incubated for 1 hour at 37ºC. HEK293-T/ACE-2 cells were added to the antibody/pseudoparticle mixture at a density 8×10^5cells per well, and incubated for 24 hours at 37ºC, 5% CO_2.

Thereafter, the media was aspirated off the cells, and 30µl of 1X passive lysis buffer was added and incubated for 10 minutes before adding 100µl of BrightGlo substrate. The contents of each well were then transferred to a 96 well white plate and luminescent signal was quantified using the SpectraMax ID3 with an integration time of 1 sec.

RLU values were recorded in Excel before plotting the normalized values vs. the antibody concentration, and applying a line of best fit in GraphPad. The statistical programme also generated IC50 values (50% inhibitory concentration).

2.7.3 Validation of the assay using human SARS-CoV-2 sera

A batch of blinded human serum samples was sent by Prof Penny Moore (NICD) to test the validity of VSV-based SARS-CoV-2 neutralization assay. The nine samples were initially centrifuged at 14 000 rpm for 1 minutes before being heat inactivated at 55ºC for 30 minutes to destroy the naturally occurring complement factors. Samples were aliquoted and stored at -80ºC.

All serum samples were initially diluted 1:20 before performing a serial 3-fold dilution. A set amount of VSVpp-spike (~100 000 RLU) was added to the plate before incubating for 1 hour at 37ºC. A suspension of HEK-293T/ACE-2 cells was prepared and added at a final density of $2X10^4$ cells/well. Cells were incubated at 37ºC at 5% CO_2.

After incubating for 24 hours, the media was aspirated off the cells and 30µl of 1X passive lysis buffer was added and incubated for 10 mins before adding 100µl of BrightGlo substrate. The contents of each well were transferred to a 96 well white plate and luciferase activity was measured.

The data generated by SoftMax Pro relative light units (RLU) reading was then processed in Excel to standardize values $\frac{RLU\ value}{RLU\ virus\ only\ value}$ x100% to give us a percentage of neuralization of each sample. The percentage of neutralization was then plotted against the corresponding serum dilution using GraphPad.

To further determine accuracy of ID_{50} values the data was processed using a Macro programme provided to us from the NICD.

Chapter 3: Results

3.1. Amplification of SARS-CoV-2 spike genes from viral cDNA

Viral SARS-CoV-2 RNA was isolated from amplified virus stocks of wild type/D614G (WT), alpha beta, and delta variants. The RNA was converted to cDNA using random hexamer and poly dT primers. The Q5® High-Fidelity PCR Kit was then used to amplify three overlapping fragments using specific primer pairs (Table 2.1)

Due to the lack of availability of commercial SARS-CoV-2 spike antibodies at the time of this experiment, a FLAG tag was added to the C-terminus of the ORF for downstream protein detection. Another modification at the C-terminus of the ORF was the deletion of the last 19 amino acids to eliminate the ER-retention motif. Research has shown that the deletion of the 19 amino acid retention sequence increases the presence of spike protein at the cell surface (Johnson, et al. 2020, Chen, et al. 2021, Wang, et al. 2021, Zhang, et al. 2023). These modifications were incorporated into the reverse primer for Fragment 3 (Table 2.1) The forward primer of fragment 1 and the reverse primer of fragment 3 also contained KpnI sites which would allow for recombination with the vector once it had been linearized at the *KpnI* site present in the multiple cloning sites. Images of the DNA gels showing successful amplification of the three fragments (approximately 1210bps,1355 bps, and 1327 bps) for each SARS-CoV-2 variant are shown in Figure 3.1 A-D.

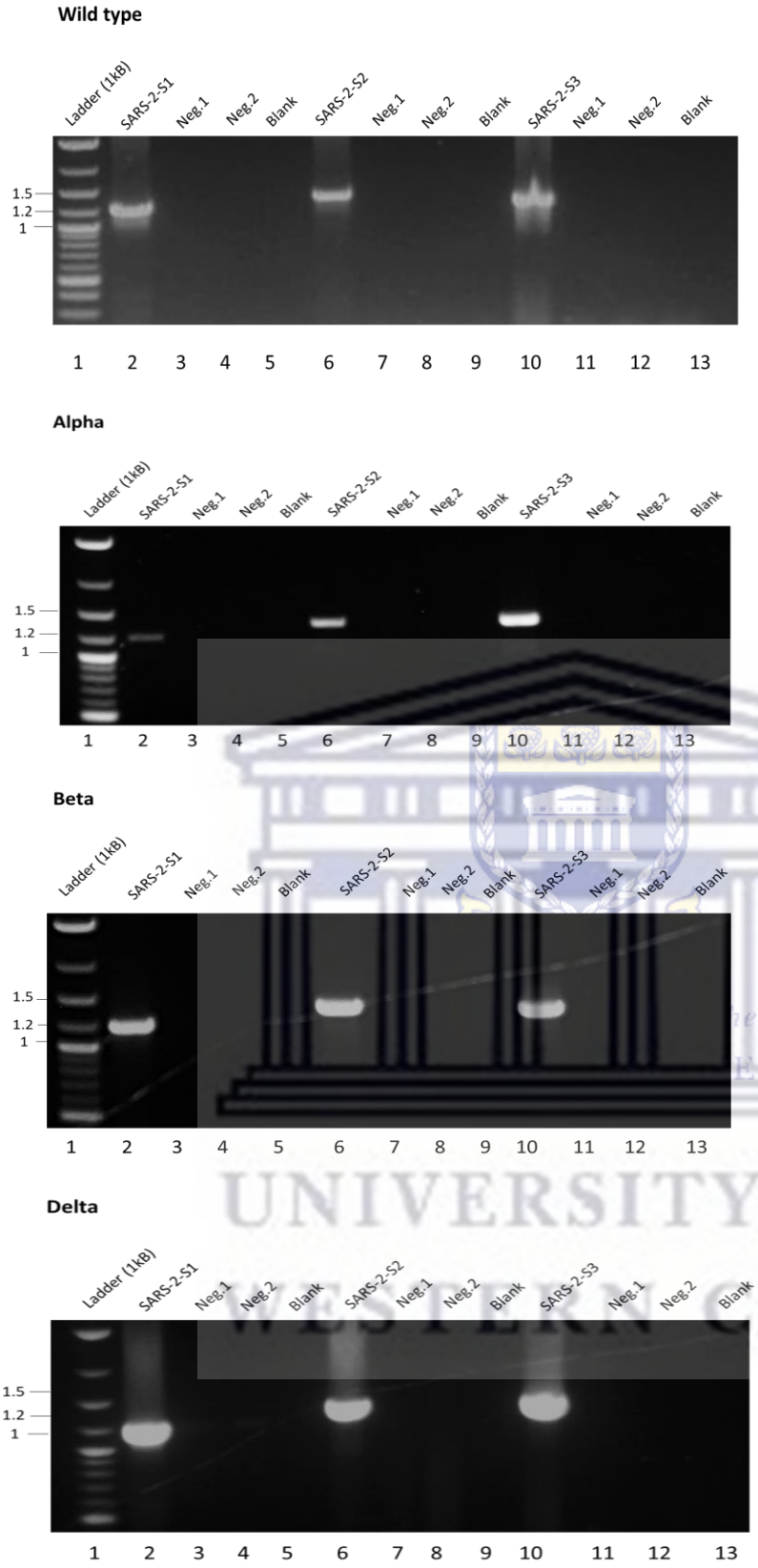

Figure 3. 1 PCR of amplicons for the construction of SARS-CoV-2-spike ORF.

A 1 % agarose gel showing the three amplicons (SARS-2-S-1, SARS-2-S-2 and SARS-2-S-3) which together comprise the full-length spike gene of the SARS-CoV-2 WT (panel

A), alpha (panel B), beta (panel C), and delta (panel D) variants, respectively. Lane 1 contains a 1kB ladder. Negative controls: Neg.1 = no reverse transcriptase (RT), Neg.2 = a no template control, Blank= empty wells

3.2. Cloning of Flag-tagged SARS-CoV-2 spike genes into pCAGGS

Once the SARS-CoV-2 spike fragments were amplified, they were purified and combined with the expression vector, pCAGGS, that had been linearised with *KpnI*. The four DNA fragments were ligated by means of recombination using NEBuilder HiFi DNA Assembly Reaction kit. To confirm the presence of the entire SARS-CoV-2 spike gene in the resultant clones, a double digest using enzymes *Xho I* and *Sac I* was performed, which should remove the SARS-CoV-2 spike gene from the pCAGGS vector. The presence of bands at approximately 3.9 kB and 4.7Kb, which represent SARS-CoV-2 spike and pCAGGS, respectively, was used to identify positive clones (Figure 3.2).

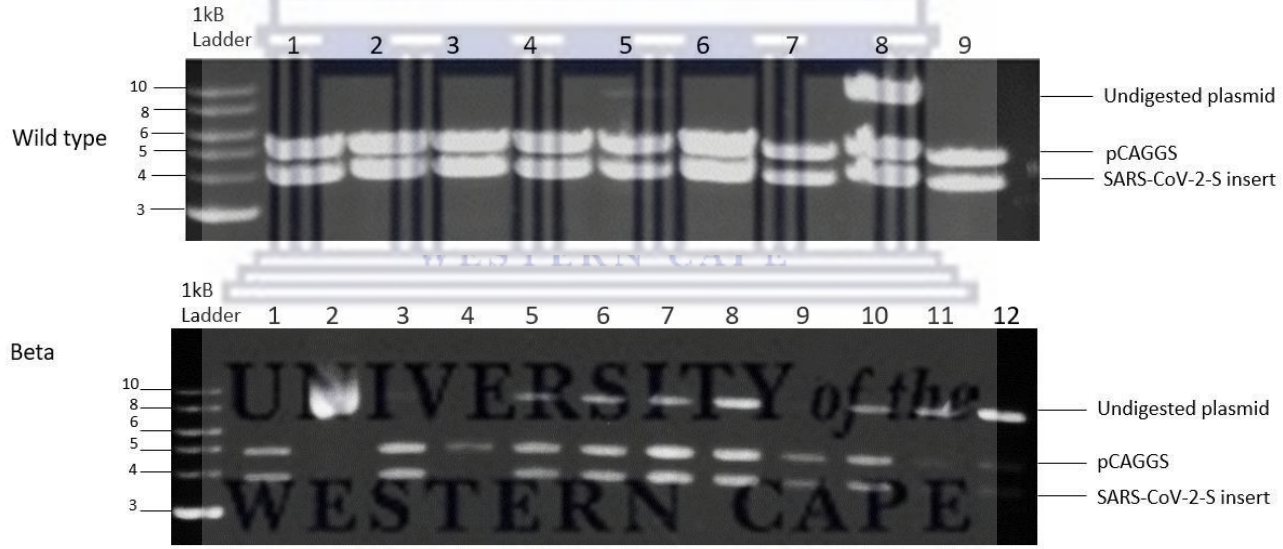

Figure 3. 2 Confirmation of SARS-CoV-2 spike WT and Beta clones by restriction enzyme digest using enzymes *Xho I* and *Sac I*. Lanes 1-9 (wild type) and lanes 1-12 (beta) contain the digest products of different plasmid clones electrophoresed on a 1% agarose gel. The positions of the pCAGGS vector at 4.7kB, the SARS-CoV-2 S gene at 3.9kB, and undigested plasmid are indicated.

3.3. Sequence confirmation of pCAGGS spike-Flag clones

Once positive clones were identified, and purified plasmid DNA was generated, it was sent for sequence confirmation. The plasmid was subjected to Sanger sequencing using the forward and reverse primers that generated each of the three PCR fragments of SARS-CoV-2 spike. In addition, forward and reverse pCAGGS primers that bind either side of the multiple cloning sites were utilized. This allowed for the generation of multiple overlapping sequences that were then aligned to reconstruct the cloned spike gene. The aligned sequences were compared to the SARS-CoV-2 Wuhan-Hu-1 reference sequence (Figures 3.3 and 3.4). For the WT spike clone, one missense mutation was detected at position 614 of the amino acid sequence which changed an aspartic acid to glycine (Figure 3.3). The results were expected because it is known that the virus acquired this mutation in the spike gene very soon after it began circulating in humans in early 2020. The viral RNA that was used as a template for the amplification of the WT spike gene was from a virus isolated in the first wave of COVID-19 in South Africa (April 2020), corresponding to the presence of the D614G mutation in spike.

Figure 3. 3 Alignment of the reference sequence for SARS-CoV-2 isolate Wuhan-Hu-1 (NC_045512.2) with the contigs generated from pCAGGS-Spike^{WT} clone.

For the pCAGGS-spike^{Beta} clone, 8 missense mutations resulting in the change of amino acids were detected, namely: L18F, D80A, D215G, K417N, E484K, N501Y D614G and A701V (Fig 3.4 and Table 3.1). In addition, a deletion of amino acids 242-244 was observed. A synonymous mutation occurred at position 1532 of the genome sequence but still encoded for the amino acid valine. These mutations correspond to the report from Tegally *et al*. (Tegally, et al. 2020) who first detected the emergence of the Beta variant in South Africa.

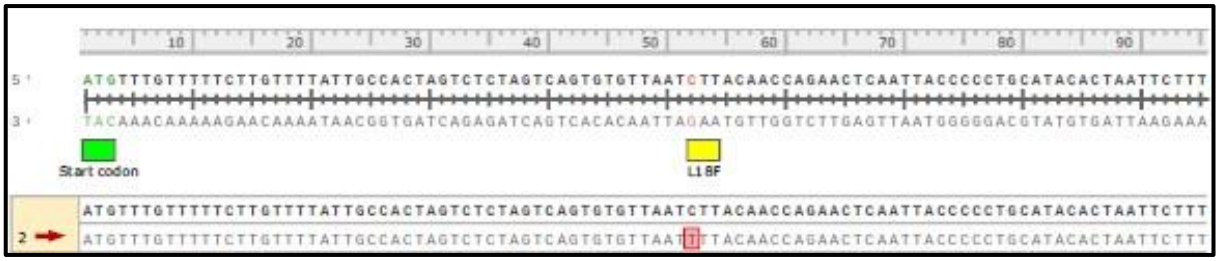

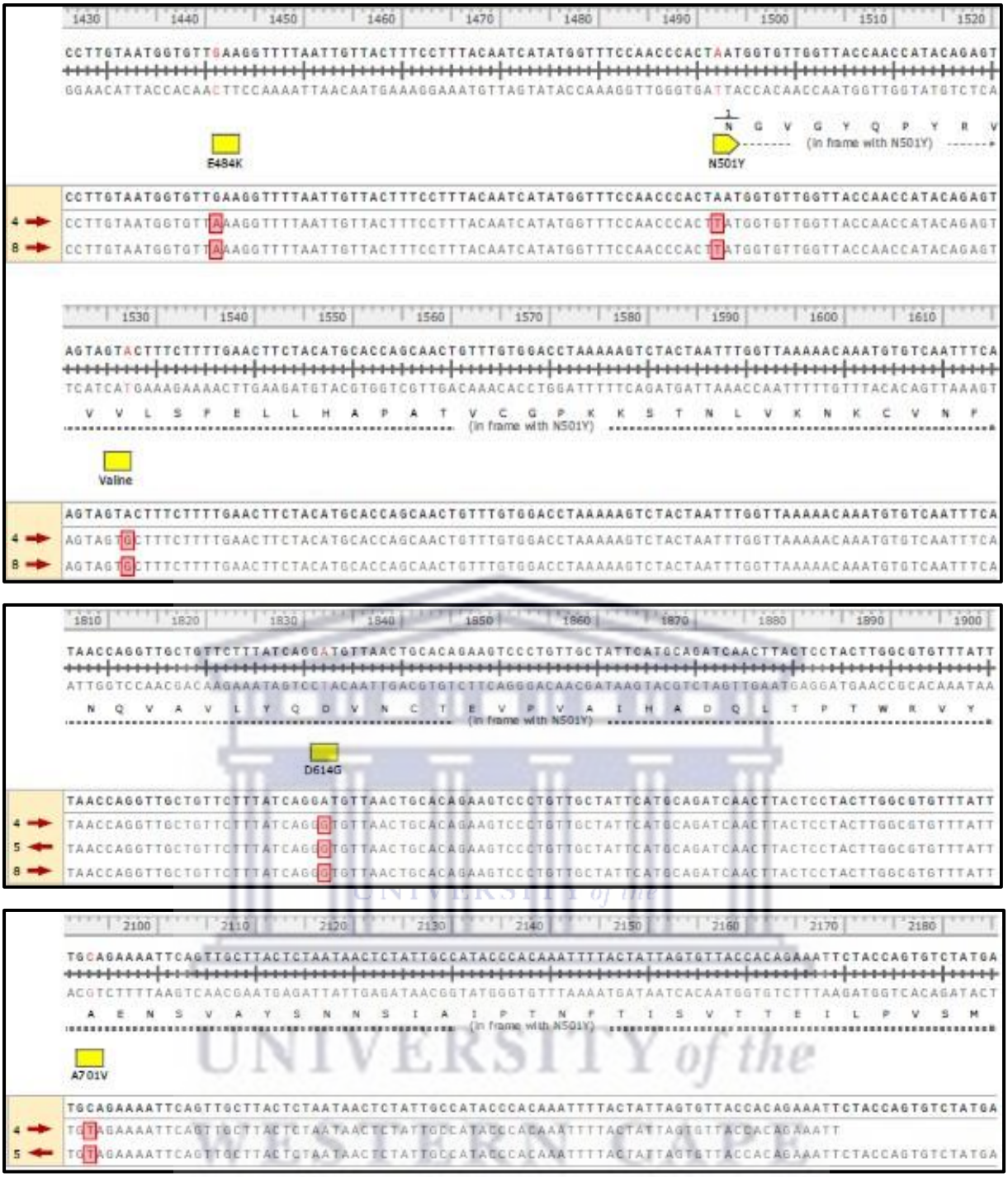

Figure 3.4 Alignment of the reference sequence for SARS-CoV-2 isolate Wuhan-Hu-1 (NC_045512.2) with the contigs generated from pCAGGS-spike ^{Beta} clone.

Table 3.1 Table of listed mutation detected in the clone of pCAGGS-spike [Beta].

Mutation	Genome position	Genome sequence	Amino acid position	Amino acid conversion
L18F	52	CTT-**T**TT	18	Leucine – Phenylalanine
D80A	239	GAT - G**C**T	80	Aspartic acid- Alanine
D215G	644	GAT - G**G**T	215	Aspartic acid - Glycine
K417N	1242	AAG - AA**T**	417	Lysine - Asparagine
E484K	1441	GAA - **A**AA	484	Glutamic acid - Lysine
N501Y	1492	TTA - T**A**T	501	Asparagine - Tyrosine
D614G	1833	GAT - G**G**T	614	Aspartic acid to Glycine
A701V	2193	GCA - G**T**A	701	Alanine to Valine

3.4. Expression and localisation of pCAGGS-spike ^{WT}-FLAG and pCAGGS-spike ^{Beta}FLAG

After cloning the SARS-CoV-2 spike gene into the mammalian vector pCAGGS, successful expression and localisation of the spike protein from pCAGGS-Spike ^{WT}-FLAG and pCAGGS-Spike ^{Beta} had to be confirmed. HEK-293T cells were transfected with plasmid DNA of pCAGGS-spike^{WT}-FLAG and pCAGGS-spike^{Beta} -FLAG. Cells were then fixed and permeabilised before adding mouse monoclonal ANTI-FLAG® M2 antibody to detect the FLAG epitope that was engineered onto the spike protein. Secondary antibody Goat anti-mouse Alexa Fluor Plus 488 (Thermo-Fisher Scientific, Catalogue No. A-10680) and DAPI were added before viewing the cells on a fluorescence microscope. As seen in Figure 3.5 no detection of the spike protein can be seen in cells transfected with pCAGGS-spike^{WT}-FLAG and pCAGGS-spike^{Beta} -FLAG. However, the positive control pCAGGS-KPNA4-FLAG showed positive staining, with KPNA-4 visible in the nucleus and perinuclear region.

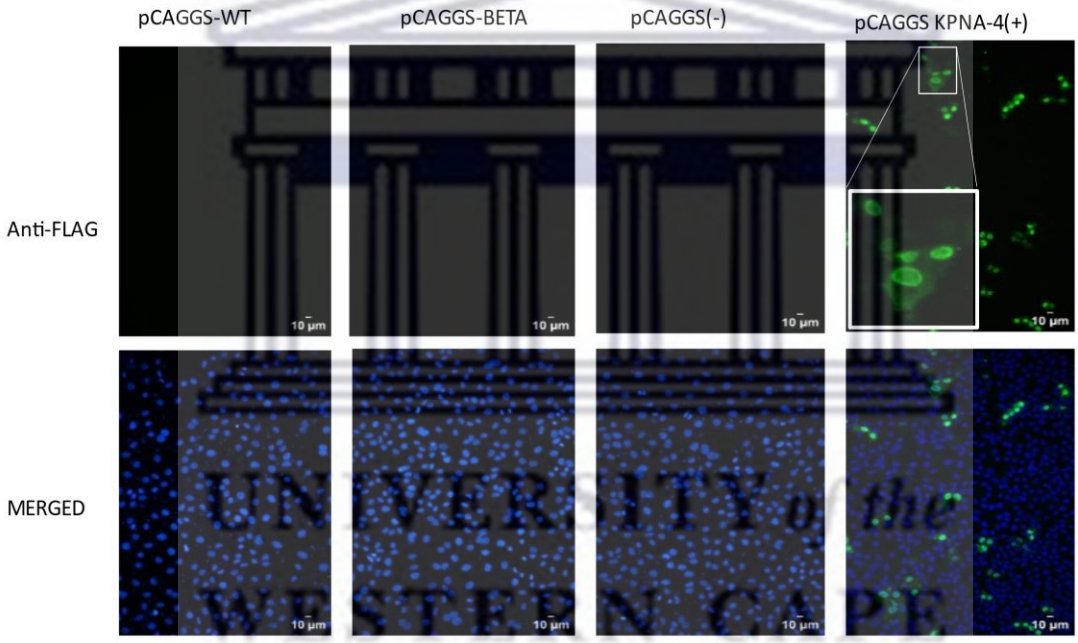

Figure 3.5 Expression and localisation of SARS-CoV-2 spike-protein using FLAG antibody. HEK293T cells were transfected with of pCAGGS-spike^{WT}-FLAG and pCAGGS-spike^{Beta} -FLAG or pCAGGS-KPNA4-FLAG. The expression of spike and KPNA4 proteins were detected with an anti-FLAG antibody and an Alexa Fluor 488 secondary antibody (green signal). Nuclei were visualised with DAPI staining (blue signal). Representative images captured by fluorescent microscopy are shown. Scale bars are indicated.

One potential explanation for why the spike protein was not being detected is that the FLAG epitope was hidden in the context of the folded protein, and therefore not accessible to the antiFLAG antibody. Thus, in a repeat experiment the transfected cells were probed with a SARSCoV-2 spike-specific antibody (Fig 3.6), but unfortunately no spike-specific signal was observed. A thorough investigation of the plasmid sequences could not provide a logical explanation for why no protein expression could be observed, as the spike ORF was intact and the FLAG sequence was in-frame. We reached out to Prof Penny Moore at NICD for assistance, and she kindly provided us with pcDNA3.1 plasmids encoding the SARS-CoV-2 spike gene from several variants.

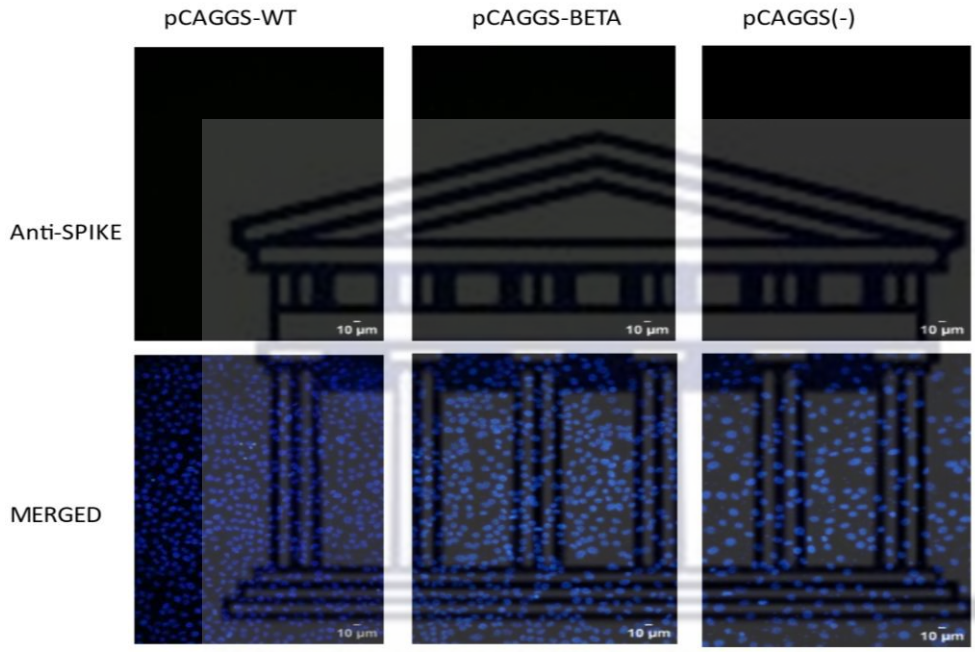

Figure 3.6 Expression and localisation of SARS-CoV-2 spike protein using SARS-CoV-2 spike antibody. HEK293T cells were transfected with, pCAGGS-spike^{WT}-FLAG and pCAGGS-spike^{Beta} -FLAG or empty pCAGGS. The expression of spike protein was detected with a SARS-CoV-2 spike S1 Subunit Antibody followed by probing with an Alexa Fluor 488 secondary antibody (green). Nuclei were stained with DAPI (blue). Representative images captured by fluorescent microscopy are shown. Scale bars are indicated

3.5. Validation of SARS-CoV-2 spike protein expression from the plasmids obtained from NICD

The NICD gifted us with pcDNA3.1 constructs encoding the spike genes of five variants – WT/D614G, Alpha, Beta, Delta, and Omicron (Table 3.2). A mutant form of the Omicron spike in which the C-terminal 18 residues had been deleted, were also received.

Table 3.2 The SARS-CoV-2 spike expression constructs received from NICD

Name of variant and sub-linage	Abbreviated names
Wild type-D614G	WT
B.1.1.7 Alpha	ALPHA
B.1.351 Beta	BETA
B.1.617.2 Delta	DELTA
B.1.1.529 Omicron	OMI-1
B.1.1.529 Omicron-d18	OMI-Δ18

All sub lineages of the variants are denoted in the table. Omi-d18 contains a deletion of the C-terminal 18 amino acid ER retention sequence for enhanced expression of SARS-CoV-2 spike protein on the cell surface.

To confirm that the SARS-CoV-2 spike ORF was cloned into the pcDNA 3.1 vector, a double restriction enzyme digest was performed using restriction enzymes *HindIII* and *ApaI* (Fig 3.7). The presence of bands at 5.4Kb and 3.4 Kb respectively indicated the vector and spike gene, respectively.

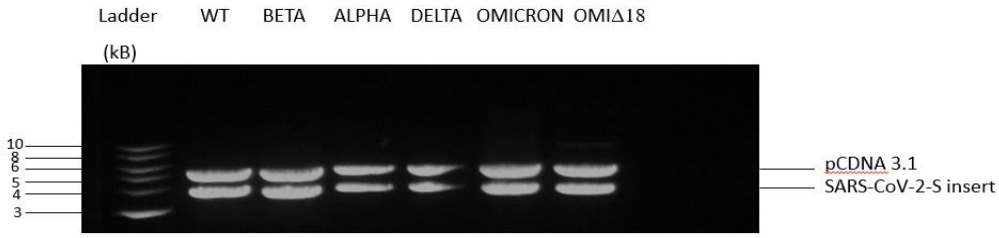

Figure 3.7 Confirmation of the presence of the SARS-CoV-2 spike gene in the plasmids obtained from NICD. Plasmid DNA was subjected to restriction enzyme digest with *HindIII* and *ApaI.* The bands representing the pcDNA 3.1 vector (5.4. Kb) and the SARS-CoV-2 spike gene (3.9Kb) are indicated.

To validate that the plasmid constructs were expressing the various spike proteins, HEK-293T cells were transfected with spike plasmids for WT and each variant (beta, alpha, delta and omicron). Cells were then fixed and probed with a specific SARS-CoV-2 S1 subunit monoclonal antibody and Alexa Fluor 488 secondary antibody. A green signal can be seen in the cytoplasm for all spike variants (Figure 3.8) with a pattern that likely represents the.ER/Golgi

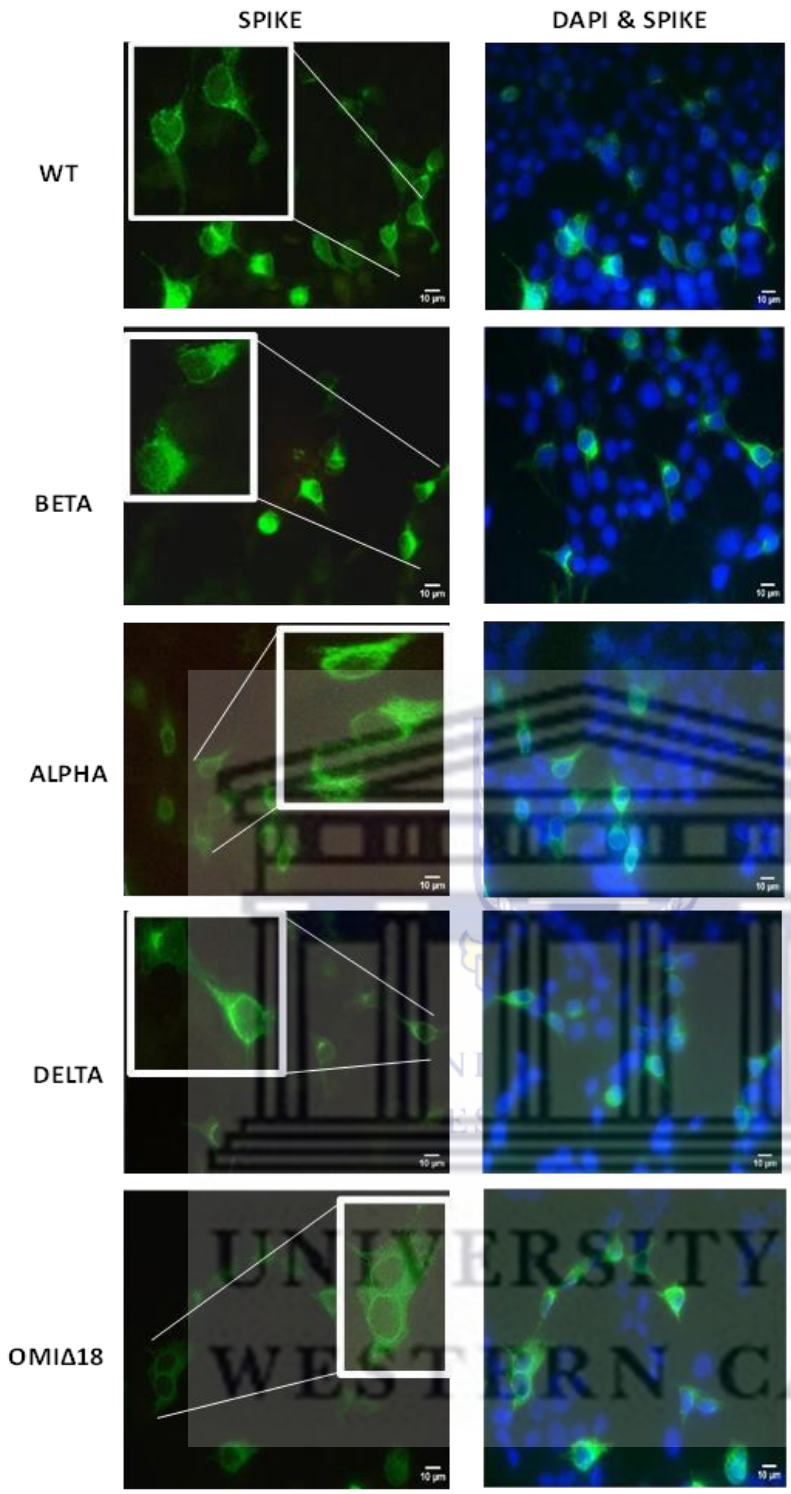

Figure 3.8 Detection and localization of SARS-CoV-2 protein. HEK293T cells were transfected with SARS-CoV-2 plasmids probed with a SARS-CoV-2 S monoclonal antibody specific to the S1 subunit and Alexa Fluor 488 secondary antibody(green). DAPI was used as a counterstain(blue). Scale bar 10µm

In order to verify the correct size of the spike protein, transfected cell lysates were run on an SDS-page gel before transferring proteins to a nitrocellulose membrane for immunostaining. An antibody raised against the S1 subunit of SARS-CoV-2 spike was able to detect the presence of the full-length spike protein (~180kDa) for all variants as indicated by the presence of a clear purple band (Fig 3.9).

Figure 3.9 Confirmation of SARS-CoV-2 spike expression by Western blot analysis. HEK293T cells were transfection with plasmids expressing SARS-CoV-2 spike protein from the indicated variants, and cell lysates were subjected to SDS-PAGE. The positive control is lysates from VeroE6 cells infected with SARS-CoV-2. The blot was probed with SARS-CoV-2 spike S1 Subunit antibody and an HRP secondary antibody. Visualization was done via colourimetric reaction. Protein ladders are shown on both sides of the gel.

3.6. Generation of VSV pseudoparticles bearing the SARS-CoV-2 spike protein

To produce SARS-CoV-2 spike-expressing pseudoparticles, the VSV packaging system was used. This system allows us to express the SARS-CoV-2 spike protein on the surface of the VSV particle. This VSV pseudoparticle system has been engineered so that it lacks expression of its own glycoprotein, G, and instead expresses a green fluorescence protein (GFP) and firefly luciferase (FLUc), which allow for downstream quantitative analysis SARS-CoV-2 spike proteins of WT and variants (beta, alpha, delta and omicron) were generated by transfecting HEK293T cells with the SARS-CoV-2 spike of interest, and then infecting the cells 24 hours later with the parent virus, VSV*ΔG(FLUc)(GFP) + (VSV-G). The pseudoparticles were harvested 24 hours later. To titrate the pseudoparticle (VSV-pp) stocks, each VSV-pp was serially diluted before adding HEK293T-ACE-2 cells. Infected cells were

incubated for 24 hours before measuring the luciferase activity (relative luciferase units) in the lysates (Fig 3.10). VSVpp-spike ^{ALPHA} generated the highest titre of $4.8x10^5$ RLU, followed by VSVpp-spike ^{WT} at $3.1x10^5$ RLU, VSVpp-spike ^{OMICRON} at $1.7x10^5$ RLU, with with the lowest values of $1.2x10^5$RLU and with the lowest values of $1.2x10^5$RLU and $7.8X10^4$ RLU respectively.

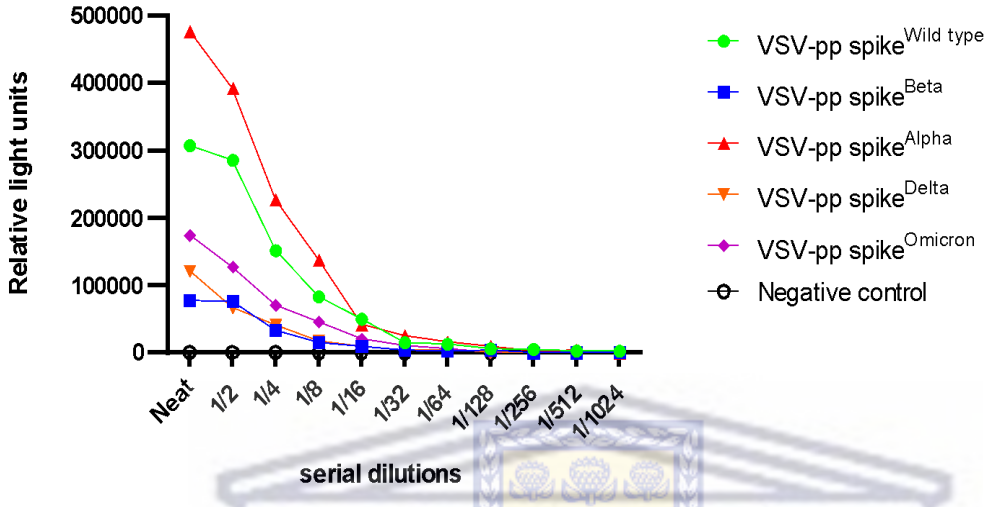

Figure 3.10 Titration of VSVpp-spike pseudoparticles in HEK293T-ACE-2 cells. Pseudoparticles were serially diluted (1:2) and incubated with HEK293T-ACE-2 cells for 24 hours. Luciferase activity was measured in cell lysates and expressed as relative luciferase units (RLU).

3.7. Optimisation of neutralization conditions using SARS-CoV-2 neutralizing human monoclonal antibodies

In the first step of optimising the neutralization assay, VSVpp-spike^{WT} was tested against a characterised SARS-CoV-2 neutralizing human monoclonal antibody, CA-1. This antibody has been shown to neutralize the SARS-CoV-2 wild type/D614G variant(Wibmer, et al. 2021). The CA-1 antibody was also titrated against VSVpp-VSV-G to control for specificity to the spike protein. A set amount of VSVpp-spike^{WT} or VSVpp-VSV-G was mixed with decreasing concentrations of CA-1, before adding HEK293T-ACE-2 cells and measuring luciferase activity 24 hours later. A clear dose-responsive neutralizing effect was observed for CA-1 vs. VSVpp-spike^{WT} with an IC_{50} of 600 ng/mL, but there was no activity observed for CA-1 vs. VSVpp-VSV-G (Fig 3.11). To ensure specificity, VSVpp-spike^{WT} was also tested against an unrelated antibody, HT103, which is specific for the influenza A virus nucleoprotein. No activity was observed for HT103 vs. VSVpp-spike^{WT} (Fig 3.11).

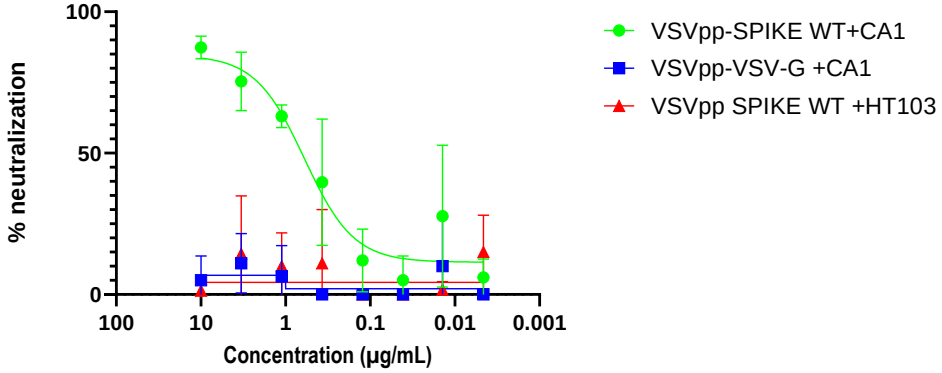

Figure 3.11 Neutralization of VSVpp-spike^{WT} and VSVpp-VSV-G by increasing concentrations of SARS-CoV-2 neutralizing monoclonal antibody, CA-1, or HT-103 antibody (anti-influenza A, nucleoprotein). The average percent neutralization (from 3 replicates) is shown +/- StdDev.

3.8. Neutralization of SARS-CoV-2 spike pseudoparticles using CA-1 antibody

Neutralization of VSVpp were tested against the human monoclonal antibody CA-1. CA-1 was discovered early in 2020 by researchers who isolated human monoclonal antibodies from a COVID-19 patient's convalescent plasma (Shi, et al. 2020). The antibody was tested against WT, Delta and Omicron pseudoparticles (Fig 3.12). In this experiment, reproducibility both within an assay, and between assays performed on separate days was also assessed. However, the CA-1 antibody was only able to neutralize the WT variant, with an IC_{50} of 2µg/mL.

(A)

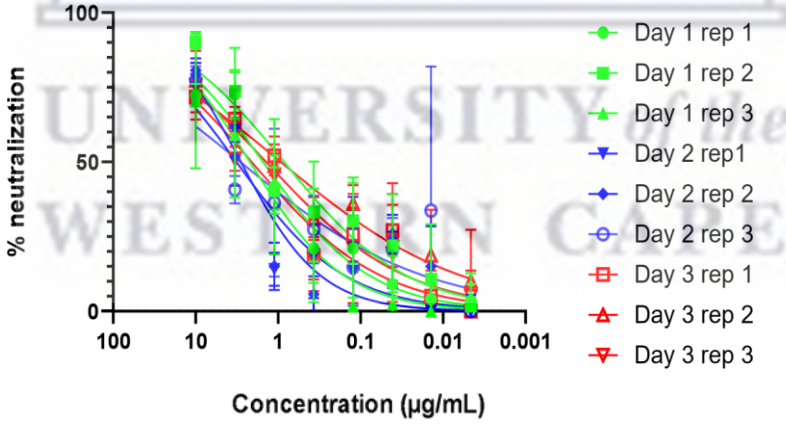

IC_{50}: 2 µg/mL

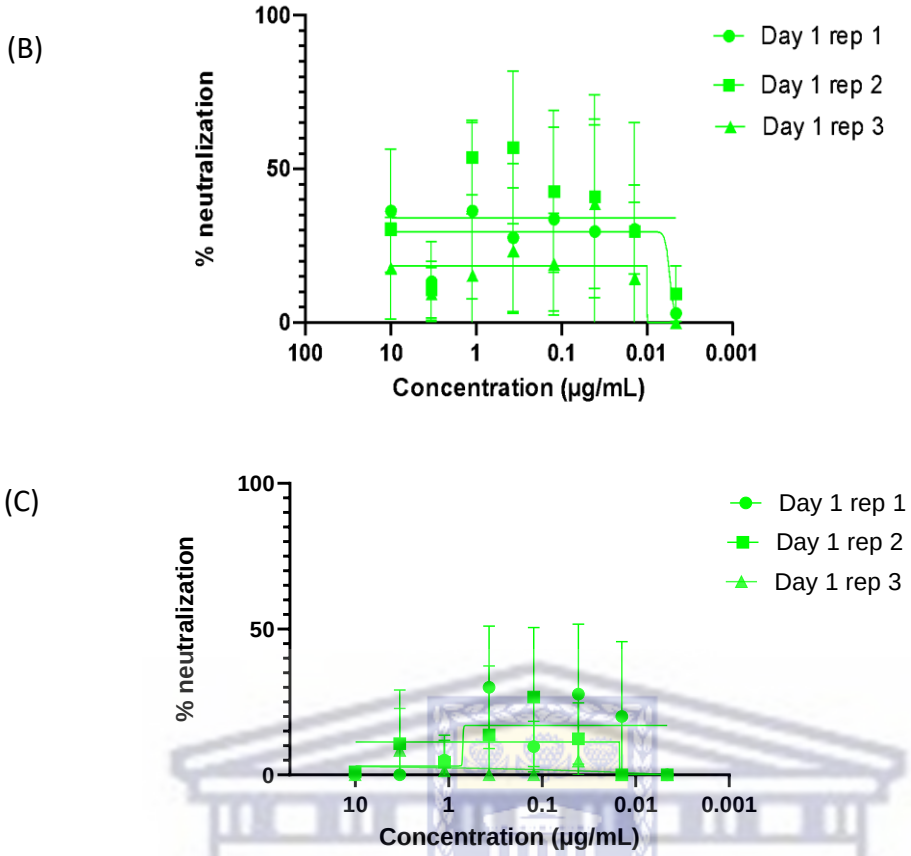

Figure 3. 12 Neutralization of SARS-CoV-2 spike pseudoparticles by CA-1 antibody. The neutralizing effect of CA-1 on (A) VSVpp-spike^{WT}, (B) VSVpp-spike^{DELTA}(C) VSVpp-spike^{OMI} expressed as percentage (%) neutralization. The assay was performed with 3 replicates, and on 3 separate days as indicated. Error bars represent StdDev, and the average IC_{50} value is shown.

3.9. Neutralization of SARS-CoV-2 spike pseudoparticles using CB-6 antibody

Thereafter, the neutralization effect of human monoclonal antibody CB-6 was assessed against pseudoparticles bearing the spike proteins of WT, Delta, and Omicron variants. CB-6 is a human monoclonal antibody isolated from a COVID -19 patient's convalescent plasma and it has been reported to neutralize SARS-CoV-2 *in vivo* and *in vitro* (Shi, et al. 2020). It is characterised as a class 1 RBD-targeting antibody and is able to prevent the interaction of ACE-2 receptors with the spike protein. The results show that CB-6 is able to neutralize both VSVpp-spike^{WT} and VSVpp-spike^{DELTA} generating IC_{50} values of 55.89 ng/mL and 19.33 ng/mL, respectively (Fig 3.13). The strongest neutralizing effect of CB-6 is seen against the Delta variant, being able to neutralize the virus at a third of the concentration needed for WT. No neutralizing effect was seen against VSVpp-spike^{OMI}.

(A)

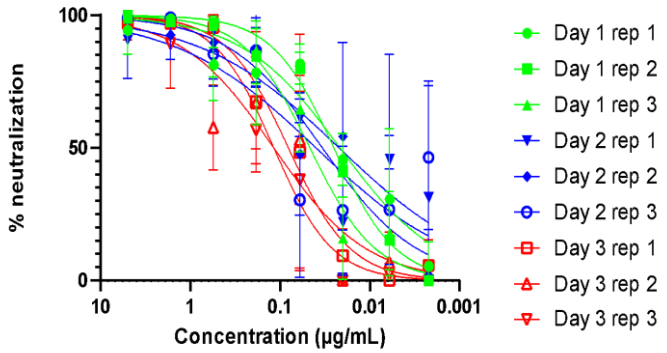

IC_{50}: 55.89 ng/mL

(B)

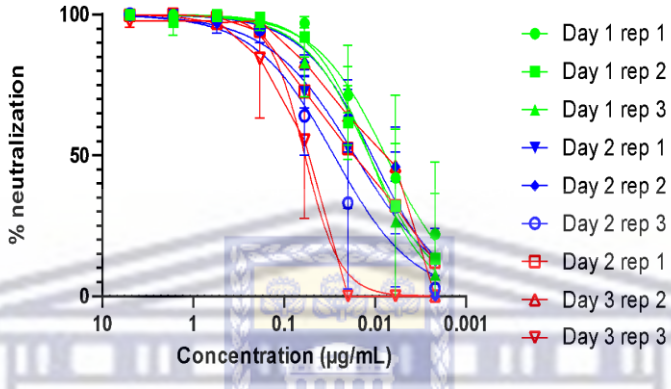

IC_{50}: 19.33 ng/mL

(C)

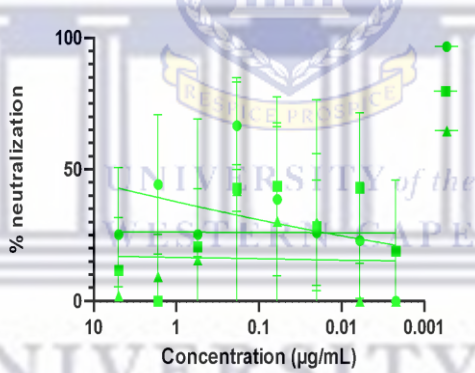

Figure 3. 13 Neutralization of SARS-CoV-2 spike pseudoparticles by CB-6 antibody. The neutralizing effect of CB-6 on (A) VSVpp-spike^{WT}, (B) VSVpp-spike^{DELTA}(C) VSVpp-spike^{OMI} expressed as percentage (%) neutralization. The assay was performed with 3 replicates, and on 3 separate days as indicated. Error bars represent StdDev, and the average IC_{50} value is shown.

3.10. Neutralization of SARS-CoV-2 spike pseudoparticles using the 084-7D antibody

Neither CA-1 nor CB-6 showed activity against the Beta variant (data not shown). So, to validate VSVpp-spike ^{BETA} in the neutralization assay, the human antibody 084-7D was used. This antibody was isolated from a patient infected with the beta variant of SARS-CoV-2 which possesses the amino acid mutation K417N. 084-7D targets the N417 mutation and has shown neutralization potency similar to the convalescent plasma (Moyo-Gwete, et al. 2022). Reproducible neutralization of VSVpp-spike ^{BETA} by 084-7D was observed, with an IC_{50} of 71 ng/mL (Fig 3.14), whereas the study conducted by Moyo-Gwete et al. (Moyo-Gwete, et al. 2022) observed an IC_{50} of 100 ng/mL.

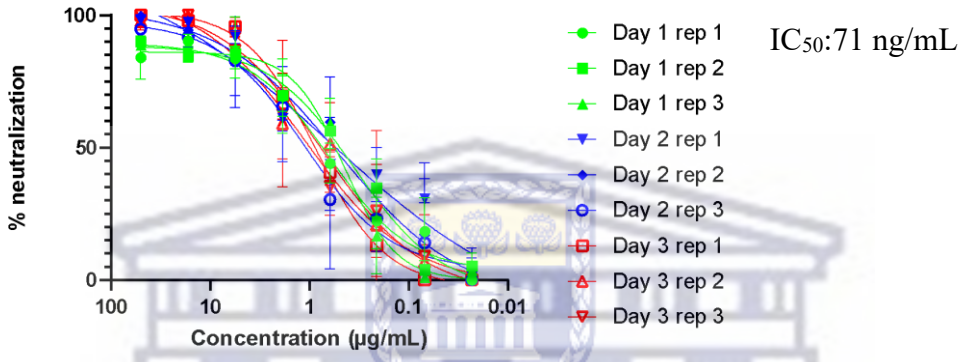

Figure 3. 14 The neutralization activity of 084-7D on VSVpp-spike^{BETA} expressed as % neutralization. The assay was performed with 3 replicates, and on 3 separate days as indicated. Error bars represent StdDev, and the average IC_{50} value is shown.

3.11. Neutralization of SARS-CoV-2 spike pseudoparticles using Bebtelovimab antibody

As the CA-1, CB-6, and 084-74 antibodies did not display neutralization activity against the Omicron variant, a fourth antibody was required to validate VSVpp-spike^{OMI} in the neutralization assay. Bebtelovimab (LY-CoV1404) is a human monoclonal antibody first detected in a B-cell high throughput screening assay. LY-CoV1404 is another RBD-specific binding antibody but according to research, the antibody binds to epitopes in domains that are less susceptible to mutation (Greaney, Loes et al. 2021). Wild type, Beta, Delta, and Omicron pseudoparticles, were all neutralized by Bebtelovimab (Fig 3.15). Comparable IC_{50} values of around 4 ng/mL were obtained for WT, Beta, and Omicron variants, while the IC_{50} for the Delta variant was slightly higher at 10.62 ng/mL.

(A)

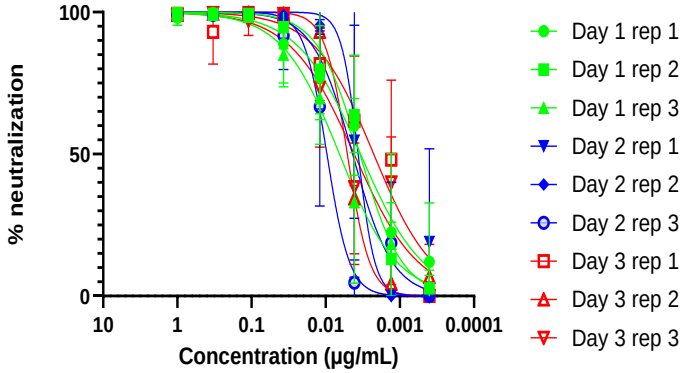

IC_{50}: 4.86 ng/mL

(B)

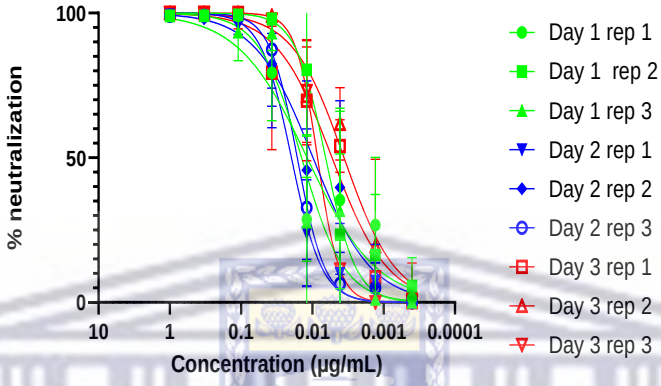

IC_{50}: 10.62 ng/mL

(C)

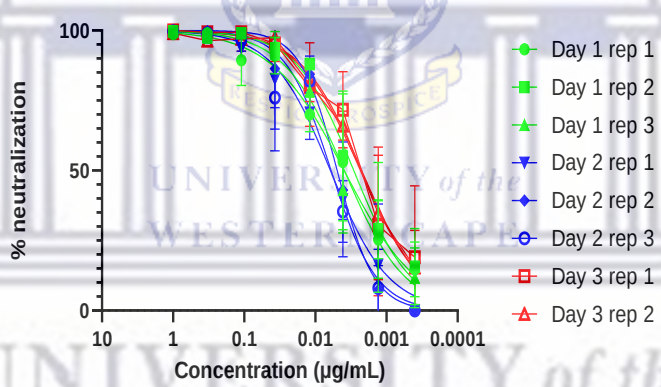

IC_{50}: 4.04 ng/mL

(D)

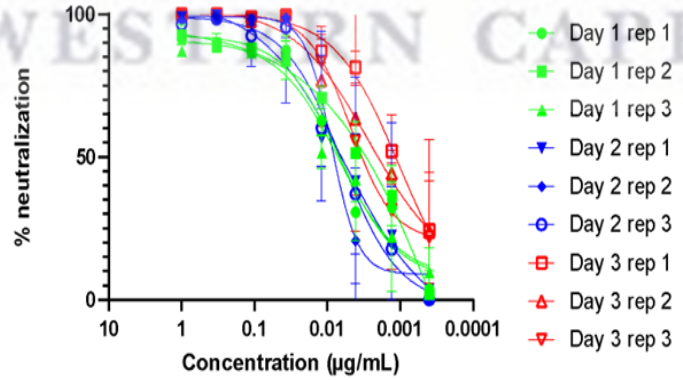

IC_{50}: 4.78 ng/mL

Figure 3. 15 Neutralization of SARS-CoV-2 spike pseudoparticles by Bebtelovimab antibody. The neutralizing effect of Bebtelovimab on (A) VSVpp-Spike^{WT}, (B) VSVpp-spike^{DELTA}, (C) VSVpp-spike^{OMI}, and (D) VSVpp-spike^{BETA} expressed as percentage (%) neutralization. The assay was performed with 3 replicates, and on 3 separate days as indicated. Error bars represent StdDev, and the average IC50 value is shown.

Table 3. 3 Summary of IC_{50} of VSVpp^{VARIANTS} against human monoclonal antibody in ng/mL

	VSVpp-spike ^{WT}	VSVpp spike^{BETA}	- VSVpp spike ^{DELTA}	VSVpp spike^{OMICRON}
CA-1	2000			
CB-6	55.9		19.33	
084-79		70		
Bebtelovimb	4.86	4.78	10.62	4.04

3.12 Validation of the SARS-CoV-2 neutralization assay with sera from COVID-19 patients

To validate the VSV-based SARS-CoV-2 neutralization assay with human serum, I tested 9 serum samples collected from COVID-19 patients during the different (most prevalent variants of concerns) waves of infection experienced in South Africa. These same sera had been tested by Prof Penny Moore's lab at NICD in their lentivirus-based SARS-CoV-2 neutralization assay, but they were blinded so I did not have any information on them besides their code name and the wave in which the sera were collected. For ease of use, I numbered them 1-9 (Table 3.4).

Table 3. 4 Table showing the sera samples and the corresponding NICD sera sample codes.

Sera sample number	NICD sera sample code	Wave of infection sera collected in
Sample 1	COV-186	4
Sample 2	COV-140	4
Sample 3	COV-158	4
Sample 4	COV-109-V1	3
Sample 5	SA-01-0079	2
Sample 6	COV-004	1
Sample 7	COV-183	4
Sample 8	COV-111-V1	3
Sample 9	COV-189	4

Before use, the serum samples were heat inactivated to destroy the complement factors. Each sample was then serially diluted before adding the respective pseudoparticles (WT, Beta, Delta, Omicron) for each experiment. HEK-293T-ACE-2 cells were added to the pseudoparticle-sera mixture and incubated for one hour before reading luciferase activity using a luminometer. This was done in replicates for each sera sample. Statistical analysis was done and normalised data were plotted to a sigmoidal dose response curve using GraphPad Prism. To interpret the neutralizing activity of the sera the inhibitory dose 50 (ID_{50}) was determined. The ID_{50} is the reciprocal of the serum dilution that causes 50% inhibition of the virus, and a high ID_{50} indicates a high level of neutralizing antibody activity in the sera. The baseline ID_{50} is 20, which is indicative of no neutralization occurring.

The data obtained with VSVpp-spike^{WT} (Fig 3.16), VSVpp-spike^{Beta} (Fig 3.17), VSVppspike^{Delta} (Fig 3.18), and VSVpp-spike^{Omicron} (Fig 3.19) are shown. With VSVpp-spike^{WT} samples 7 and 2 produced the highest ID values of 448 and 116, respectively. Samples 1 and 6 also produced ID_{50} above the threshold of detection at 40 and 41, respectively, whereas, samples 3,4,5,8 and 9 produce no neutralization (Fig 3.16)

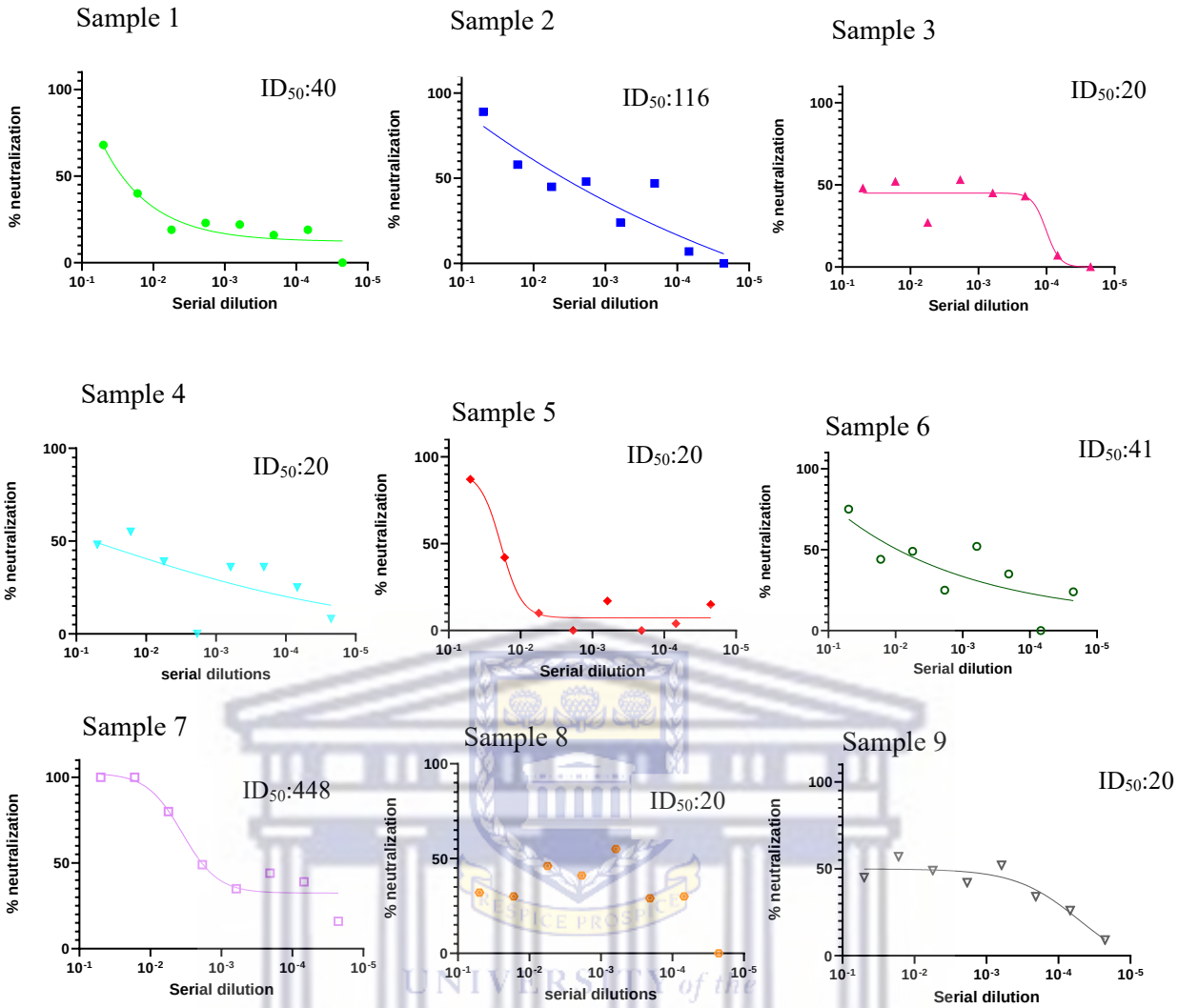

Figure 3.16 Neutralization of VSVpp-spike^{WT} by serum samples 1-9. The percent neutralization relative to the dilution of serum is shown as a best fit curve for each sample. Data points represent the average of duplicates. The ID_{50} for each sample is indicated

The sera were also tested against VSVpp-spike^{BETA} and samples 7, 8, and 9 showed the highest levels of neutralization with ID_{50} values of 389, 5073, and 417, respectively (Fig 3.17). Low neutralization activity was observed for samples 1 and 3 with ID_{50} values of 82 and 33, respectively. No neutralizing antibodies were detected in samples 2, 3 ,4, and 6.

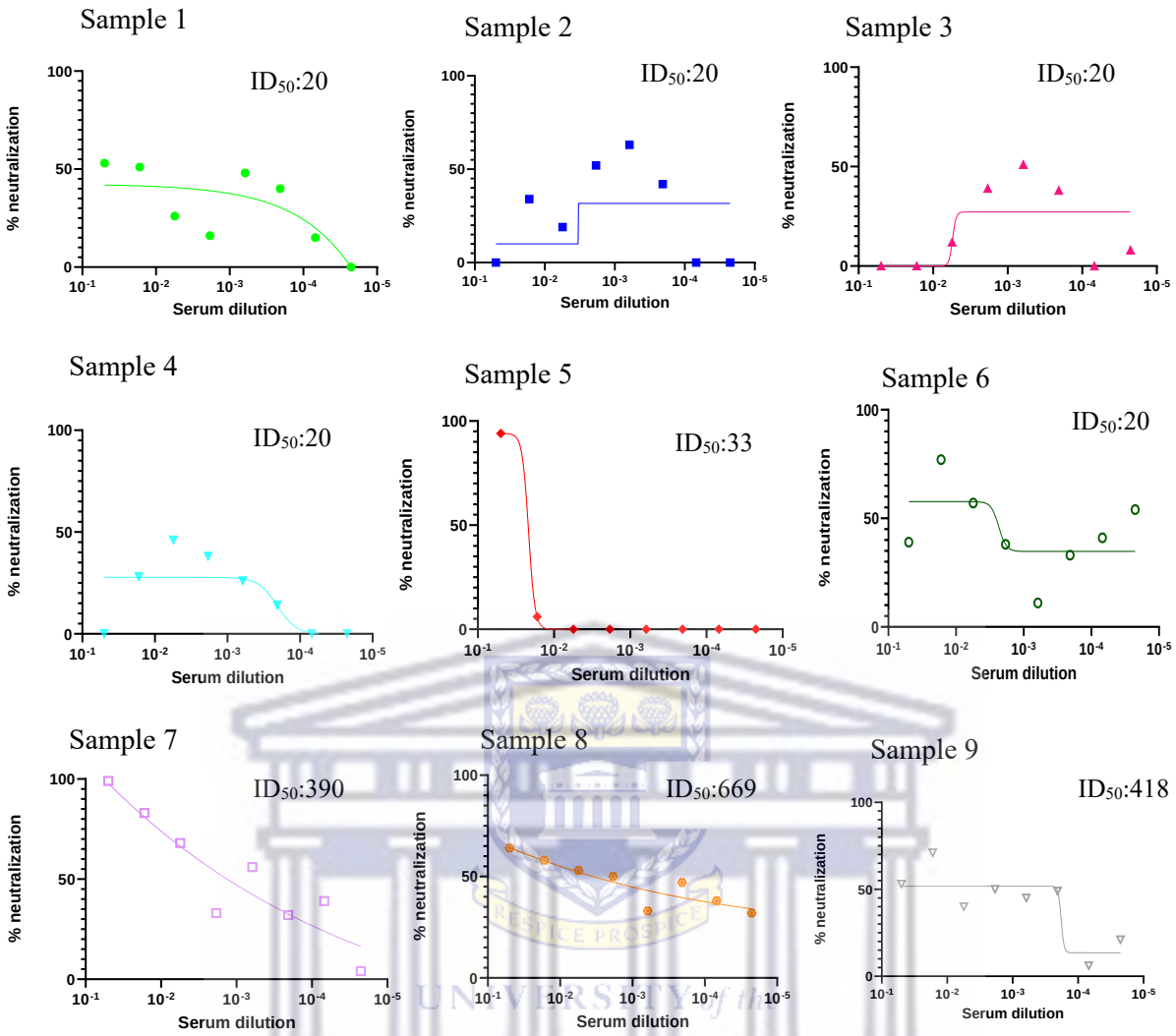

Figure 3. 17 Neutralization of VSVpp-spike^{Beta} by serum samples 1-9. The percent neutralization relative to the dilution of serum is shown as a best fit curve for each sample. Data points represent the average of duplicates. The ID_{50} for each sample is indicated

For VSVpp-spike^{Delta} samples 7 and 2 showed the highest neutralization activity with ID_{50} values of 18603 and 87, respectively (Fig 3.18). Sample 8 displayed low activity with an ID_{50} of 29, whereas samples 1, 2, 4, and 9 showed no neutralization.

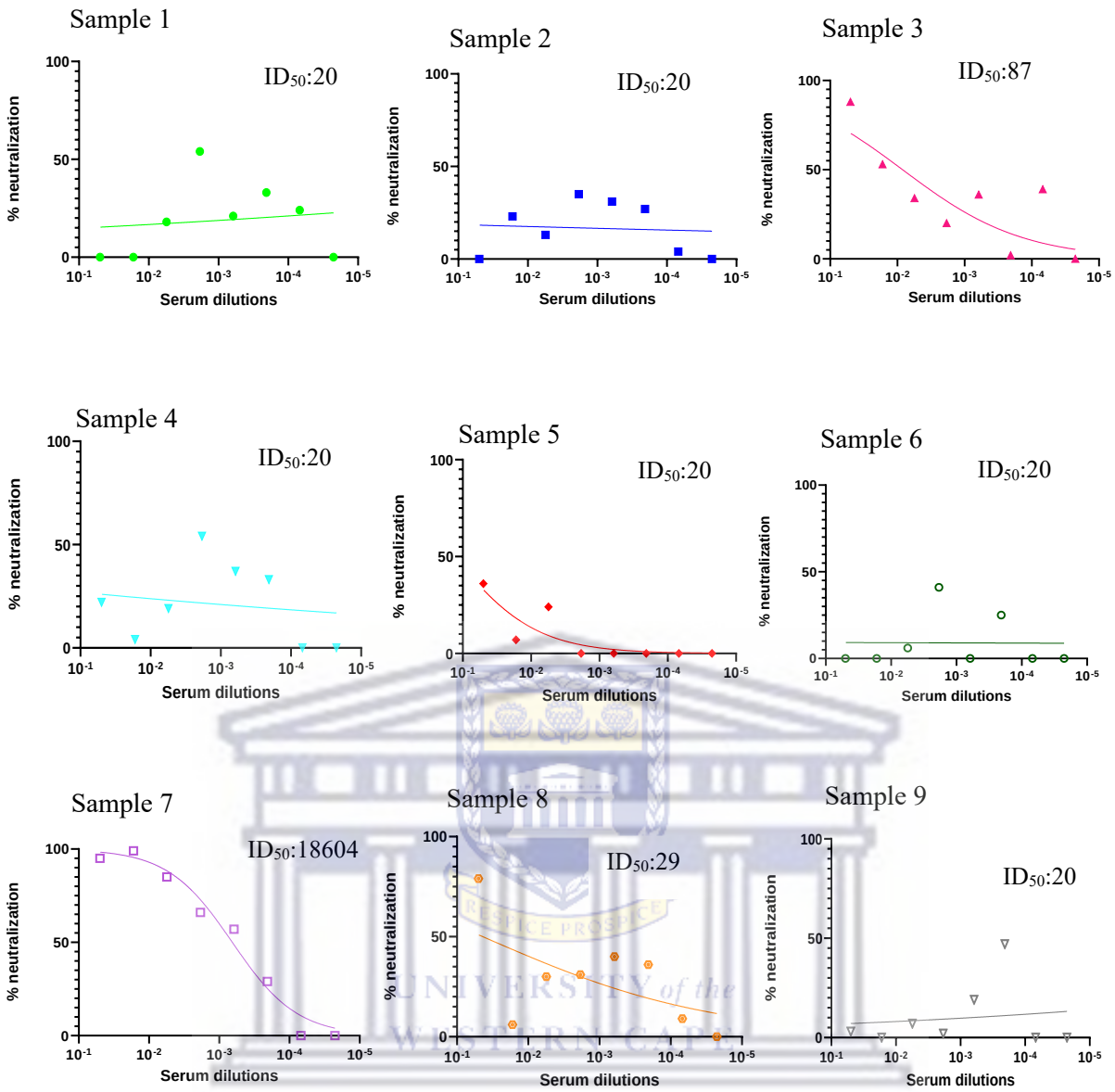

Figure 3.18 Neutralization of VSVpp-spike^{Delta} by serum samples 1-9. The percent neutralization relative to the dilution of serum is shown as a best fit curve for each sample. Data points represent the average duplicates. The ID_{50} for each sample is indicated

Finally, the sera were tested against VSVpp-spike^{Omicron} (Fig 3.19). Serum samples 1, 2, 3, 7, and 9 displayed high ID_{50} values of 1030, 2431, 5850, 13727, and 836, respectively. Sample 5 showed low neutralization activity with a ID_{50} of 52, while no neutralization activity was seen in samples 4, 6, and 8.

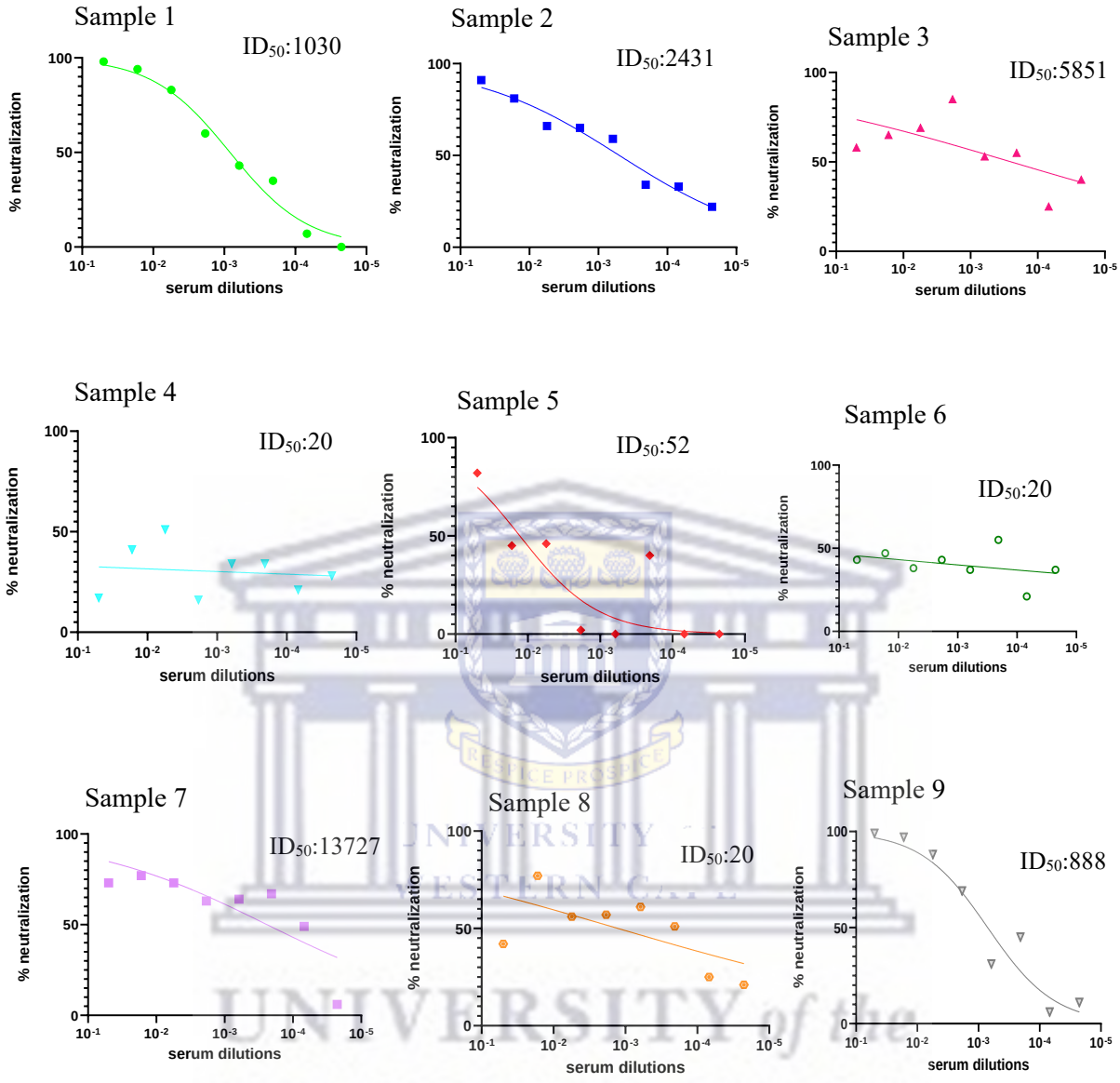

Figure 3.19 Neutralization of VSVpp-spike^{Omicron} by serum samples 1-9. The percent neutralization relative to the dilution of serum is shown as a best fit curve for each sample. Data points represent the average of duplicates. The ID_{50} for each sample is indicated

To compare the data generated above in Figure 3.16 to 3.19, a dot plot of the ID50 values was generated (Fig 3.20) allowing visualisation of the relative neutralization activities of the sera against each SARS-CoV-2 variant.

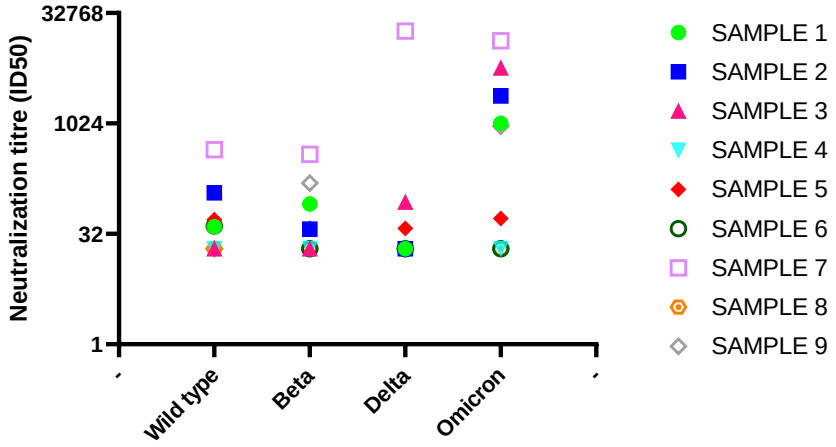

Figure 3.20 Dot plot of the ID50s of each serum sample tested against the WT, Beta, Delta, and Omicron variants of VSVpp-spike.

Each shape represents an individual patient serum tested against the VSV-pp^{SPIKE} variants. Any values below 20 were assigned an arbitrary value of 20 as a baseline value.

3.13 Comparison of neutralization activities obtained using the VSV or lentivirus SARS CoV-2 neutralization assays

The neutralization titres obtained for the 9 sera using the VSV-based assay were then compared to the data obtained for the same sera using the lentivirus-based assay (these data were supplied by Prof Penny Moore, NICD). The purpose of comparing the ID_{50} values is to determine if there is concordance between the two pseudoparticle systems used for the neutralization assays. Neutralization titres obtained with the VSV system (UWC) are shown in blue, and those for the lentivirus system (NICD) are shown in orange (Fig 3.21).

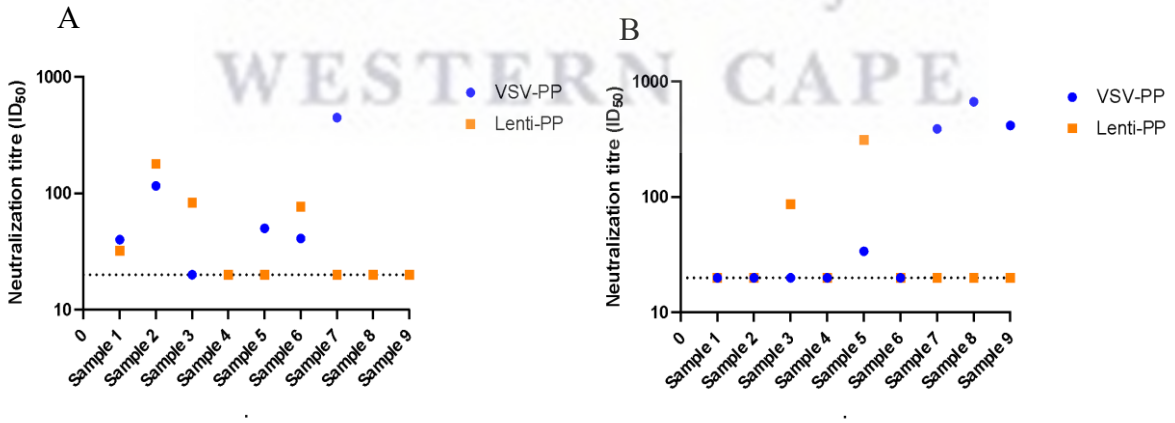

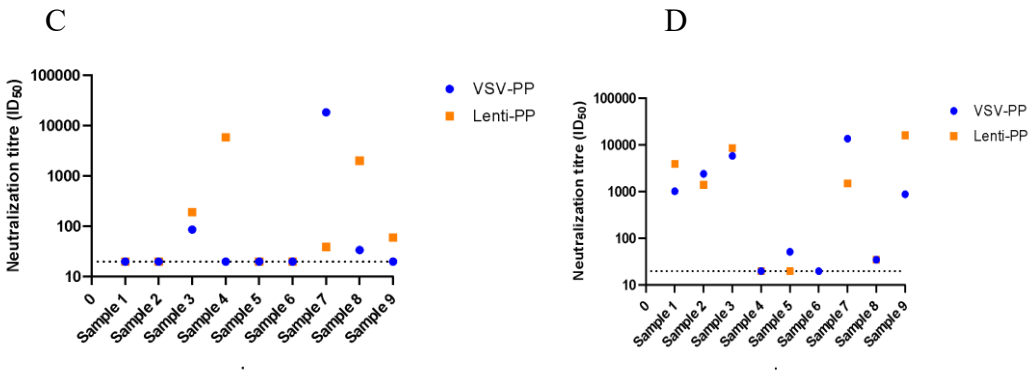

Figure 3.21 Comparison of VSV- or lentivirus-based SARS-CoV-2 neutralization data. ID50 data for n=9 sera tested with either the VSV (blue) or the lentivirus (orange) SARS-CoV-2 neutralization assays are shown for each variant. (A) WT, (B) Beta, (C) Delta, and (D). The dotted line represents the minimum ID_{50} value of 20.

Chapter 4: Discussion

The sudden emergence of SARS-CoV-2 highlights the significance of zoonotic viral infections and their ability to cause devastating effects, not only on local public health, but on a global scale (Morens and Fauci 2020). Reports suggest that SARS-CoV-2 highly likely originated in the bat species *Rhinolophus* but there is still much speculation over which animal served as an intermediary host and was able to transmit the virus to the human population. Identifying the intermediatory host is important as this may help curb the transmission of the virus and also help scientists investigate the mechanism of cross species transmission (Nova 2021).

After early investigation showed that SARS-CoV-2 spike protein had a high affinity for ACE2 expressing cells (Huang, et al. 2020), researchers started studying the virus entry mechanisms into host cells and exploiting this as an avenue for vaccine development and potential therapeutic treatment. A rapid accumulation of mutations in the spike glycoprotein has seen an influx of variants of concern (VOC) from all across the world. As more SARS-CoV-2 spike variants emerged, this put more pressure on scientists to create vaccines and antiviral treatments that would effectively target all variants.

Due to the pathogenicity, all studies of SARS-CoV-2 that use live virus are limited to BSL-3 facilities which are scarce and require skilled personnel. To circumvent this obstacle, the pseudoparticle system has been developed as a means to study viral entry mechanisms while mitigating the risk of infection. In this study I generated SARS-CoV-2 spike expressing pseudoparticles using the VSV packaging system, and successfully produced pseudoparticles expressing the spike proteins of SARS-CoV-2 Wild Type/D614G and Beta, Delta and Omicron VOCs. Furthermore, I quantified the neutralizing effect of human monoclonal antibodies against the abovementioned pseudoparticles, and these was used as a standard for the establishment of a neutralizing assay to test the potency of convalescent patient sera against VSV-spike pseudoparticles.

Cloning and expression of the SARS-CoV-2 spike proteins were an essential first step towards generating the VSV-spike pseudoparticles. However, even though clones of pCAGGS-spike^{WT} and pCAGGS-spike^{Beta} were verified through double restriction enzyme digest, and through Sanger sequencing, no expression of spike^{WT} or spike^{Beta} could be observed from these constructs. One explanation for this could be due to conformational folding of the protein masking the FLAG epitope that was added to the C-terminus. Perhaps inserting a 3xFLAG tag or repositioning of the FLAG tag to the N-terminus might increase the likelihood of detection. However, this hypothesis might not be valid as expression was also tested using a SARS-CoV2 anti-spike antibody, and there was still no protein detected. It is possible that there was

something wrong with the promoter region in the pCAGGS plasmid vector, so another alternative could be to clone the spike ORF into an alternative expression vector such as pcDNA3.1. In the interest, of time, I obtained SARS-CoV-2 spike plasmids from Prof Penny Moore at the National Institute for Communicable Disease (NICD) and I used these to successfully generate spike-expressing VSV pseudoparticles. Prof Moore and Dr Craig Fenwick (Lausanne University Hospital, Lausanne, Switzerland) also kindly provided human monoclonal antibodies that are known to have SARS-CoV-2 neutralizing activity which I was able to use as positive controls. This not only validated that my pseudoparticles were in fact expressing spike proteins on the surface but also provided us with information regarding the neutralizing potency of the antibodies against the respective spike variants.

CA-1 and CB-6 antibodies were some of the first neutralizing antibodies found in human plasma in early 2020, with CA-1 displaying weaker potency than CB-6 (Shi, et al. 2020). I demonstrated that CA-1 antibody was only able to neutralize the wild type variant at an IC_{50} value of 2µg/mL, whereas CB-6 was able to neutralize the wild type variant at an IC_{50} 40 times lower than CA-1 (shown in Fig 3.12 A and Fig 3.13B). This corresponds with data published by (Zhou, et al. 2022) using SARS-CoV-2 spike lentivirus pseudoparticles to test neutralization potency of human monoclonal antibodies against VOC. Even though the assay used to measure neutralization was different, the IC_{50} values are similar to the values from my study (Zhou, Wang et al. 2022). CB-6 was able to neutralize the wild type variant with an IC_{50} of 50.5 ng/mL in their study compared to an IC_{50} of 55.89 ng/mL in my study. CB6 is also able to neutralize the delta variant with an IC_{50} of 19.33 ng/mL which is very similar to the IC_{50} of 14.8 ng/mL obtained by Zhou *et al*. The epitope that is bound by CB-6 is highly mutated in the Beta and Omicron variants (Cao, et al. 2023), which explains the lack of neutralization activity against the Beta and Omicron spike pseudoparticles. Cheng *et al*. (Cheng, et al. 2022) suggests this might be due to one key residue mutation, K417N, decreasing the binding affinity of CB-6.

The antibody, 084-7D, was the control used to neutralize Beta pseudoparticles, and produced an IC_{50} of 71ng/mL which is similar to the IC_{50} value of 100 ng/mL reported by Moyo-Gwete *et al.* (Moyo-Gwete, et al. 2022). Data on this neutralizing antibody are very limited due to the short-lived dominance of the Beta variant in countries other than South Africa and France.

Bebtelovimab was the antibody with the most potent and broadest neutralizing effect. It was able to neutralize all WT, Beta, Delta, and Omicron pseudoparticles with IC_{50} values ranging from 4-10ng/mL. This correlates with a number of studies such as Westendorf *et al*. (Westendorf, et al. 2022) who also reported IC_{50} values for Bebtelovimab against the above-mentioned variants ranging from 2-5 ng/mL in a VSV-pseudoparticle system. Syed *et al*. (Syed,

et al. 2022) conducted a similar experiment but used virus-like particles (VLP) and generated IC_{50} for Bebtelovimab of <10ng/mL for both Delta and Omicron. Similar results were also found by Zhou *et al*. (Zhou, et al. 2022) using lentivirus pseudoparticles for Wild Type, Beta, Delta, and Omicron with IC_{50} values ranging from 3-5 ng/mL. Together these results support the significant efficacy and potency of Bebtelovimab and also the validate the spik-pseudoparticles that I produced. In a phase 2 clinical trial (Gottlieb, et al. 2021), patients with mild-to-moderate COVID-19 were treated with Bebtelovimab on its own or in combination of Bebtelovimab, Bamlanivimab and Etesevimab (CB-6) which were delivered via slow intravenous push (Dougan, et al. 2022). The results showed significant viral clearance and reduction in symptom resolution. But despite this success, on the 10th of November 2022, the FDA ended its emergency authorization of Bebtelovimab due to resistance observed with a number of omicron subvariants (BQ.1, BQ1.1, BJ.1, XBB, BR.1, CH.1.1 and BA.4.6.3) circulating in the USA (Cao, et al. 2023). And since the BQ.1 and BQ1.1 variants accounted for >50% of COVID-19 cases (Ma 2023), the usefulness of Bebtelovimab was limited. This highlights the struggle of antiviral therapy development in the face of constant evolution of viruses that may render the drug or antibody useless if resistance develops. (Strasfeld and Chou 2010)

As we have observed, the development of a successful vaccine is crucial for being able to control a pandemic. As part of this process, the ability to detect neutralizing antibodies is an extremely useful tool in vaccine development (Pang, et al. 2021). It is important to gather data on the levels of protective neutralizing antibodies that are elicited upon vaccination, and for how long these levels are sustained. The ability to detect neutralizing antibodies in convalescent sera is also important for seroprevalence studies (Khoury, et al. 2021). In South Africa there is a high incidence of comorbidities such as HIV and TB which increases the risk of COVID-19 disease severity and fatalities (Tolossa, et al. 2021). Therefore, seroprevalence studies in populations like South Africa is important to identify vulnerable people and prioritize them for vaccination if their neutralizing antibodies are below the protective threshold.

Choosing an appropriate pseudoparticle packaging system is also of utmost importance, with the most popular systems being VSV, MLV and lentivirus. It has also been reported that sera from HIV patients on antiretroviral therapy (ART) may also cause false positives. This could be due to the inhibitory effect of the compounds found in ART on the replication machinery of the HIV-based pseudovirus (Garcia-Beltran, et al. 2021, Huang, et al. 2021, De La Torre-Tarazona, et al. 2023) Consequently, this could can bias the results as it may cause an overestimation in neutralization titres. This is particularly concerning for Africa as the WHO

reported more than 68% of individuals living with HIV from the African continent and 7.52 million of those people reside in South Africa. Interference with the readouts of neutralization activity impede the accuracy and efficacy of data which may form the basis for major public health decisions.

Additionally, the generation of VSV pseudoparticles is also less time consuming. The VSV system requires the spike expressing plasmid to be transfected into permissive cells in suspension on day 1, followed by infection with the carrier virus VSV*ΔG(FLUc)(GFP) on day 2, and then collection of the pseudoparticles in the supernatant on day three, so taking a total of three days to generate. In contrast, the generation of lentivirus pseudoparticles requires cells to be seeded in a monolayer before co-transfecting the cells with multiple plasmids for 24 hours. Thereafter, cells incubate for a further 48-72 hours before collection of the pseudoparticles. From start to finish this requires 5-6 days to generate.

To validate my VSV-based neutralization assay for SARS-CoV-2, I received a set of 9 blinded sera from Prof Penny Moore's lab that had previously been assayed with their lentivirus-based SARS-CoV-2 neutralization assay. The sera were from COVID-19 patients that had experienced an infection in either wave 1 (WT/D614G), wave 2 (beta), wave 3 (delta) or wave 4 (omicron) of the pandemic in South Africa. I observed strong concordance between the neutralizing titres (ID_{50} values) from the lentivirus vs the VSV system for the WT and omicron variants. However, there were discrepancies observed for the beta and delta variants between the lentivirus, and the VSV system. The reasons for this are not exactly clear. We could theorize that sample 4 (COV-109-V10 and sample 8 (COV-111-V1), which showed high neutralizing titres against Delta in the lentivirus assay, but low in the VSV assay, could possibly have come from HIV positive patients on ART. Thus, the ID_{50} values might be elevated in the lentivirus assay due to non-specific antibody neutralization occurring. This could be a similar explanation for sample 5 which showed a neutralization titre 10 times higher with the delta lentivirus pseudoparticles than the delta VSV pseudoparticles. The problem with this theory is that if this was the case, the titres obtained with the sera should have been elevated across all variants, not just Delta.

Sample 7 (COV-183), which was collected during the Omicron wave, generated positive activity across all variants in the VSV system. After much speculation an article by Richardson *et al*. (Richardson, et al. 2022) may have provided a possible explanation. The study showed that vaccinated individuals who subsequently become infected with the Omicron variant have elevated levels of cross-neutralization, thus increasing the overall neutralizing titres observed with the Wild type, Beta, and Delta variants. Furthermore Khan *et al.* (Khan, et al. 2022) stated

that vaccinated individuals infected with Omicron can show increase neutralization activity against the Delta variant. This corresponds with the variability and elevation of neutralization titres for sample 7(COV-183) that I observed, however the same was not seen with the lentivirus system. One can make an inference that the sera collected from the patient was most likely a vaccinee who contracted the omicron variant of SARS-CoV-2. This could suggest that the VSV packaging system might more sensitive and specific to neutralization than a lentivirus system. In fact, Steeds et al. (Steeds et al. 2020), who tested pseudotyped particles expressing the Ebola virus glycoprotein, reported that the VSV system was more sensitive for detecting Ebola virus neutralizing activity than a lentivirus system.

Another explanation for the increase in ID_{50} values for sample 7 could be that the patient developed anti-VSV antibodies, as the virus is most commonly found in farm animals. Occupational interaction with farm animals such as a veterinarian or farm worker who contracted the VSV and then later contracted the omicron-variant of SARS-CoV-2. This could be an explanation for the elevated neutralization titres. However, the likelihood for this occurrence is low as VSV is endemic to the western hemisphere (Rozo-Lopez, et al. 2018). Which indicates the patient would have needed to travel countries in South and North America and have contracted a VSV infection before travelling back to South Africa and contracting SARS-CoV-2 omicron variant.

Limitations of the study

This study had certain limitations that need to be considered when interpreting the findings. One of the limitations include the availability of only a small sample size of sera from patients. The NICD provided only one sera sample for the wild type and beta variant and two samples for the delta variant, for testing purposes. If the sample size is too small, one may include a disproportionate number of sera, which are outliers and anomalies. This skews the results which might not be a fair picture of the whole population.

Further limitations include inter and intra experimental variation when testing concordance between the Lentivirus vs VSV neutralization assay. Lentivirus sera was tested in a different laboratory (NICD) at different time periods to that of my study which was conducted at UWC.

Conclusion

Virus pseudoparticles are a safe and versatile tool that can be used for a number of applications such as developing neutralizing assays. Prior to this study, the only SARS-CoV-2 neutralization assays in use by the South African virology community were a live-virus assay (requiring a

BSL3) and the lentivirus-based pseudoparticle assay. Both of these methods have limitations as were discussed earlier in the thesis (e.g. need for enhanced biosafety, or issues with false positives when conducting studies on sera from HIV-positive patients on ARVs). Therefore, it was necessary to investigate alternative approaches.

The establishment of a VSV-based neutralization assay for SARS-CoV2 is thus an important and significant contribution, and it can now be applied to studies assessing SARS-CoV-2 vaccine immunogenicity, sero-surveillance studies, etc.

Recent research has also shown various advantages of the VSV system including favouring its use when testing patient sera from HIV-positive individuals on ART. This is a significant discovery as South Africa and the African continent account for more than 68% of the global HIV population. The wider use of the VSV system will allow for more accurate and precise results when conducting studies on virus neutralizing activity in the South African and African population.

Appendix A: List of Materials

Table 1: Bacterial strains

Table Bacterial strains		
Strain	**Source**	**Identifier**
JM109 Competent *E. coli* cells	Promega	Catalogue No.PR-L1001
NEB 5 alpha Competent *E. coli cells*	New England BioLabs	Catalogue No.C2987H

Table 2: Cell lines

Table Cell lines		
Cell Lines	**Source**	**Identifier**
Hek-293 T cells	Prof Penny Moore	
Hek-293T-ACE-2 cells	Prof Penny Moore	
Vero E6	Cellonex	CVER-FL (flask)

Table 3: Plasmids

Table Plasmids	
Plasmid names	**Source**
pCAGGS	Shaw Lab
pCAGGS-KPNA-FLAG	Shaw Lab
pCAGGS-spike Beta-FLAG	Shaw Lab
pCAGGS-spike WT-FLAG	Shaw Lab
pcDNA 3.1 B.1.1.529 Omicron d18	NICD
pcDNA3.1 B.1.1.7 Alpha	NICD
pcDNA3.1 B.1.1529 Omicron	NICD
pcDNA3.1 B.1.351 Beta	NICD
pcDNA3.1 B.1.617.2 Delta	NICD
pcDNA3.1 WTD614G	NICD

Table 4: Viruses

Table of viruses	
Virus	**Source**
VSV*ΔG(FLUc)+VSV-G	Dr Gert Zimmer

Table 5: Molecular Reagents

Table of Molecular Reagents		
Name	**Source**	**Identifier**
10x Phosphate buffered salt	Thermo-Fisher Scientific	Catalogue No.70011044
Agarose powder (Molecular grade)	Invitrogen	Catalogue No.17850
Ampicillin sodium salt	Sigma-Aldrich	Catalogue No. A9518
Bovine albumin serum powder	Sigma-Aldrich	Catalogue No. A2153
DTT	Roche	Catalogue No.3483-12-3
EDTA	Sigma-Aldrich	Catalogue No. E9884
Ethidium bromide	Sigma-Aldrich	Catalogue No. E7637
HindIII	New England Biolabs	Catalogue No. R0104S
KpnI	New England Biolabs	Catalogue No. R3142S
Non-fat dried milk	Sigma-Aldrich	Catalogue No.M7409
S.O.C media	New England Biolabs	Catalogue No.15544034
SacI	New England Biolabs	Catalogue No. R3156S
TEMED	Sigma-Aldrich	Catalogue No. 1.10732
TRIS	Bio-Rad	Catalogue No.1610719

Table 6: Cell culture reagents

Table of cell culture reagents		
Name	**Source**	**Identifier**
1 X Dulbecco's Modified Eagles media	Gibco	Catalogue No.41966052
1 X PBS	Gibco	Catalogue No.10010023
1 X Trypsin	Gibco	Catalogue No.25200056
Fetal Bovine Serum	Gibco	Catalogue No.16000044
Lipofectamine 3000	Thermo-Fisher Scientific	Catalogue No. L3000015

OptiPro Serum free media	Gibco	Catalogue No.12309050
Penicillin/Streptomycin/Amphotericin B	Pan Biotech	Catalogue No. P0607350
Poly-L-lysine	Sigma-Alrich	Catalogue No. P8920
Puromycin	Gibco	Catalogue No. A1113803

Table 7:Antibodies

Table of antibodies		
Name	**Source**	**Identifier**
Anti-Influenza A, Nucleoprotein [HT103] Antibody	Sigma-Alrich	Catalogue No. MABF2164
Goat anti-Mouse IgG (H+L) Secondary Antibody, HRP	Thermo-Fisher Scientific	Catalogue No. 31430
Goat anti-Mouse IgG, IgM (H+L) Secondary Antibody, Alexa Fluor™ 488	Thermo-Fisher Scientific	Catalogue No. A-10680
Monoclonal ANTI-FLAG ® M2 antibody produced in mouse	Sigma-Aldrich	Catalogue No. F3165
SARS-CoV-2 spike S1 subunit antibody	R&D	Catalogue No. MAB105407

Table 8: Software

Table of software	
Table of Software	**Name of Version**
ApE_win_current	2.0.49.0
GraphPad Prism	9
ImageJ	N/A
Snapgene	7
SoftmaxPro	7
Windows Excel	Microsoft 360

Table 9:Buffers and solutions

Table of Buffers and Solutions		
Name	**Recipe**	**Identifier**
0.1% Wash Buffer	Dilute 200µl of Tween 20 in 2L of 1xPBS	
0.5 M Tris pH (6.8)	6.06g of Tris base in 100mL of distilled water	
10% APS	10% (w/v) of APS into 10mL of distilled water	
10% SDS	Dissolve 10 g of SDS in 100 mL of distilled water	
10X Transfer buffer	5,76g of Tris base,2,95g of glycine,3, 75mL of 10% SDS,200mL methanol,800 mL of distilled water	
10X TRIS-Glycine SDS Running buffer	30g of Tris base,144g pf glycine,10g of SDS and 100 mL of distilled water	
10XPBS	From manufacturer-Gibco	Catalogue No.70011044
1M DTT	Mix 1.54g of DTT powder to 10mL of distilled water	
1M Tris pH (7.8)	12.11g of Tris base in 100mL of distilled water	
20% SDS	Dissolve 20 g of SDS in 100 mL of distilled water	
2X Sample buffer		
30% Bis-acrylamide solution	From manufacturer-Sigma-Alrich	Catalogue No. A3699
5% Blocking buffer	Dissolve 1g of Non-fat dried milk powder in 20mL of 5% Blocking buffer	
KPL TMB Peroxidase Substrate	From manufacturer-SeraCare	Catalogue No. 4200025
Luria Bertani (Miller's broth) solution	Add 25 g of pre-mixed powder containing Tryptone, NaCl and Yeast Extract to 950 mL of Milli-Q H2O	Condalabs Catalogue No.1551
S.O.C media	From manufacturer- Invitrogen	Catalogue No.15544034

Appendix B

Appendix B:Alignment of pCAGGS-spike ^{WT} with reference sequence isolate Wuhan-Hu-1 (NC_045512.2)

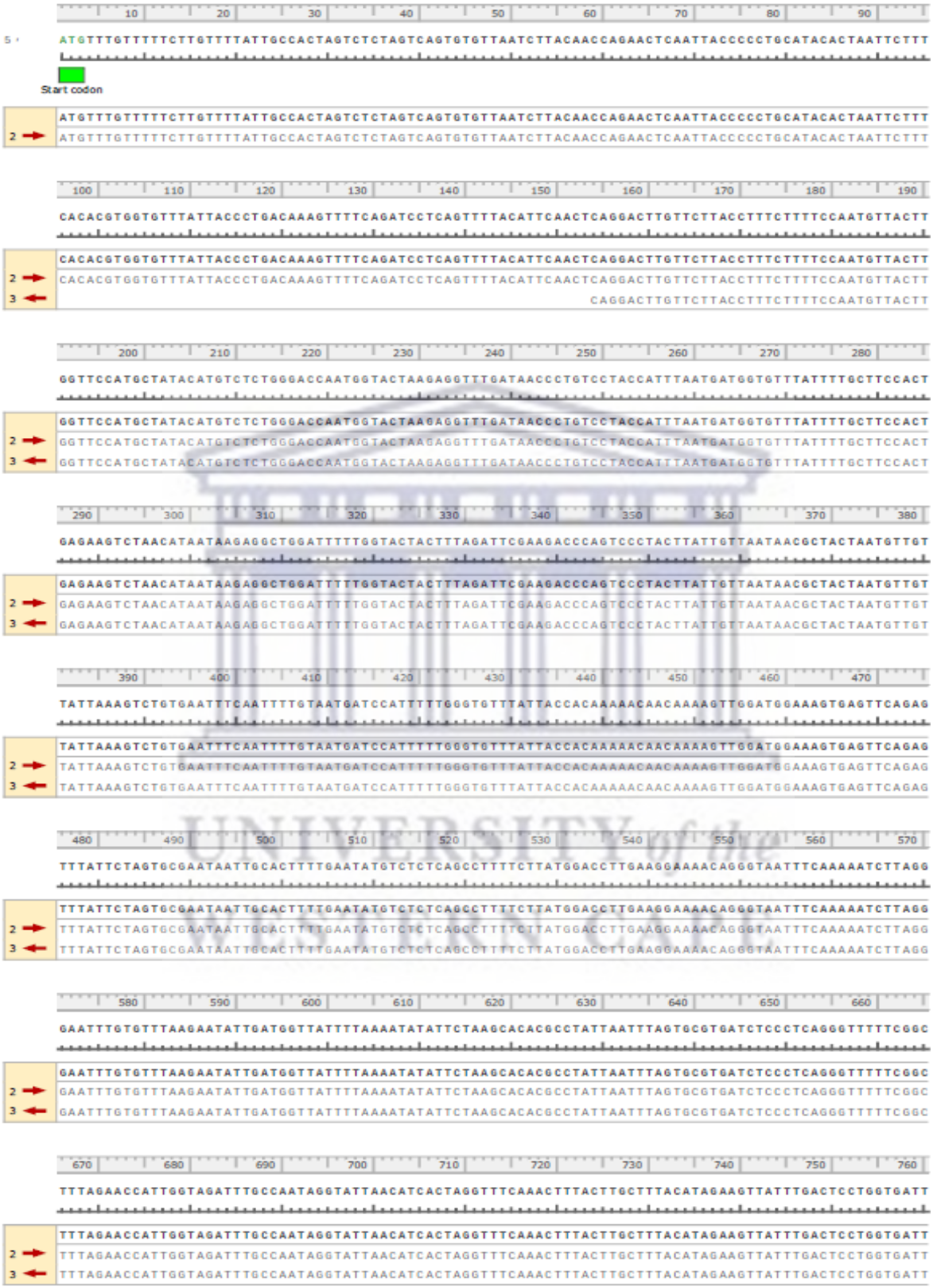

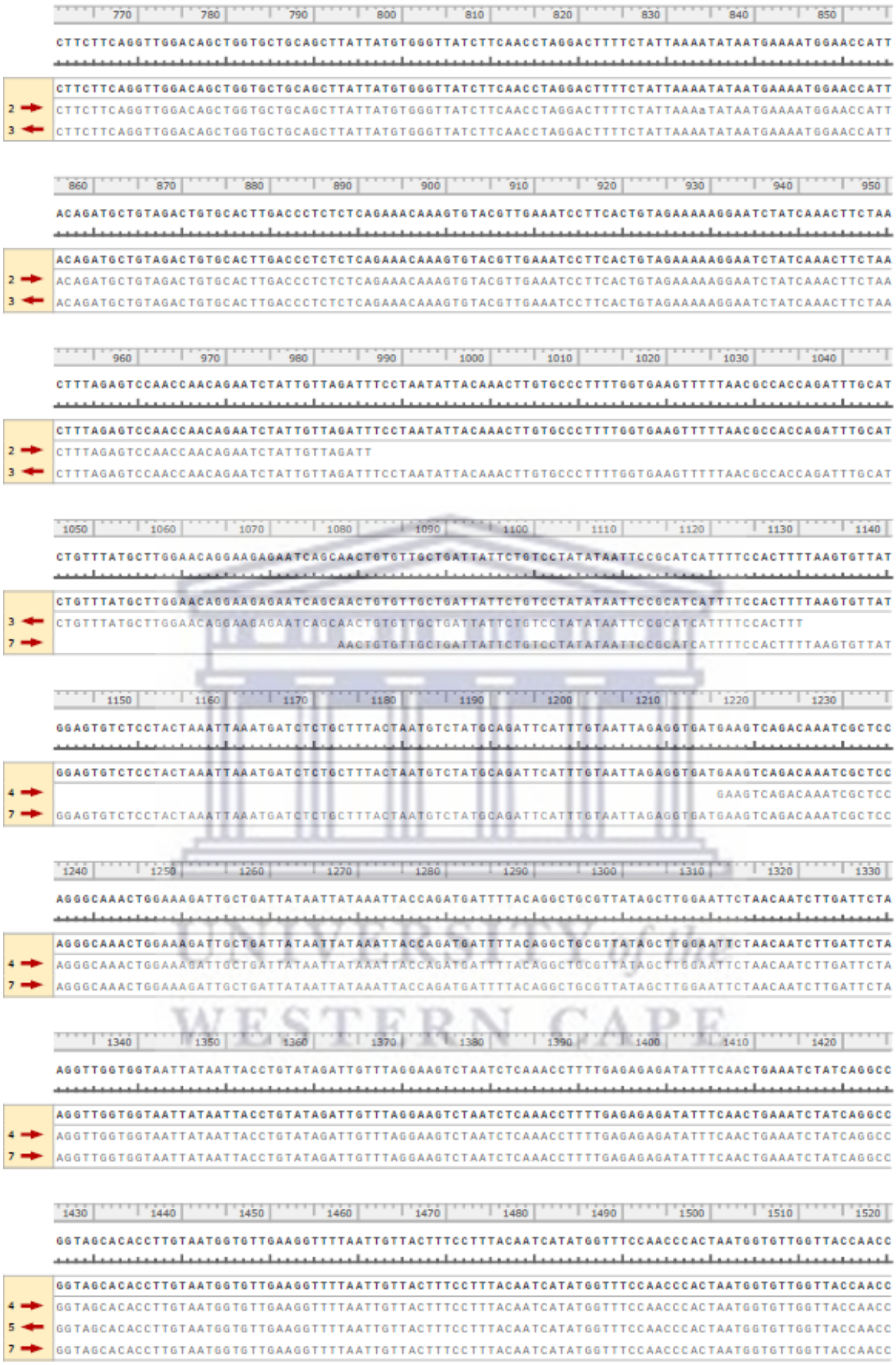

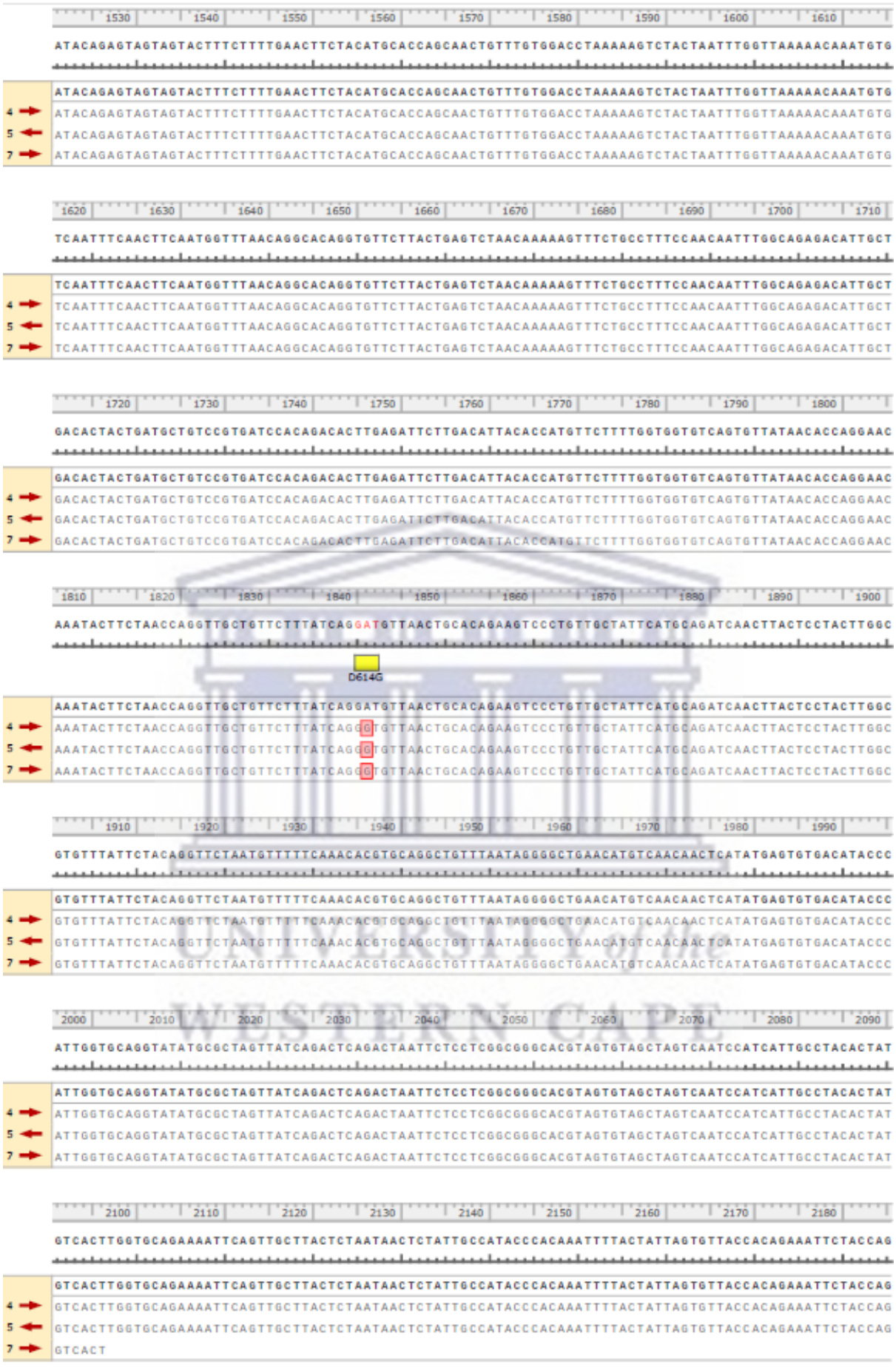

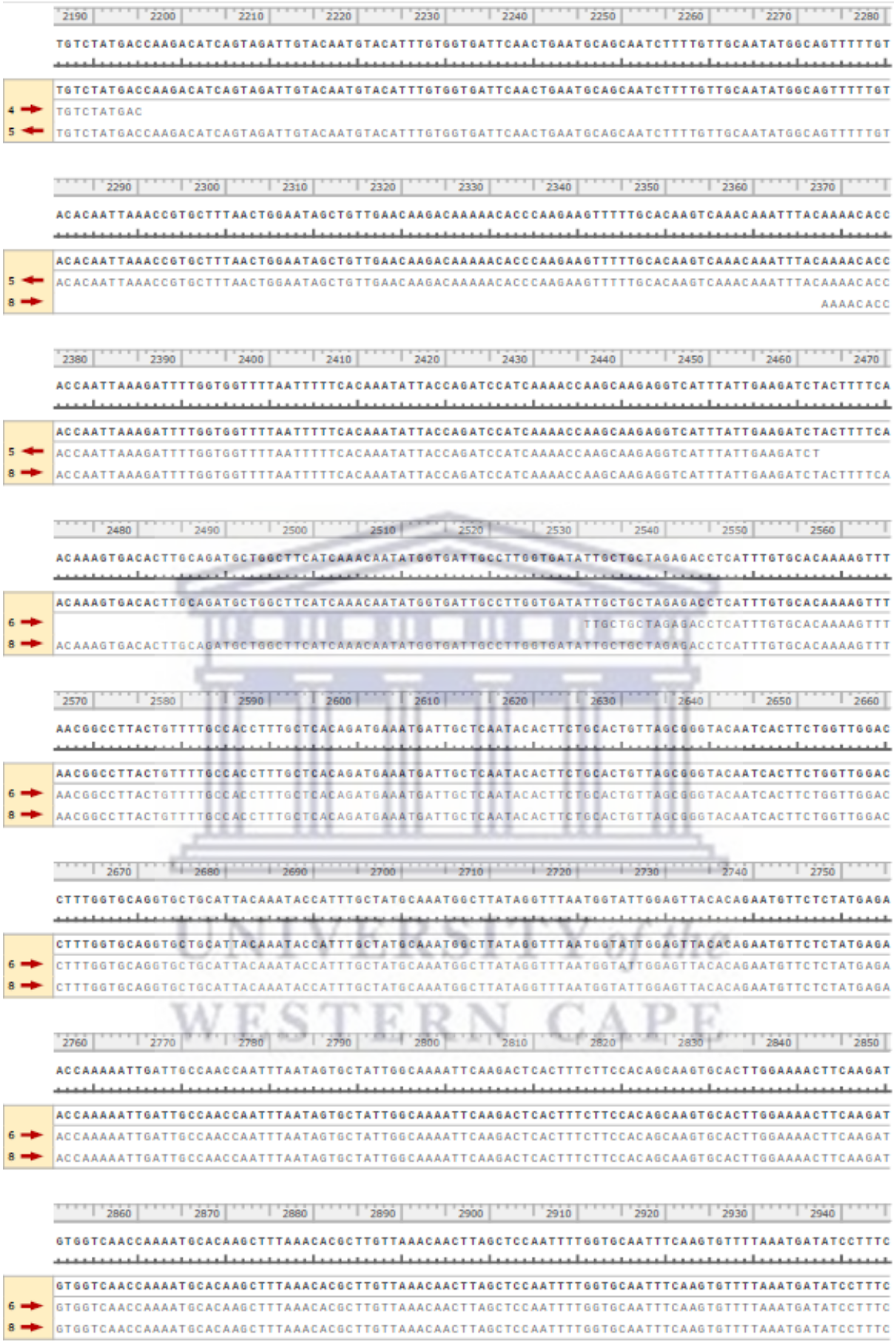

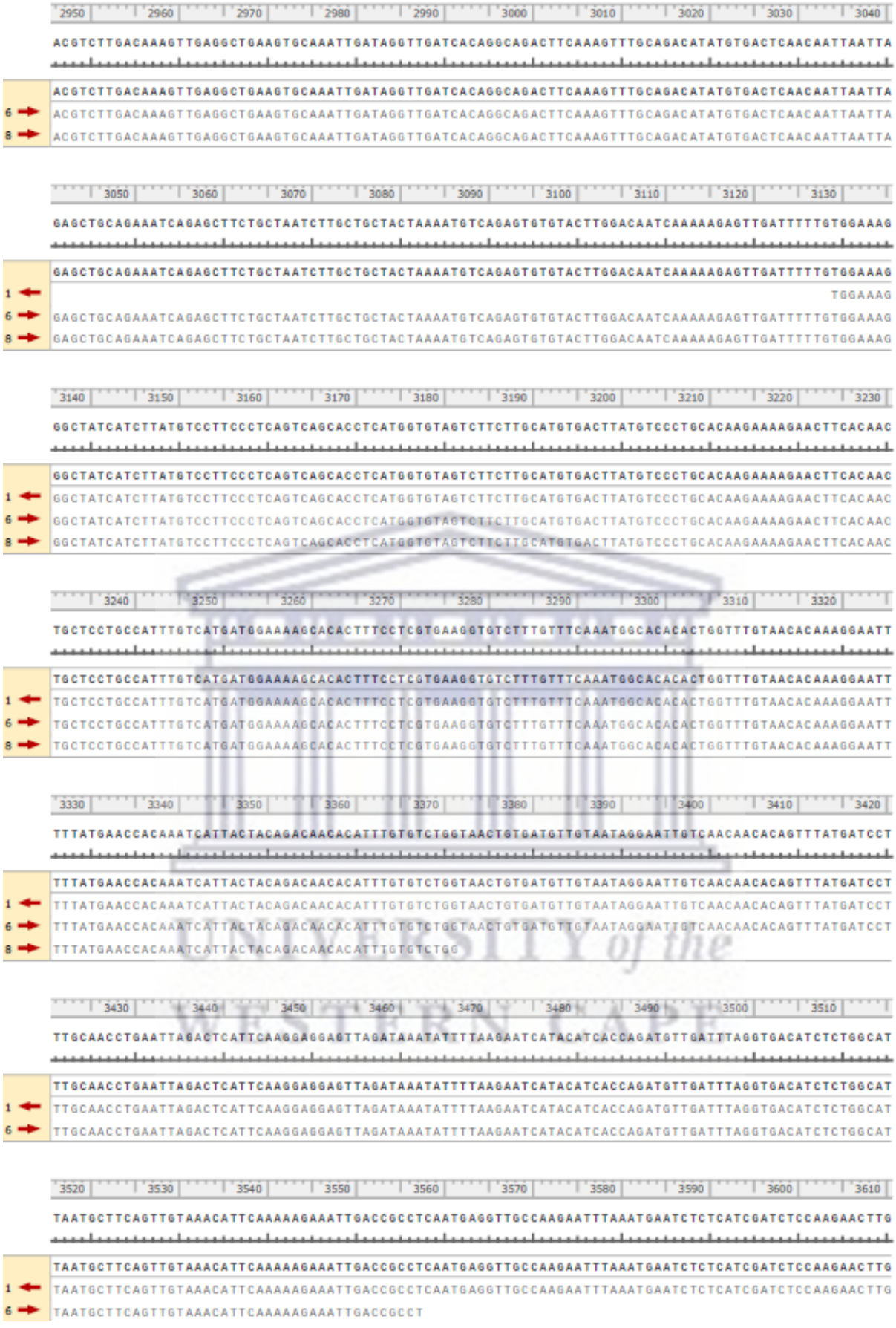

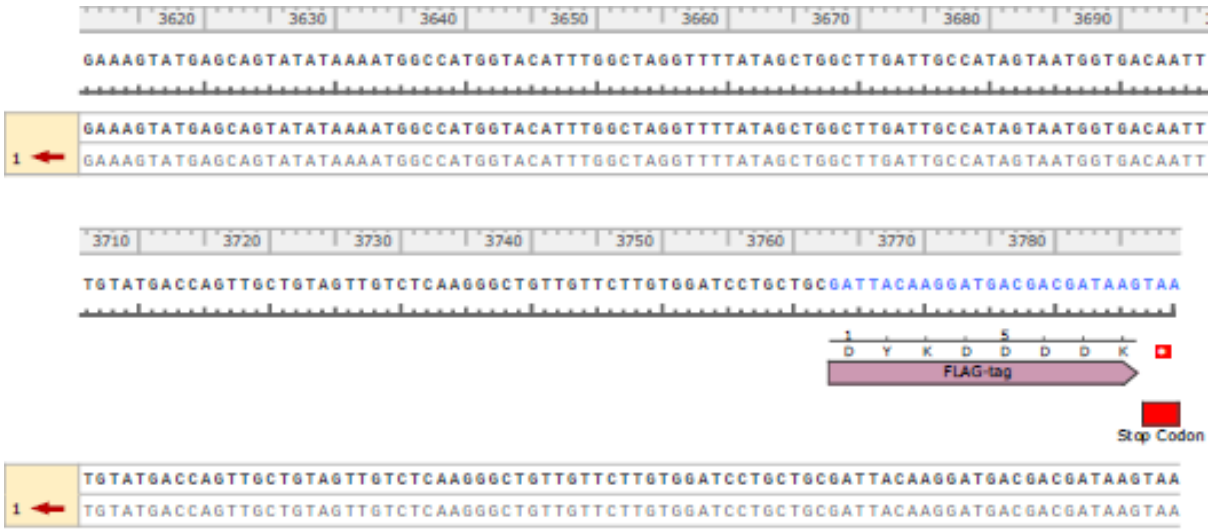

Appendix C

Appendix C :Alignment of pCAGGS-spikeBETA with reference sequence isolate Wuhan-Hu-1(NC_045512.2)

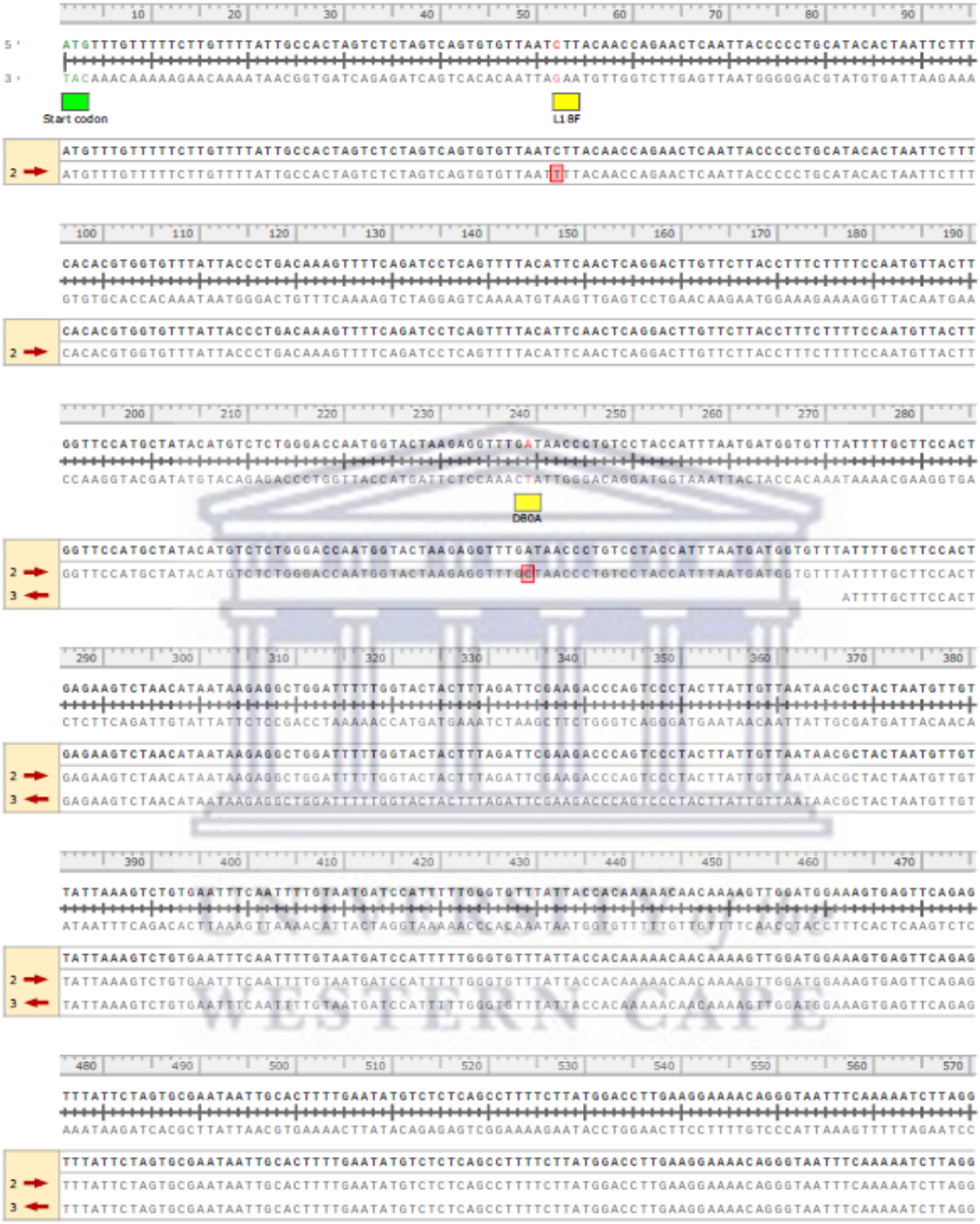

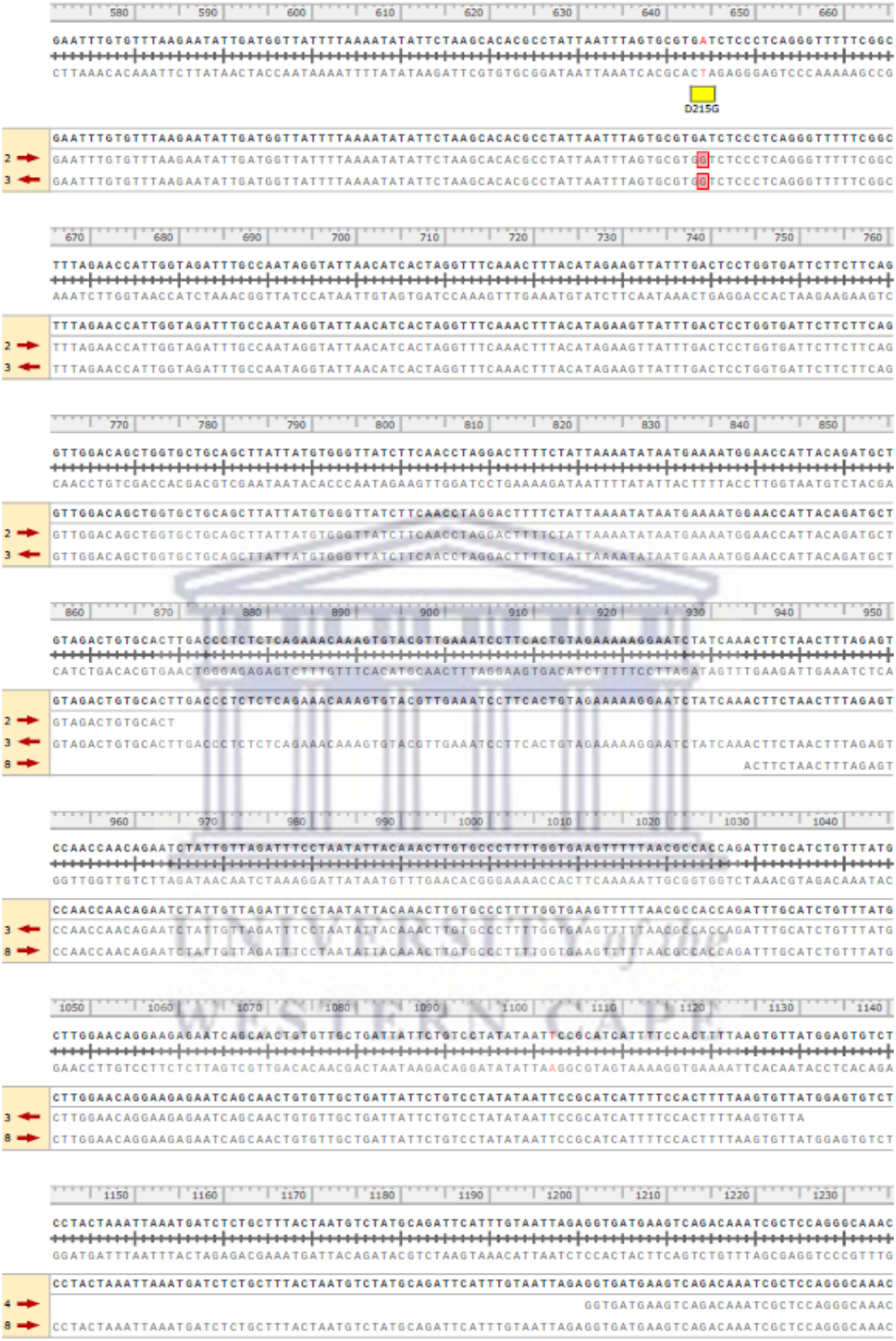

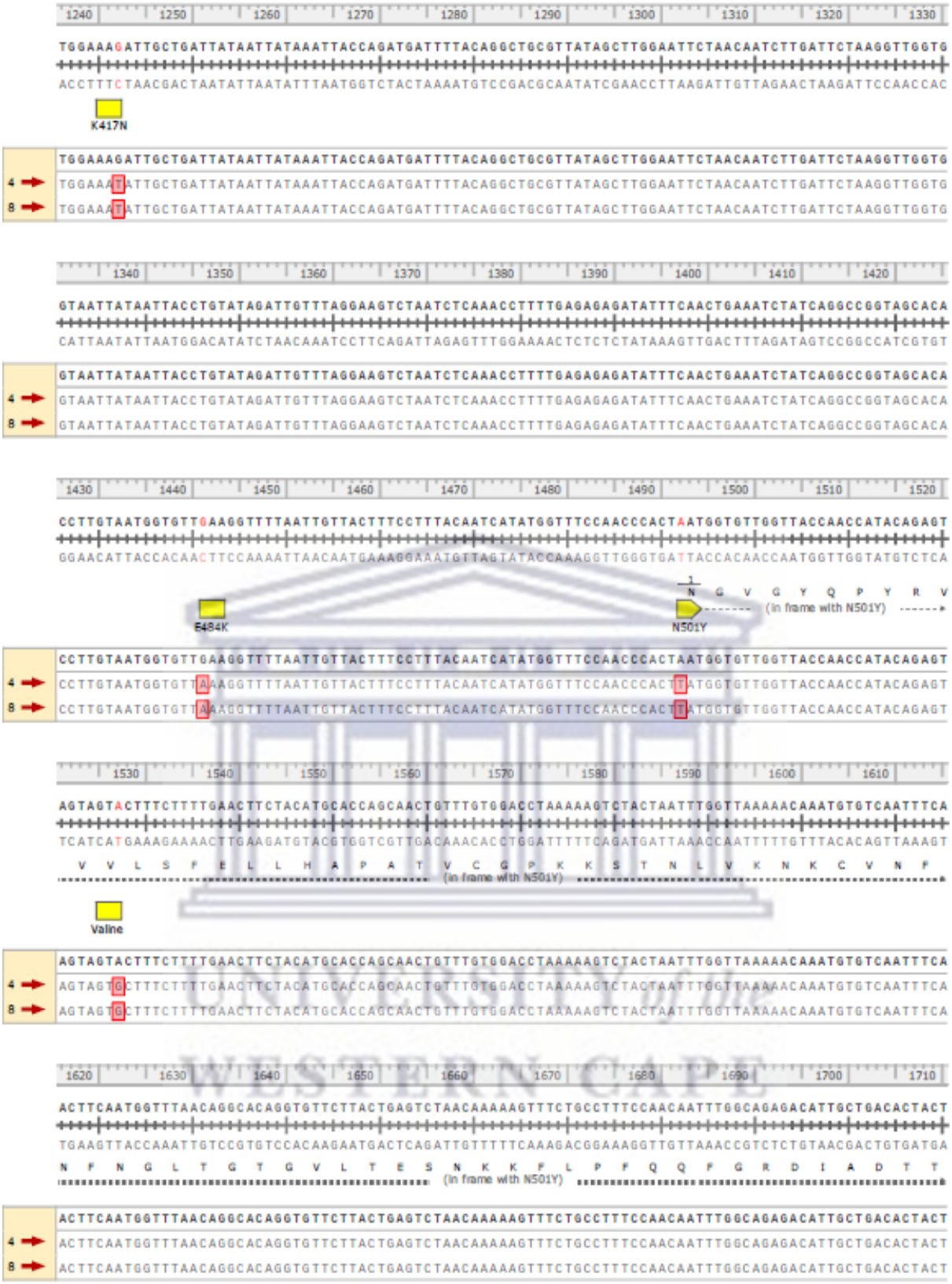

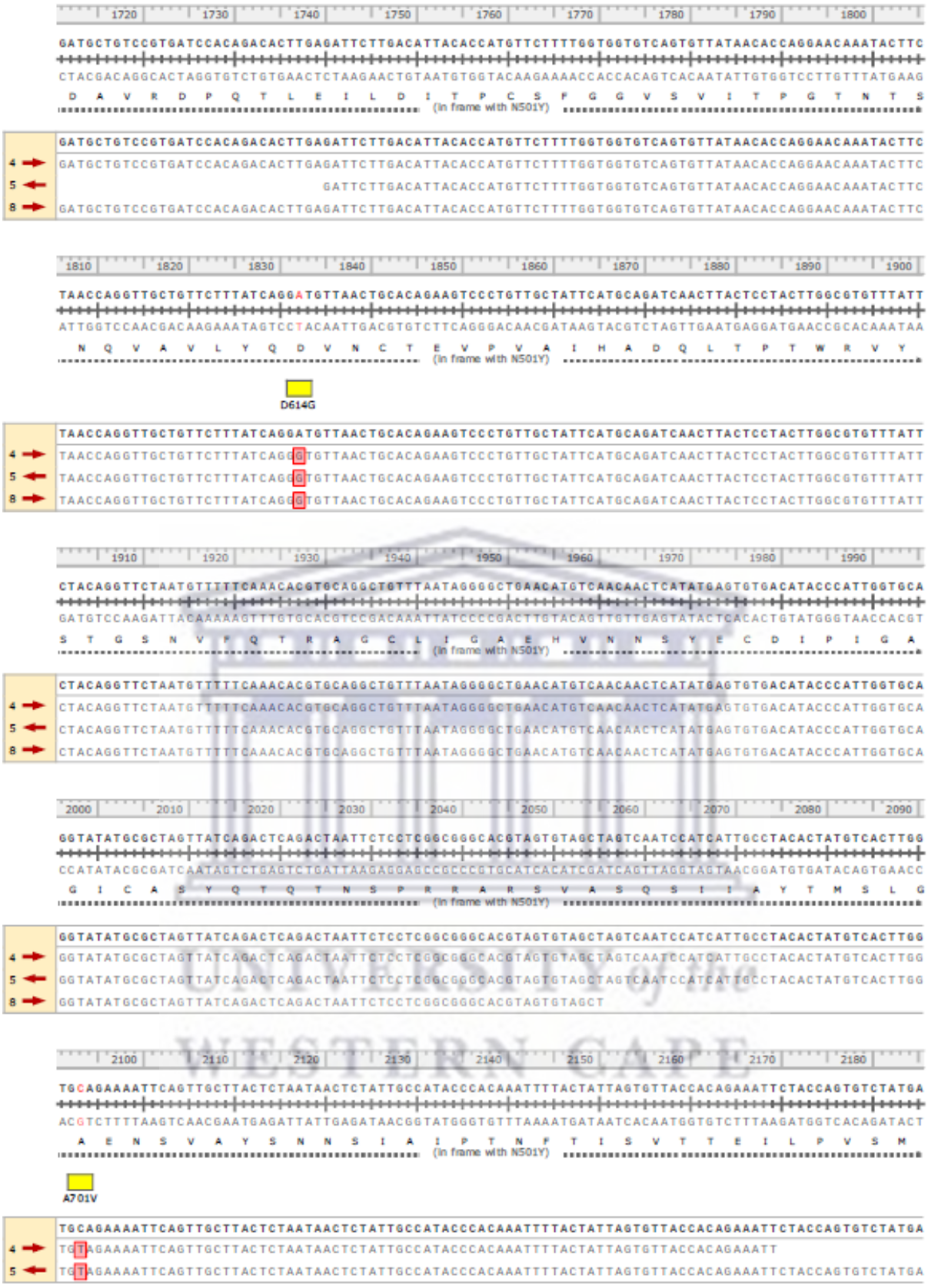

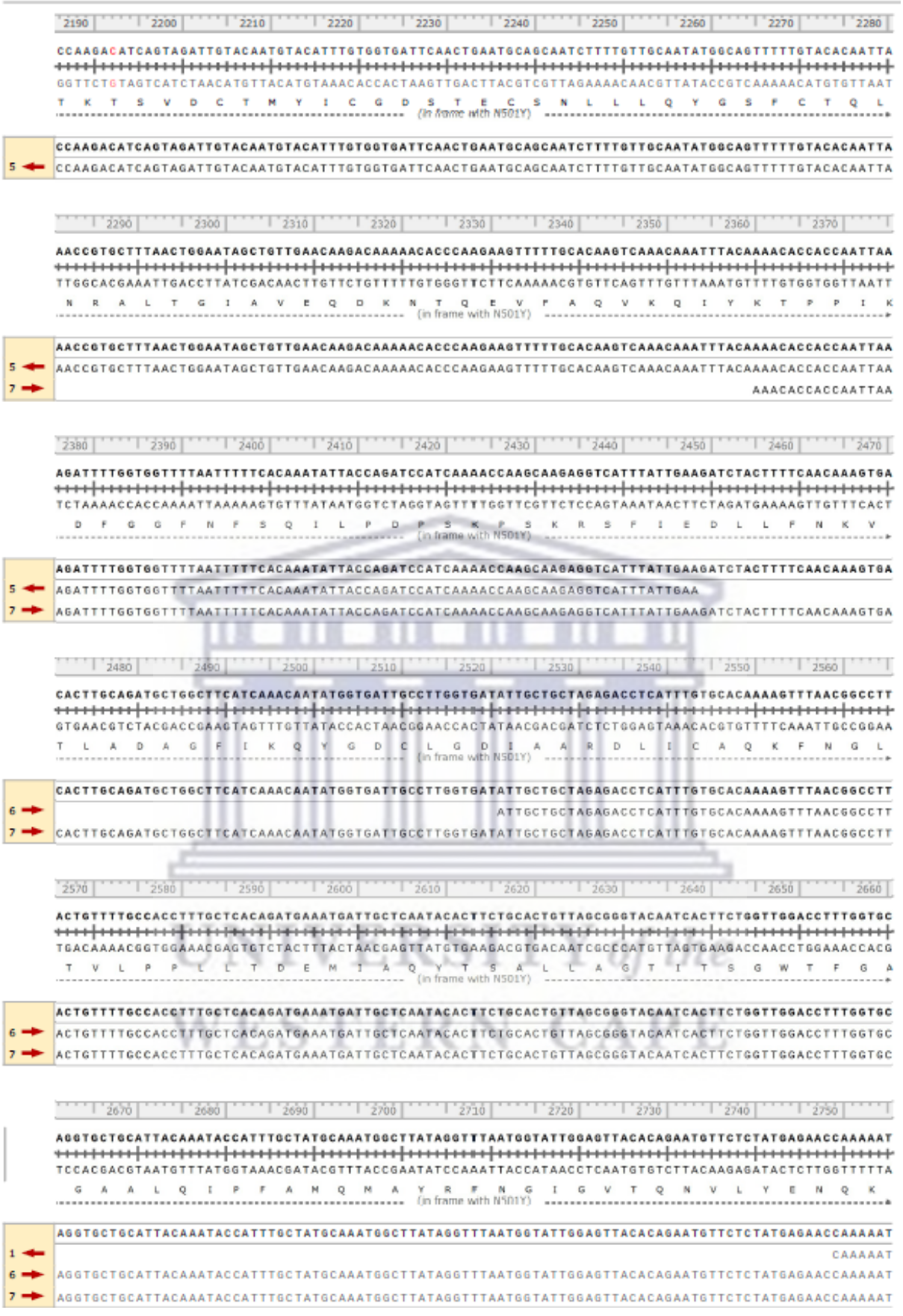

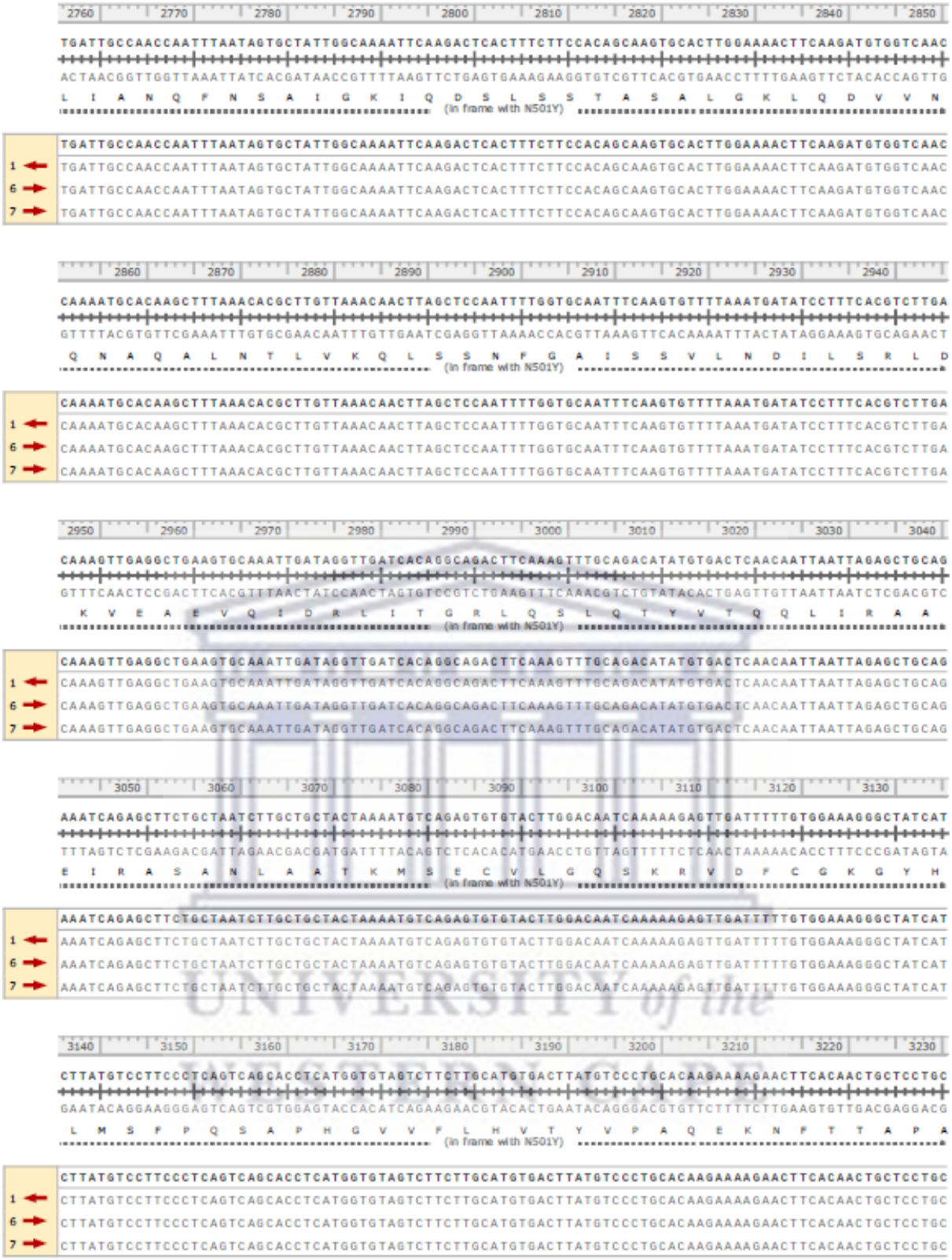

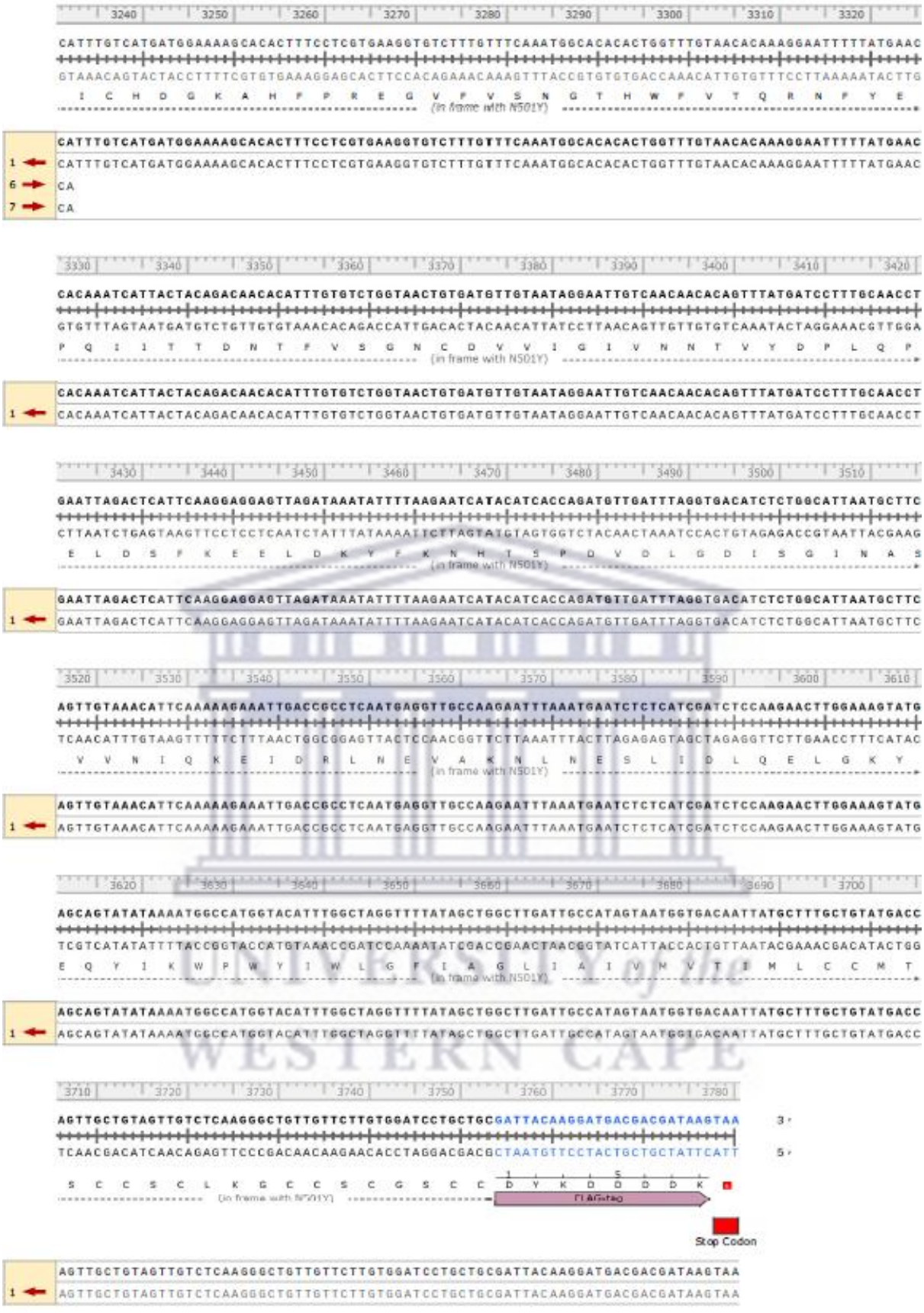

References

(2023). NEBuilder HiFi DNA Assembly Cloning Kit. New England Biolabs. Ipswich, Massachusetts, New England Biolabs**:** 3.

Abebe, E. C. and T. A. Dejenie (2023). "Protective roles and protective mechanisms of neutralizing antibodies against SARS-CoV-2 infection and their potential clinical implications." Frontiers in Immunology **14**: 1055457.

Andersen, K. G., et al. (2020). "The proximal origin of SARS-CoV-2." Nature medicine **26**(4): 450-452.

Arya, R., et al. (2021). "Structural insights into SARS-CoV-2 proteins." Journal of molecular biology **433**(2): 166725.

Biolabs, N. E. (2022). "NEBuilder HiFi DNA assembly reaction (E2621)."

Burger, C., et al. (2022). "The health impact of free access to antiretroviral therapy in South Africa." Social Science & Medicine **299**: 114832.

Burnett, L. C., et al. (2009). "Biosafety: guidelines for working with pathogenic and infectious microorganisms." Current protocols in microbiology **13**(1): 1A. 1.1-1A. 1.14.

Cao, Y., et al. (2023). "Imprinted SARS-CoV-2 humoral immunity induces convergent Omicron RBD evolution." Nature **614**(7948): 521-529.

Cao, Y., et al. (2021). "Characterization of the SARS-CoV-2 E protein: sequence, structure, viroporin, and inhibitors." Protein Science **30**(6): 1114-1130.

Chakraborty, S. (2022). "E484K and N501Y SARS-CoV 2 spike mutants Increase ACE2 recognition but reduce affinity for neutralizing antibody." International immunopharmacology **102**: 108424.

Chen, H.-Y., et al. (2021). "Cytoplasmic tail truncation of SARS-CoV-2 spike protein enhances titer of pseudotyped vectors but masks the effect of the D614G mutation." Journal of Virology **95**(22): 10.1128/jvi. 00966-00921.

Chen, K.-W. K., et al. (2022). "SARS-CoV-2 variants–evolution, spike protein, and vaccines." biomedical journal **45**(4): 573-579.

Cheng, M. H., et al. (2022). "Impact of new variants on SARS-CoV-2 infectivity and neutralization: A molecular assessment of the alterations in the spike-host protein interactions." Iscience **25**(3).

Chmielewska, A. M., et al. (2021). "Immune response against SARS-CoV-2 variants: the role of neutralization assays." Npj Vaccines **6**(1): 142.

Chvatal-Medina, M., et al. (2021). "Antibody responses in COVID-19: a review." Frontiers in Immunology **12**.

Condor Capcha, J. M., et al. (2021). "Generation of SARS-CoV-2 spike pseudotyped virus for viral entry and neutralization assays: a 1-week protocol." Frontiers in cardiovascular medicine **7**: 618651.

Cui, X., et al. (2023). "Future trajectory of SARS-CoV-2: Constant spillover back and forth between humans and animals." Virus research **328**: 199075.

De La Torre-Tarazona, E., et al. (2023). "Treatment with integrase inhibitors alters SARS-CoV-2 neutralization levels measured with HIV-based pseudotypes in people living with HIV." Journal of Medical Virology **95**(2): e28543.

Dispinseri, S., et al. (2021). "Neutralizing antibody responses to SARS-CoV-2 in symptomatic COVID-19 is persistent and critical for survival." Nature communications **12**(1): 1-12.

Dougan, M., et al. (2022). "Bebtelovimab, alone or together with bamlanivimab and etesevimab, as a broadly neutralizing monoclonal antibody treatment for mild to moderate, ambulatory COVID-19." medrxiv: 2022.2003. 2010.22272100.

Duffy, S. (2018). "Why are RNA virus mutation rates so damn high?" PLoS biology **16**(8): e3000003.

Elena, S. F. and R. Sanjuán (2005). "Adaptive value of high mutation rates of RNA viruses: separating causes from consequences." Journal of Virology **79**(18): 11555-11558.

Fani, M., et al. (2020). "Comparison of the COVID-2019 (SARS-CoV-2) pathogenesis with SARS-CoV and MERS-CoV infections." Future Virology **15**(5): 317-323.

Fukushi, S., et al. (2005). "Vesicular stomatitis virus pseudotyped with severe acute respiratory syndrome coronavirus spike protein." Journal of general virology **86**(8): 2269-2274.

Fukushi, S., et al. (2008). "Pseudotyped vesicular stomatitis virus for analysis of virus entry mediated by SARS coronavirus spike proteins." SARS-and Other Coronaviruses: Laboratory Protocols: 331-338.

Galipeau, Y., et al. (2020). "Humoral responses and serological assays in SARS-CoV-2 infections." Frontiers in Immunology **11**: 610688.

Garcia-Beltran, W. F., et al. (2021). "COVID-19-neutralizing antibodies predict disease severity and survival." Cell **184**(2): 476-488. e411.

Gattinger, P., et al. (2022). "Vaccine based on folded receptor binding domain-PreS fusion protein with potential to induce sterilizing immunity to SARS-CoV-2 variants." Allergy **77**(8): 2431-2445.

Gottlieb, R. L., et al. (2021). "Effect of bamlanivimab as monotherapy or in combination with etesevimab on viral load in patients with mild to moderate COVID-19: a randomized clinical trial." Jama **325**(7): 632-644.

Greaney, A. J., et al. (2021). "Comprehensive mapping of mutations in the SARS-CoV-2 receptor-binding domain that affect recognition by polyclonal human plasma antibodies." Cell host & microbe **29**(3): 463-476. e466.

Gupta, S. L. and R. K. Jaiswal (2022). "Neutralizing antibody: a savior in the Covid-19 disease." Molecular Biology Reports: 1-10.

Harvey, W. T., et al. (2021). "SARS-CoV-2 variants, spike mutations and immune escape." Nature Reviews Microbiology **19**(7): 409-424.

Hossain, M. G., et al. (2021). "SARS-CoV-2 host diversity: An update of natural infections and experimental evidence." Journal of Microbiology, Immunology and Infection **54**(2): 175-181.

Huang, D., et al. (2021). "A rapid assay for SARS-CoV-2 neutralizing antibodies that is insensitive to antiretroviral drugs." The Journal of Immunology **207**(1): 344-351.

Huang, Y., et al. (2020). "Structural and functional properties of SARS-CoV-2 spike protein: potential antivirus drug development for COVID-19." Acta Pharmacologica Sinica **41**(9): 1141-1149.

Hui, K. P., et al. (2020). "Tropism, replication competence, and innate immune responses of the coronavirus SARS-CoV-2 in human respiratory tract and conjunctiva: an analysis in ex-vivo and in-vitro cultures." The Lancet Respiratory Medicine **8**(7): 687-695.

Jackson, C. B., et al. (2022). "Mechanisms of SARS-CoV-2 entry into cells." Nature reviews Molecular cell biology **23**(1): 3-20.

Jassat, W., et al. (2022). "Clinical severity of COVID-19 in patients admitted to hospital during the omicron wave in South Africa: a retrospective observational study." The Lancet Global Health **10**(7): e961-e969.

Jassat, W., et al. (2021). "Difference in mortality among individuals admitted to hospital with COVID-19 during the first and second waves in South Africa: a cohort study." The Lancet Global Health **9**(9): e1216-e1225.

Jayakar, H. R., et al. (2004). "Rhabdovirus assembly and budding." Virus research **106**(2): 117-132.

Johnson, M. C., et al. (2020). "Optimized pseudotyping conditions for the SARS-COV-2 spike glycoprotein." Journal of Virology **94**(21): 10.1128/jvi. 01062-01020.

Kendall, E., et al. (1962). "Virus isolations from common colds occurring in a residential school." British medical journal **2**(5297): 82.

Khan, K., et al. (2022). "Omicron infection of vaccinated individuals enhances neutralizing immunity against the Delta variant." medrxiv.

Khoury, D. S., et al. (2021). "Neutralizing antibody levels are highly predictive of immune protection from symptomatic SARS-CoV-2 infection." Nature medicine: 1-7.

Klasse, P. and Q. Sattentau (2002). "Occupancy and mechanism in antibody-mediated neutralization of animal viruses." Journal of general virology **83**(9): 2091-2108.

Lam, T. T.-Y., et al. (2020). "Identifying SARS-CoV-2-related coronaviruses in Malayan pangolins." Nature **583**(7815): 282-285.

Lan, J., et al. (2020). "Structure of the SARS-CoV-2 spike receptor-binding domain bound to the ACE2 receptor." Nature **581**(7807): 215-220.

Lau, E. H., et al. (2021). "Neutralizing antibody titres in SARS-CoV-2 infections." Nature communications **12**(1): 1-7.

Letchworth, G., et al. (1999). "Vesicular stomatitis." The Veterinary Journal **157**(3): 239-260.

Li, C., et al. (2021). "Overview of the pathogenesis of COVID-19." Experimental and Therapeutic Medicine **22**(3): 1-10.

Li, C., et al. (2020). "Genetic evolution analysis of 2019 novel coronavirus and coronavirus from other species." Infection, Genetics and Evolution **82**: 104285.

Li, D., et al. (2021). "In vitro and in vivo functions of SARS-CoV-2 infection-enhancing and neutralizing antibodies." Cell **184**(16): 4203-4219. e4232.

Li, Q., et al. (2018). "Current status on the development of pseudoviruses for enveloped viruses." Reviews in medical virology **28**(1): e1963.

Liu, G., et al. (2021). "Vesicular stomatitis virus: from agricultural pathogen to vaccine vector." Pathogens **10**(9): 1092.

Liu, P., et al. (2020). "Are pangolins the intermediate host of the 2019 novel coronavirus (SARS-CoV-2)?" PLoS Pathogens **16**(5): e1008421.

Lu, Y., et al. (2021). "Advances in neutralization assays for SARS-CoV-2." Scandinavian Journal of Immunology **94**(3): e13088.

Ma, K. C. (2023). "Genomic Surveillance for SARS-CoV-2 Variants: Circulation of Omicron Lineages—United States, January 2022–May 2023." MMWR. Morbidity and Mortality Weekly Report **72**.

Magazine, N., et al. (2022). "Mutations and evolution of the SARS-CoV-2 spike protein." Viruses **14**(3): 640.

Malone, B., et al. (2022). "Structures and functions of coronavirus replication–transcription complexes and their relevance for SARS-CoV-2 drug design." Nature reviews Molecular cell biology **23**(1): 21-39.

Martinez, D. R., et al. (2021). "Prevention and therapy of SARS-CoV-2 and the B. 1.351 variant in mice." Cell reports **36**(4).

Matusali, G., et al. (2021). "SARS-CoV-2 serum neutralization assay: a traditional tool for a brand-new virus." Viruses **13**(4): 655.

Millet, J. K. and G. R. Whittaker (2015). "Host cell proteases: critical determinants of coronavirus tropism and pathogenesis." Virus research **202**: 120-134.

Min, L. and Q. Sun (2021). "Antibodies and Vaccines Target RBD of SARS-CoV-2." Frontiers in Molecular Biosciences **8**: 247.

Mishra, N., et al. (2021). "Cross-neutralization of SARS-CoV-2 by HIV-1 specific broadly neutralizing antibodies and polyclonal plasma." PLoS Pathogens **17**(9): e1009958.

Morales-Núñez, J. J., et al. (2021). "Overview of neutralizing antibodies and their potential in COVID-19." Vaccines **9**(12): 1376.

Morens, D. M. and A. S. Fauci (2020). "Emerging pandemic diseases: how we got to COVID-19." Cell **182**(5): 1077-1092.

Motozono, C., et al. (2021). "SARS-CoV-2 spike L452R variant evades cellular immunity and increases infectivity." Cell host & microbe **29**(7): 1124-1136. e1111.

Moyo-Gwete, T., et al. (2022). "Shared N417-dependent epitope on the SARS-CoV-2 omicron, beta, and delta plus variants." Journal of Virology **96**(15): e00558-00522.

Naqvi, A. A. T., et al. (2020). "Insights into SARS-CoV-2 genome, structure, evolution, pathogenesis and therapies: Structural genomics approach." Biochimica et Biophysica Acta (BBA)-Molecular Basis of Disease **1866**(10): 165878.

Neuman, B. W., et al. (2011). "A structural analysis of M protein in coronavirus assembly and morphology." Journal of structural biology **174**(1): 11-22.

Nova, N. (2021). "Cross-species transmission of coronaviruses in humans and domestic mammals, what are the ecological mechanisms driving transmission, spillover, and disease emergence?" Frontiers in Public Health **9**: 717941.

Noy-Porat, T., et al. (2020). "A panel of human neutralizing mAbs targeting SARS-CoV-2 spike at multiple epitopes." Nature communications **11**(1): 1-7.

Palmer, E. and T. Freeman (2004). "Investigation into the use of C-and N-terminal GFP fusion proteins for subcellular localization studies using reverse transfection microarrays." Comparative and functional genomics **5**(4): 342-353.

Pang, N. Y.-L., et al. (2021). "Understanding neutralising antibodies against SARS-CoV-2 and their implications in clinical practice." Military Medical Research **8**(1): 1-17.

Papageorgiou, A. C. and I. Mohsin (2020). "The SARS-CoV-2 spike glycoprotein as a drug and vaccine target: structural insights into its complexes with ACE2 and antibodies." Cells **9**(11): 2343.

Peck, D. E., et al. (2020). "Management strategies for reducing the risk of equines contracting vesicular stomatitis virus (VSV) in the western United States." Journal of equine veterinary science **90**: 103026.

Pedenko, B., et al. (2023). "SARS-CoV-2 S Glycoprotein Stabilization Strategies." Viruses **15**(2): 558.

Perkmann, T., et al. (2021). "Spike protein antibodies mediate the apparent correlation between SARS-CoV-2 nucleocapsid antibodies and neutralization test results." Microbiology Spectrum **9**(1): 10.1128/spectrum. 00218-00221.

Petrovszki, D., et al. (2022). "Penetration of the SARS-CoV-2 spike protein across the blood–brain barrier, as revealed by a combination of a human cell culture model system and optical biosensing." Biomedicines **10**(1): 188.

Pinto, D., et al. (2020). "Cross-neutralization of SARS-CoV-2 by a human monoclonal SARS-CoV antibody." Nature **583**(7815): 290-295.

Polatoğlu, I., et al. (2023). "COVID-19 in early 2023: Structure, replication mechanism, variants of SARS-CoV-2, diagnostic tests, and vaccine & drug development studies." MedComm **4**(2): e228.

Redondo, N., et al. (2021). "SARS-CoV-2 accessory proteins in viral pathogenesis: knowns and unknowns." Frontiers in Immunology: 2698.

Richardson, S. I., et al. (2022). "SARS-CoV-2 Omicron triggers cross-reactive neutralization and Fc effector functions in previously vaccinated, but not unvaccinated, individuals." Cell host & microbe **30**(6): 880-886. e884.

Robba, C., et al. (2020). "Multiple organ dysfunction in SARS-CoV-2: MODS-CoV-2." Expert review of respiratory medicine **14**(9): 865-868.

Rozo-Lopez, P., et al. (2018). "Vesicular stomatitis virus transmission: A comparison of incriminated vectors." Insects **9**(4): 190.

Sanyaolu, A., et al. (2021). "The emerging SARS-CoV-2 variants of concern." Therapeutic Advances in Infectious Disease **8**: 20499361211024372.

Sarzotti-Kelsoe, M., et al. (2014). "Optimization and validation of a neutralizing antibody assay for HIV-1 in A3R5 cells." Journal of immunological methods **409**: 147-160.

Schmidt, F., et al. (2020). "Measuring SARS-CoV-2 neutralizing antibody activity using pseudotyped and chimeric viruses." Journal of Experimental Medicine **217**(11): e20201181.

Scialo, F., et al. (2020). "ACE2: the major cell entry receptor for SARS-CoV-2." Lung **198**: 867-877.

Seydoux, E., et al. (2020). "Characterization of neutralizing antibodies from a SARS-CoV-2 infected individual." BioRxiv.

Shang, J., et al. (2020). "Structural basis of receptor recognition by SARS-CoV-2." Nature **581**(7807): 221-224.

Shereen, M. A., et al. (2020). "COVID-19 infection: Emergence, transmission, and characteristics of human coronaviruses." Journal of advanced research **24**: 91-98.

Shi, J., et al. (2020). "Susceptibility of ferrets, cats, dogs, and other domesticated animals to SARS–coronavirus 2." Science **368**(6494): 1016-1020.

Shi, R., et al. (2020). "A human neutralizing antibody targets the receptor-binding site of SARS-CoV-2." Nature **584**(7819): 120-124.

Steeds, K., et al. (2020). "Pseudotyping of VSV with Ebola virus glycoprotein is superior to HIV-1 for the assessment of neutralising antibodies." Scientific Reports **10**(1): 14289.

Stephens, D. S. and M. J. McElrath (2020). "COVID-19 and the Path to Immunity." Jama **324**(13): 1279-1281.

Strasfeld, L. and S. Chou (2010). "Antiviral drug resistance: mechanisms and clinical implications." Infectious Disease Clinics **24**(2): 413-437.

Stremlau, M., et al. (2004). "The cytoplasmic body component TRIM5α restricts HIV-1 infection in Old World monkeys." Nature **427**(6977): 848-853.

Syed, A. M., et al. (2022). "Omicron mutations enhance infectivity and reduce antibody neutralization of SARS-CoV-2 virus-like particles." Proceedings of the National Academy of Sciences **119**(31): e2200592119.

Tang, Y., et al. (2020). "Laboratory diagnosis of COVID-19: current issues and challenges. McAdam AJ, ed." J Clin Microbiol **58**(6): e00512-200520.

Tegally, H., et al. (2020). "Emergence and rapid spread of a new severe acute respiratory syndrome-related coronavirus 2 (SARS-CoV-2) lineage with multiple spike mutations in South Africa." medrxiv: 2020.2012. 2021.20248640.

Tiwari, R., et al. (2020). "COVID-19: animals, veterinary and zoonotic links." Veterinary Quarterly **40**(1): 169-182.

Tolossa, T., et al. (2021). "Survival from a triple co-infection of COVID-19, HIV, and tuberculosis: a case report." International Medical Case Reports Journal: 611-615.

Travieso, T., et al. (2022). "The use of viral vectors in vaccine development." Npj Vaccines **7**(1): 75.

Tulimilli, S. V., et al. (2022). "Variants of severe acute respiratory syndrome coronavirus 2 (SARS-CoV-2) and vaccine effectiveness." Vaccines **10**(10): 1751.

V'kovski, P., et al. (2021). "Coronavirus biology and replication: implications for SARS-CoV-2." Nature Reviews Microbiology **19**(3): 155-170.

Van Der Hoek, L., et al. (2006). "Human coronavirus NL63, a new respiratory virus." FEMS microbiology reviews **30**(5): 760-773.

Velusamy, P., et al. (2021). "SARS-CoV-2 spike protein: Site-specific breakpoints for the development of COVID-19 vaccines." Journal of King Saud University-Science **33**(8): 101648.

Vogt, I. (2008). Analysis of Biological Screening Data and Molecular Selectivity Profiles Using Fingerprints and Mapping Algorithms, Universitäts-und Landesbibliothek Bonn.

von der Thüsen, J. and M. van der Eerden (2020). "Histopathology and genetic susceptibility in COVID-19 pneumonia." European journal of clinical investigation **50**(7): e13259.

Wang, J., et al. (2021). "Specific cytokines in the inflammatory cytokine storm of patients with COVID-19-associated acute respiratory distress syndrome and extrapulmonary multiple-organ dysfunction." Virology Journal **18**(1): 1-12.

Wang, Q., et al. (2023). "Key mutations in the spike protein of SARS-CoV-2 affecting neutralization resistance and viral internalization." Journal of Medical Virology **95**(1): e28407.

Wang, Q., et al. (2020). "Structural and functional basis of SARS-CoV-2 entry by using human ACE2." Cell **181**(4): 894-904. e899.

Wang, X., et al. (2021). "Deletion of ER-retention motif on SARS-CoV-2 spike protein reduces cell hybrid during cell–cell fusion." Cell & Bioscience **11**(1): 1-12.

Wang, Y., et al. (2022). "Structural basis for SARS-CoV-2 Delta variant recognition of ACE2 receptor and broadly neutralizing antibodies." Nature communications **13**(1): 871.

Weissenhorn, W., et al. (2007). "Virus membrane fusion." FEBS letters **581**(11): 2150-2155.

Westendorf, K., et al. (2022). "LY-CoV1404 (bebtelovimab) potently neutralizes SARS-CoV-2 variants." Cell reports **39**(7).

Whitt, M. A. (2010). "Generation of VSV pseudotypes using recombinant ΔG-VSV for studies on virus entry, identification of entry inhibitors, and immune responses to vaccines." Journal of virological methods **169**(2): 365-374.

Wibmer, C. K., et al. (2021). "SARS-CoV-2 501Y. V2 escapes neutralization by South African COVID-19 donor plasma." Nature medicine **27**(4): 622-625.

Wolfe, M., et al. (2022). "Detection of SARS-CoV-2 variants Mu, Beta, Gamma, Lambda, Delta, Alpha, and Omicron in wastewater settled solids using mutation-specific assays is associated with regional detection of variants in clinical samples." Applied and Environmental Microbiology **88**(8): e00045-00022.

Wong, N. A. and M. H. Saier Jr (2021). "The SARS-coronavirus infection cycle: a survey of viral membrane proteins, their functional interactions and pathogenesis." International journal of molecular sciences **22**(3): 1308.

Wrapp, D., et al. (2020). "Cryo-EM structure of the 2019-nCoV spike in the prefusion conformation." Science **367**(6483): 1260-1263.

Yadav, R., et al. (2021). "Role of structural and non-structural proteins and therapeutic targets of SARS-CoV-2 for COVID-19." Cells **10**(4): 821.

Yang, W. and J. L. Shaman (2022). "COVID-19 pandemic dynamics in South Africa and epidemiological characteristics of three variants of concern (Beta, Delta, and Omicron)." Elife **11**.

Ye, Z.-W., et al. (2020). "Zoonotic origins of human coronaviruses." International journal of biological sciences **16**(10): 1686.

Yoon, E., et al. (2022). "Severe acute respiratory syndrome coronavirus 2 variants–Possibility of universal vaccine design: A review." Computational and Structural Biotechnology Journal **20**: 3533-3544.

Young, M., et al. (2022). "Covid-19: virology, variants, and vaccines." BMJ medicine **1**(1).

Yuan, S., et al. (2020). "Analysis of possible intermediate hosts of the new coronavirus SARS-CoV-2." Frontiers in Veterinary Science: 379.

Yurkovetskiy, L., et al. (2020). "Structural and functional analysis of the D614G SARS-CoV-2 spike protein variant." Cell **183**(3): 739-751. e738.

Zandi, M., et al. (2022). "The role of SARS-CoV-2 accessory proteins in immune evasion." Biomedicine & Pharmacotherapy: 113889.

Zárate, S. and I. S. Novella (2004). "Vesicular stomatitis virus evolution during alternation between persistent infection in insect cells and acute infection in mammalian cells is dominated by the persistence phase." Journal of Virology **78**(22): 12236-12242.

Zhang, L., et al. (2023). "Cytoplasmic Tail Truncation Stabilizes S1-S2 Association and Enhances S Protein Incorporation into SARS-CoV-2 Pseudovirions." Journal of Virology **97**(3): e01650-01622.

Zhang, Y.-Z. and E. C. Holmes (2020). "A genomic perspective on the origin and emergence of SARS-CoV-2." Cell **181**(2): 223-227.

Zhang, Z., et al. (2022). "Structure of SARS-CoV-2 membrane protein essential for virus assembly." Nature communications **13**(1): 4399.

Zhao, J., et al. (2020). "The potential intermediate hosts for SARS-CoV-2." Frontiers in microbiology **11**: 2400.

Zhou, H., et al. (2020). "A novel bat coronavirus closely related to SARS-CoV-2 contains natural insertions at the S1/S2 cleavage site of the spike protein." Current biology **30**(11): 2196-2203. e2193.

Zhou, T., et al. (2022). "Structural basis for potent antibody neutralization of SARS-CoV-2 variants including B. 1.1. 529." Science **376**(6591): eabn8897.